A STUDY OF MECHANICAL AND STRUCTURAL PROPERTIES OF APPLE AND POTATO

Ph. D. THESIS

by

FATEH SINGH

DEPARTMENT OF MATHEMATICS
INDIAN INSTITUTE OF TECHNOLOGY ROORKEE
ROORKEE- 247 667 (INDIA)
FEBRUARY, 2015

A STUDY OF MECHANICAL AND STRUCTURAL PROPERTIES OF APPLE AND POTATO

A THESIS

Submitted in partial fulfilment of the requirements for the award of the degree

of

DOCTOR OF PHILOSOPHY

in

MATHEMATICS

by

FATEH SINGH

DEPARTMENT OF MATHEMATICS
INDIAN INSTITUTE OF TECHNOLOGY ROORKEE
ROORKEE- 247 667 (INDIA)
FEBRUARY, 2015

INDIAN INSTITUTE OF TECHNOLOGY ROORKEE
ROORKEE

CANDIDATE'S DECLARATION

I hereby certify that the work which is being presented in the thesis entitled "**A STUDY OF MECHANICAL AND STRUCTURAL PROPERTIES OF APPLE AND POTATO"** in partial fulfilment of the requirements for the award of the Degree of Doctor of Philosophy and submitted in the Department of Mathematics of the Indian Institute of Technology Roorkee, Roorkee is an authentic record of my own work carried out during a period from December, 2009 to February, 2015 under the supervision of Dr. V.K. Katiyar, Professor, Department of Mathematics, Indian Institute of Technology Roorkee, Roorkee, UK, India and Dr. B.P. Singh, Director, Central Potato Research Institute (CPRI) Shimla, HP, India.

The matter presented in this thesis has not been submitted by me for the award of any other degree of this or any other Institute.

(FATEH SINGH)

This is to certify that the above statement made by the candidate is correct to the best of our knowledge.

(B. P. Singh)
Supervisor

(V. K. Katiyar)
Supervisor

Date: February , 2015

Abstract

Among various fruits and vegetables, apple and potato are the most widely used products for consumption. Consumers select the food products which retain a natural texture, color and freshness. The overall quality and freshness of apple and potato depend on their mechanical properties (cell-wall tension, cell-wall stiffness, stretch ratios, turgor pressure, tissue strength etc.) and structural properties (moisture content, shrinkage, porosity, density, surface area etc.).

From harvesting to consumption of apple and potato, mechanical and structural properties of these products are affected badly at several stages. Due to the application of external mechanical forces during post-harvest handling, several types of damage occur in these products. Mechanical damage is one of the major causes for the degradation of the quality of these products. On the other hand, during storage, drying and processing, water removal from apple and potato leads to change their structural properties. The first step in reduction of damage in apple and potato is the understanding of cell-wall mechanical properties. The mechanical properties of cell-wall can be calculated by developing constitutive relations/-mathematical models for cell-wall material during deformation.

The dehydration process is frequently used to extend shelf-life of foods by increasing their stability during storage [95]. Previous research indicates that the water removal, from apple and potato during dehydration, caused the contraction in the cell material which results the formation of pores [11]. As drying process proceeds, moisture content in apple and potato decreases, consequently internal pressure in these products generated on pore surface. This pressure is responsible for change in porosity. Basically, the dependence of porosity on moisture content variation has been discussed in literature [81, 184]. The effect of initial

porosity and the stress, originated in cellular structure during water removal, have not been studied yet. Therefore, a suitable model is required to describe porosity variation with respect to pressure generated on the cell surface.

It is evident from previous studies [82, 83, 184] that the mathematical models, developed by several researchers to predict structural properties of various food products, are the function of moisture content only. During dehydration, the effect of drying time on the structural properties has not been considered so far. For industries point of view, variation in structural properties with respect to time is important for allocation and optimization of resources. Therefore, more work is required for the development of mathematical models, so that, the moisture content variation and structural properties can be studied as function of drying time.

Outline of the thesis

The present thesis is compiled in 6 chapters, and the chapter wise description is given below.

Chapter 1 is an introductory and contains some basic definitions related to thesis. It gives brief description of mechanical and structural properties, mathematical modeling and work done by various authors for apple and potato.

In **Chapter 2**, we have proposed a strain energy function to study the mechanical properties (cell-wall tension and stretch ratios) of apple and potato by considering tissues as a lattice of hexagonal cellular structure under an external load. It has been considered that the tissues are isotropic, incompressible, homogeneous, thin, and shows hyperelastic behavior. The aptness of the proposed model is explored in the light of numerous experimental data [50, 87] of apple and potato tissues in isotropic condition. A Levenberg-Marquardt algorithm is used to estimate material constants of the model, which is based on the regression between predicted results and experimental data. A good fit of the proposed model is obtained with available experimental data. Comparisons are made between our results and previous studies. It is noticed that our results are better in respect of coefficient of determination (R^2) and standard deviation (SD) than the previous results. It can be concluded that our model can describe those mechanical properties of apple and potato tissues for which different model

were proposed earlier.

In **Chapter 3**, a generalized form of the strain energy function, which has been developed in Chapter 2, is proposed. Turgor pressure plays an important role in stiffness of apple and potato cells and hence freshness of the whole product. To determine the quality of these food products, it is important to understand the effect of turgor pressure in the cells. The effects of turgor pressure can also be analyzed by using constitutive relations between turgor pressure and stretches in cell-wall material. Therefore, in this chapter, we have developed a relation between turgor pressure and stretch ratio by using strain energy function developed in Chapter 2. The developed relation is validated with the help of experimental data taken from literature [87]. A Levenberg-Marquardt algorithm is employed for regression analysis to calibrate the model constants by correlating predicted and experimental values of turgor pressure and stretch ratio for apple and potato tissues. A good fit of the developed relation to experimental data is obtained with the coefficients of determination of 98.02% for apple and 98.0% for potato.

In **Chapter 4**, variation of porosity in apple and potato is discussed during dehydration. Porosity (volume fraction of pores) is one of the key parameter that affects the quality and other properties of foods (such as apple and potato). Therefore, to examine the porosity variation during dehydration in apple and potato, an arbitrary small cubic volume element is considered which contains pores (intracellular spaces) distributed in it. Further, it is assumed that each pore in the cubic volume element is spherical. A mathematical relation is developed between porosity and pressure generated (due to contraction of cells during water removal) in outward direction on the surface of spherical elements containing pore. The developed relation is tested with the help of experimental data [81, 83] for several drying methods for apple and potato and found satisfactory in respect of experimental observations. For the given pressure range, acquired porosity range is 0.1 to 0.92 for apple and 0.03 to 0.89 for potato which is matched with the existing experimental values.

In **Chapter 5**, drying behavior and structural properties of apple and potato are investigated as a function of drying time. It is well known that mathematical modeling is a frequently used tool to study the drying kinetics of various fruits and vegetables. Therefore, in

this chapter we have proposed a thin-layer drying (mathematical) model for investigating the drying characteristics of apple and potato. For validation of the proposed model, we have conducted experiments for one apple variety, namely, Fuji and three potato varieties, namely, Kufri Chipsona-1, Kufri Himsona and Kufri Bahar at temperature 60, 70 and 80^oC. A non-linear regression procedure is employed to fit the drying model to the experimental data. The model is compared with several existing thin-layer drying models according to chi-square (χ^2), coefficient of determination (R^2) and root mean square error (RMSE). Results based on our model has close resemblance with experimental observations and are better in comparison of other models cited in literature. The effect of temperature on drying characteristics of apple and potato is determined. It is observed that the moisture content in all the samples decreases exponentially as the drying process progresses. On the successful validation of the drying model by experimental observations, drying model is used to calculate structural properties in terms of drying time. Our model is able to describe these properties suitably.

Finally, **Chapter 6** presents the summary and concluding remarks of this thesis and the possible directions of the future scope.

Acknowledgments

It is a pleasure to convey my gratitude to few of the many sources of inspiration for me and to all the people who have helped in successful realization of this Thesis.

First and foremost I thank the incessant source of divine blessings, the almighty God, who always motivates me to move forward with his omens and love.

I express my deep sense of gratitude to my supervisors Dr. V.K. Katiyar, Professor, Department of Mathematics, Indian Institute of Technology Roorkee, UK, India and Dr. B.P. Singh, Director, Central Potato Research Institute Shimla, HP, India. I feel privileged to express my sincere regards to my guides for their valuable guidance, support and constant encouragement throughout the course of my research work. Their truly scientific intuition and broad vision inspired and enriched my growth as a student and researcher. The critical comments, rendered by them during the discussions, are deeply acknowledged.

I express my regards to Prof. R.C. Mittal, Prof. Rama Bhargava, former Head of the Department, Prof. Kusum Deep, DRC Chairperson, Prof. P.N. Agrawal, Prof. T.R. Gulati and Prof. G.S. Srivastva, former DRC Chairperson, for their support. Special thanks to my SRC members: Prof. R.R. Bhargava and Prof. R. Prasad for spending their valuable time during the discussions over seminars. I am also thankful to Dr. Sandip Banerjee, Dr. P. Bera and Dr. Uaday Singh for their support and encouragement. I am indebted to the Department of Mathematics, IIT Roorkee, to all its faculty members and staff for their academic support and encouragement. I am really thankful to Dr. R.P. Pandey, Scientist - F, NIH Roorkee for his constant support and inspiration.

I wish to express my thanks to PHT Laboratory, Central Potato Research Institute (CPRI) Shimla, HP, India for providing facility to conduct experiments. It is my pleasure to express

my gratitude to Dr. Brajesh Singh, Principal Scientist & Head, and staff members, specially, Sh. Vinod Kumar, Technical officer, Division of CPB & PHT, CPRI Shimla, India for their valuable suggestions and constant support during experimental work.

I am thankful to my lab seniors Dr. Sushil Kumar, Dr. Kamini Rawat, Dr. Anju Saini, Mr. Devdatta, Dr. Kranti Kumar, Dr. Demeke Fisseha and lab colleagues Dr. Virendra Kumar, Mr. K. Venkateshwarlu, Mrs. Shashi Sharma, Mr. Ajay Kumar and Mrs. Bharti Sharma for providing their cooperation, support, healthy and progressive research environment. I am also thankful to CFD Lab members Dr. Ashok Kumar, Dr. Manish Khandelwal, Mr. Abhishek and Ms. Moumita for their cooperation.

I consider myself truly blessed as I have always been in a good company of friends. Their love, inspiration, support and cooperation is beyond the scope of my acknowledgement, yet I would like to express my heartfelt gratitude to my friends Dr. Sanoj Saini, Dr. Sandeep Mogha, Dr. Surendra Kumar, Dr. Manish Garg, Mr. Vikas Tayagi, Mr. Sumit Malik, and those, who helped me directly and indirectly. I would like to say special thanks to Mr. Amit Sharma for his incentive, valuable suggestions, cooperation, and support not only mentally but also financially at every stage during my Ph.D. work.

I feel a deep sense of gratitude for my father Late Sumer Singh and mother Smt. Bugri, who raised me with their unconditional love, inculcated in me the values that really matter in life, formed part of my vision and taught me to always believe in myself; and my elder brothers Sh. Balmukund Saini, Sh. Vedprakash Saini and other family members, who worked hard in fields and made every possible effort so that I can get good education despite so many odds. Without their support, it is not possible to achieve this goal. Thanks to my elder sisters Smt. Bala Saini, Smt. Ratikor Saini and Smt. Kusum Saini for their unconditional love. Finally, I would like to thank my beloved wife, Mrs. Ravita Saini for her constant support, enormous patience and unwavering love in my frustrations and long working days.

I gratefully acknowledge the CSIR, New Delhi, India for providing financial assistance during my Ph.D. work in the form of JRF and SRF.

Roorkee (Fateh Singh)

February , 2015

Table of Contents

List of Tables

List of Figures

List of Publications

1. **Fateh Singh**, V.K. Katiyar and B.P. Singh. (2013). A new strain energy function to characterize apple and potato tissues. *Journal of Food Engineering*, 118 (2), 178-187. **Elsevier, IF-2.576**.

2. **Fateh Singh**, V.K. Katiyar and B.P. Singh. (2014). Analytical study of turgor pressure in apple and potato tissues. *Postharvest Biology and Technology*, 89, 44-48. **Elsevier, IF-2.628**.

3. **Fateh Singh**, V.K. Katiyar and B.P. Singh. (2014). Mathematical modeling to study influence of porosity on apple and potato during dehydration. *Journal of Food Science and Technology*. DOI 10.1007/s13197-014-1647-5. **Springer, IF-2.024**.

4. **Fateh Singh**, V.K. Katiyar and B.P. Singh. (2014). Modeling of time dependent variation of moisture content, density, porosity and specific volume during drying of apple and potato. **Submitted to Journal**.

Chapter 1

Introduction

1.1 Fruits and Vegetables

Foods are the primordial unit for survival of all living organisms and have a scrumptious world in itself. These can be demonstrated as those materials which are consumed by animals or humans for health, growth, blissfulness, contentment and satisfying social needs. These materials can be in the form of raw, processed or formulated products. Food products can be categorized as fresh, harvested, processed, minimally processed, perishable, nonperishable, manufactured, preserved, functional, synthetic, primary, secondary derivatives and medical foods [127].

In the view of fruits and vegetables, the whole world is aware of the importance of these foods. Due to the invaluable importance of these foods, there is a great need to prevent the deteriorations which can be occurred due to improper management of postharvest factors, such as handling, packaging, transportation and processing. These factors are responsible for 20-30% spoilage of the total production of fruits and vegetables [84]. Now-a-days, consumers are increasing their demand for products with higher quality and freshness. They select those fruits and vegetables, which retain a natural texture, flavor, color, and preserve nutritional values. Therefore, it is a matter of attention for food processors and producers to fulfill the requirements of fresh and quality fruits and vegetables for consumers [152]. Usually, consumers check the quality of fruits and vegetables by its external appearance.

On the other hand, the internal quality of food products is checked during the consumption. Consumers prefer quality foods as well as damage free products. The quality of foods can be defined according to their use in different purposes. Nutritionists considered the quality of foods by its nutritional values, for microbiologists quality refers to safety of foods, while for chemists food items stability is important [20].

Preservation of fruits and vegetables is required to use these products for long time. Preservation methods start with the complete analysis and understanding of the whole food chain including growing, harvesting, packaging, processing, storing and distribution. The degradation of food quality is dependent on types of formulation, composition, storage and packaging of foods [156]. The loss in food quality can be reduced at any stage of food harvesting, processing, distribution and storage.

1.1.1 Apple and Potato

Apple [152] and potato [142] have momentous significance among the various fruits and vegetables due to their invaluable ingredients. Due to high enrichment, consumers have special attention towards these food products (unless otherwise stated, 'food products' refers to apple and potato throughout the thesis). Both of these have major components in the human diet, which are necessary for human being in daily life.

Due to the high nutritional values, apple may be considered as one of the best foods in the human diet. Antioxidants in apple have several health promoting and disease prevention properties, and thereby, truly justifying the adage, "An apple a day keeps the doctor away." An apple fruit anatomy is presented in Fig. (1.1)

Potato (Solanum tuberosum L.) popularly known as 'The king of vegetables'. It has emerged as fourth most important food crop in India after rice, wheat and maize. The dry matter, edible energy and edible protein content of potato makes it nutritionally superior vegetable as well as staple food not only in India but also throughout the world [142]. Now it becomes as an essential part of breakfast, lunch and dinner worldwide. A potato tuber anatomy is presented in Fig. (1.2) and terms related to figure are defined as follows:

- **Sprouting Bud:** Sprouting buds are the potato eyes, from which new potato plants

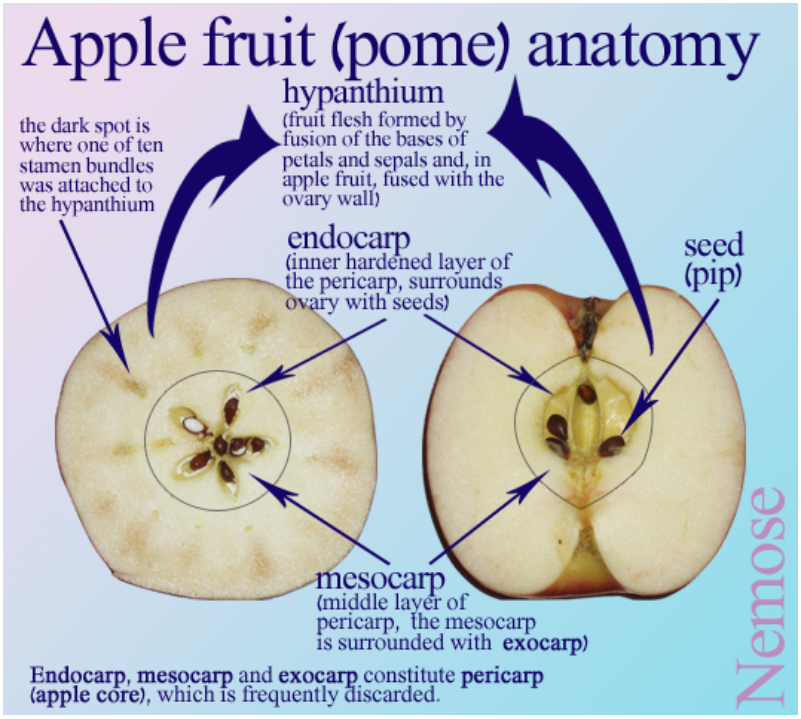

Figure 1.1: Apple fruit anatomy
(Source: http://www.geochembio.com/biology/organisms/apple/)

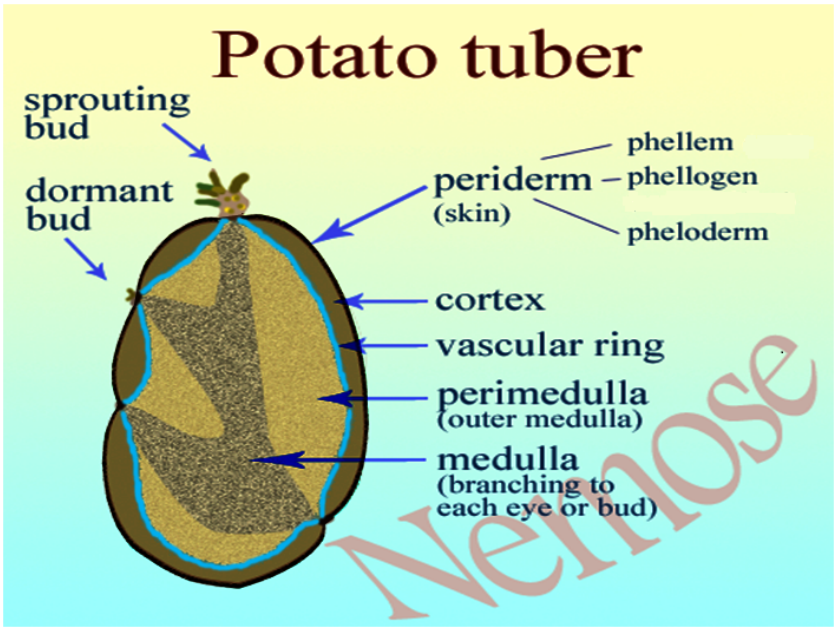

Figure 1.2: Potato tuber anatomy
(Source: http://www.geochembio.com/biology/organisms/potato/)

growth emerge.

- **Periderm (skin):** Tuber skin is composed by two layers of cells: an outer layer of cells called the epidermis, underlain by several layers of corky cells called the periderm.
- **Medulla:** Medulla represents the primary storage area for the potato tuber.
- **Vascular ring:** Vascular ring contains cells that transport nutrients from the above ground stems to the medulla.
- **Cortex:** Tissues between skin and a vascular ring are known as cortex.
- **Perimedulla (outer medulla):** It is located between the vascular ring and medulla.

1.1.2 Cell and Tissue

The cell is the basic structural, functional, and biological unit of all known living organisms. A tissue is a collection of likeminded cells and extracellular matrices that consists of fibers (for example, elastin and the proteins collagen). To respond mechanical loadings, cells in the tissues maintain and organize the structure of tissue by developing a large amount of tissue constituents and adjusting the tissue structure. A frequently change in the structure of tissues can be observed due to response and growth of mechanical environment. The mechanical environment of tissues means the mechanical loading applied on the tissues in some particular time [34].

The edible part of apple and potato mainly consist of parenchyma cells. Pitt [119] reported that the parenchyma cell is composed of a cell-wall surrounding the cytoplasm, nucleus and a vacuole which contains over 90% of the cell's liquid. These cells are bonded together by a pectin layer, called the middle lamella, which is responsible for cohesion between the cell-walls. The volume outside the cell, that does not include the middle lamella, consists of interstitial air spaces and the extracellular fluid. Cell-walls are composed of middle lamella components, cellulose microfibril, xyloglucans and pectin. In parenchyma cells, the cell-wall is a primary one with no secondary deposition of additional layers; hence, the cell-wall is relatively thin and elastic, and contains less than 10% cellulose volume [46].

The cell-wall is the stiffest component of the cellular conglomerate, and thus, the mechanical properties of the cell-walls are extremely important in determining the mechanical properties of the cellular conglomerate (tissue).

The factors such as cell size, cell-wall thickness, cell adhesion, cell shape and cell organization characterize the cellular structure of fruits and vegetables. The rigidity of cells is affected by the elasticity of cell-walls, osmotic potential of the cell contents and turgor pressure. However, some biological cells and molecules (especially Red Blood Cells) are generally considered as diamagnetic material [58]. The mode of failure under an applied load will also depend on the structure of the raw material.

The structure of tissue in apple and potato is very complex. Every component in the structure exerts a determinate effect on the mechanical properties of the tissue. Cellular liquid can fall in the category of these components. When an external load is applied to apple or potato, tissue in the product is compressed, and each cell in the tissue subjected to equal load. According to Nilsson et al. [107] and Haman et al. [60], following processes are the consequence of compression/laoding: (i) cell shape changes; (ii) the increase in the ratio between cell-wall surface and volume resulting in the increase of cell-wall tension; (iii) increase in the turgor pressure; and (iv) intracellular liquids flow out of the cell. The strength of tissues basically depends on the cell-walls [121]. Due to the applied higher load on food products, a continuous deformation in the cell results in increase of tensile stresses in the cell-walls which cause cell-wall cracking and hence failure of the tissue.

1.2 Damages in Apple and Potato

The overall quality and recency of apple and potato depend on their mechanical properties (cell-wall tension, stiffness, turgor pressure, rupture, tissue strength, force-deformation relation, stretch ratio etc.) and structural properties (moisture content, shrinkage, porosity, density, specific volume, surface area etc.) (definitions are given in section 1.3). Mechanical properties are related to the harvesting and postharvest handling (packaging, transportation

and storage) process, while structural properties are related to storage, processing and dehydration process.

Overall handling process of apple and potato, from harvesting to consumption, is a long chain. During this process at several stages, mechanical and structural properties of these products are affected badly. During the process of postharvest handling, apple and potato are subjected to external loads/forces. There are various types of external loads, which are subjected to these products during postharvest handling. High speed, impact loads, long term loads, static loads and small-repeated loads are included in this category [120]. Due to the application of external mechanical forces, several types of damages can be occurred in apple and potato. Mechanical damage is one of the major causes for degradation of the quality of these products. Another physical changes, that can be seen in vegetables, are the loss of water and loss of turgidity, which can be controlled by selecting the appropriate packaging [10].

1.2.1 Mechanical Damage

Various types of damages can take place in apple and potato during harvesting, packaging, transportation and storage. These damages occur due to compression and impact of products. Visual characteristics, such as appearance and shape of apple and potato, are first criterion for consumers to choose disorder and defect free products. The external quality/appearance such as shape, size and color of food products play an important role in selecting the high quality products.

According to Mohsenin [103], mechanical damage in food products is defined as the spoilage of products when they are subjected to excessive deformation during impact. The spoilage of apple and potato is generally consequence of external or internal forces applied under dynamic or static conditions. Internal forces are responsible for physical changes, whereas external forces results mechanical injuries in these products. The injury or damage in these products reduces the income of farmers as well as reduces the quality of processed products obtained from them. Hence, during harvesting and packaging of these products, the prevention of mechanical damages can ameliorate the quality and recency of processed

food products and in turns to farmers' income. During harvesting and packing operations, mechanical damages can be reduced in apple and potato products by identifying the components which cause bruising.

1.2.2 Types of Mechanical Damage

In apple and potato, damage can be generally divided into two categories, external damage and internal damage. These are defined by Chiputula [31] as follows:

1.2.2.1 External Damage

External damages are shown in Fig. (1.3).

- **Shatter Bruise:** Shatter bruise causes the cracking or splitting of the products during mechanical impact. The splitting may be inside or on the surface of the product.
- **Skinning:** Skinning (abrasion) is an injury, in which areas of the product are rubbed off, giving the product a feathered appearance or scuffed.
- **Pressure Bruise:** Pressure bruise is the depression or flattening of the product surface formed as a result of external pressure at a point of contact with another product and storage structure or equipment.
- **Cut:** Cut is a division or penetration by a sharp edge of an object.

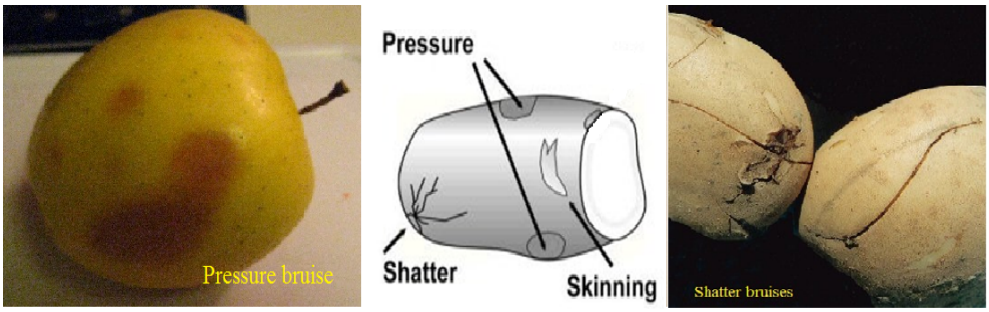

Figure 1.3: External damage in apple and potato

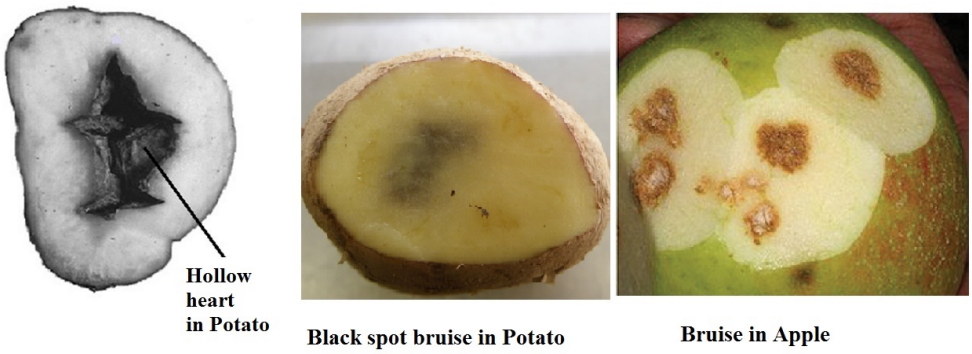

Figure 1.4: Internal damage in apple and potato

1.2.2.2 Internal Damage

Internal damages are shown in Fig. (1.4).

- **Hollow Heart:** Hollow heart is an internal noninfectious physiological disorder of the potato tuber. It appears due to cell damage in response to stresses in the pith of the tuber that occurred early in the tuber's development.

- **Black Spot Bruise:** Black spot is an internal discoloration resulting from impact, that damages cells in the tissue beneath the periderm.

1.2.3 Causes of Mechanical Damage

At microscopic level, the mechanical damage (or loss of freshness and quality) is the consequence of failure (breakage) of cells/tissues in apple and potato. According to the hypothesis of Pitt [119] and Pitt and Chen [121], the failure of cells may be the consequence of three mechanism: intercellular debonding, cell-wall rupture and cell relaxation from the migration of fluid out of the cells. These three mechanism are the main reasons for initiation of failure of soft tissue, and hence damage of the whole product. These mechanism take place due to either internal forces or external forces under dynamic or static conditions. These forces can be the result of uncontrolled temperature, and physical changes such as biological, chemical and variation in moisture content [31].

At macroscopic level, Pang [116] reported the following three main sources of mechanical damage in apple and potato, i.e. compression damage, vibration damage and impact damage (bruising).

- **Compression Damage:** This type of damage occurs in these products mainly due to applied excessive external pressure on upper product to lower product and compression of the products against containers.

- **Vibration Damage:** This type of damage results in these products due to prolonged and repeated vibration during handling and transport operations.

- **Impact Damage:** It can be occurred at any stage of product handling system from harvesting through to the consumers. This type of damage occurs due to free falling of products against a hard surface, on another products, on the parts of any grading and treatment machinery and due to mechanically applied force on these products.

Severity of damage to the product is primarily related to: (i) number of impacts; (ii) height of fall; (iii) type of impact surface and size; and (iv) physical properties of the products related or not to maturity [7]. The apple industry is particularly concerned about fruit damage during handling and transport operations.

During postharvest handling, deformation occurs in apple and potato due to excessive pressure. This deformation is responsible for cell-wall fracture, that leads to internal crash (no skin breakage), shatter, cracking and splitting (skin breakage). Cell membrane damage is the consequence of deformation that leads to black spot bruise [31]. The major reason for mechanical damage or deformation in apple and potato is the impact and shock during mechanical handling.

1.2.4 Damage Control

To reduce the damage in apple and potato, it is necessary to understand the mechanical properties of their soft tissues first. An important step in the control of damage and improvement of food quality is the development of methods for prediction and quantification of damage

in food products. To prevent the mechanical damage of food products, it is necessary first to identify the damages or bruises in these products as soon as possible. It is important to determine causes and nature of the damage before a beginning can be made towards reducing such losses. The understanding of mechanism behind the food bruising and development of suitable techniques for the rapid assessment of bruise damage is an crucial issue for packers and growers to improve the food quality. Special attention should be kept when time is short for harvesting and packaging. Food products quality is normally influenced by bruise depth, number of bruises and the bruise size.

Then et al. [167] mentioned that the study of mechanical properties of biological tissues is growing rapidly by applying computational tissue modeling in various fields of biomechanics. The first step in reduction of damage in apple and potato (in general, fruits and vegetables) is the understanding of mechanical failure in these products during handling, transportation and distribution. The better way to explore the mechanical failure is the study of cell-wall mechanical properties, which can be calculated by developing the constitutive relations for cell-wall material during deformation. The mechanics analysis can also be used to study the relationship between whole tissue properties and individual cell properties. The study of mechanical properties, such as stress-strain relation, stiffness, turgor pressure, failure characteristics, strength of cell-wall and gross mechanical properties of tissue, is essential. It is very difficult to relate the stress in the cell-wall to applied stress or strain. Therefore, development of some mathematical formulations/models are required to understand the elastic properties of cell-wall.

1.3 Structural Properties

Density, shrinkage, porosity, pore size distribution and specific volume are the invaluable structural properties that characterize the structure of food materials. However, porosity and density are the most common structural properties reported in the literature [81, 176]. Specially, porosity is a crucial structural property due to controlling the speed of re-wetting, reconstitution, appearance and taste of the dried products [83]. These structural properties

depend on several components, for example, moisture content, pretreatment, process conditions and processing methods. The demand of shelf-stable high-quality dried fruits and vegetables is increasing day by day. During dehydration process, external and internal changes occur in food products due to water removal . The internal changes in these products are responsible for apparent changes of the products (for example, textural changes, deformation and shrinkage). These internal changes can be noticed by using various imaging techniques. The structural properties as a function of moisture content can be estimated by developing suitable mathematical models. Structural properties, which are used in drying technology [130, 145, 184], are defined as follows:

Assumptions: Before defining these properties, following assumptions are considered:

- Food materials are composed of water, dry solids and air phases.

- Volumes of water, dry solids and air phases, that compose the porous system (e.g., food products), are additive, i.e.

$$V = V_w + V_s + V_a\,, \tag{1.1}$$

where V, V_w, V_s and V_a (m^3) are the total volume and volumes of water, dry solids and air pores, respectively.

- Mass of air phase is negligible with respect to mass of water and dry solids, i.e.

$$m = m_w + m_s, \tag{1.2}$$

where m, m_w, and m_s (kg) are the total mass and the masses of water and dry solids, respectively.

Now, the following definitions (Table 1.1) can be considered:

Table 1.1: Definitions of structural properties.

Property	**Definition**	**Expression**
Moisture Content (X) (kg water / kg solid)	The material moisture content on a dry basis can be defined as the amount of water per unit mass of dry solids in the sample.	$X = m_w/m_s$
Density (ρ) (kg/m^3)	Density is defined as mass per unit volume. For the characterization and process calculation of food products, different forms of density can be used as follows:	$\rho = m/V$
(i) Solid density (ρ_s)	Solid density is the density of the solid material (including water), excluding any interior pores that are filled with air.	$\rho_s = m_s/V_s$
	The density of enclosed water (ρ_w)	$\rho_w = m_w/V_w$
(ii) Particle density (ρ_p)	Particle density is the density of a particle, which includes the volume of all closed pores but not the externally connected pores.	$\rho_p = m/V_p$, $V_p = V_s + V_w$
(iii) Apparent density (ρ_a)	Apparent density is the density of a substance including all pores remaining in the material.	$\rho_a = m/V$
Porosity (ε)	Porosity is defined as the volume fraction of the air or the void fraction in the sample.	$\varepsilon = V_a/V$
Shrinkage (S)	Shrinkage is the decrease in volume of the food during processing such as drying. It is defined as the ratio of the volume at a given moisture content to the initial volume (V_0) of materials before processing.	$S = V/V_0$
Specific Volume (v) (m^3/kg, dry basis)	The specific volume of the sample is defined as the total volume per unit mass of dry solids.	$v = V/m_s$

1.4 Basic Definitions

1.4.1 Mechanical Properties

The properties of a material that reveal its elastic and inelastic behavior when force is applied, thereby indicating its suitability for mechanical applications; for example, modulus of elasticity, tensile strength, elongation, hardness and fatigue limit etc.

1.4.2 Strain Energy

Strain energy is the energy stored by a system undergoing deformation. When the load is removed, strain energy is released gradually as the system returns to its original shape.

1.4.3 Hyperelasticity

Hyperelasticity refers to those materials which can experience large elastic deformation on applying the force and that is return to original shape after removal of the force without dissipation of any energy in the process.

1.4.4 Turgor Pressure

The cell-wall is an indispensable component of cells which is semipermeable to water and certain solutes; it is also able to hold water under pressure by having a high internal concentration of solutes. The high concentration of solutes inside the cell dilute the internal water as compared to that outside. By osmosis, water can move into the cell through the semipermeable membrane. The diffusion of water inside the cell reduces its concentration gradient [137]. The solutes cannot cross the membrane and remain inside the cell. Further, as water enters into the cell, the cell starts to swell and a pressure is generated on the cell-wall. This pressure is known as turgor pressure [177]. In other words, turgor is a force exerted outward on a cell-wall by the fluid contained in the cell. This force gives the cell-wall rigidity, and may help to keep it firm. The turgidity of a cell is shown in Fig. (1.5)

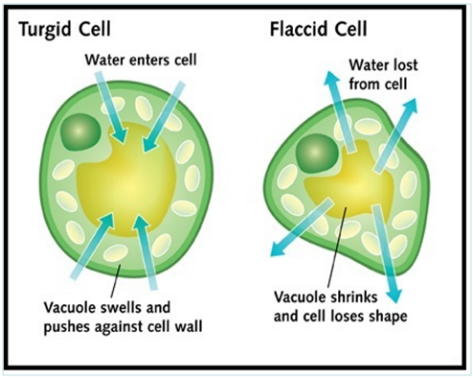

Figure 1.5: Turgor pressure

1.5 Mathematical Modeling

Mathematical modeling is the best tool for optimizing and characterizing innovative food processing technologies and the analysis of mechanical and physical problems of biological structures. By using mathematical modeling, real world (biological) problems can be translated into mathematical models and solution of these problems again can be interpreted in the language of real world [118]. The numbers of experiments, which need to be conducted to determine the influence of parameters, can be minimized by mathematical modeling. For the successful mathematical modeling of living tissues, relationships between cellular deformation and tissue deformation need to be investigated. Shahari [147] suggested that the mathematical modeling approach is an approach that is complementary to existing laboratory experiments. At present, the concept of mathematics and biology are widely used together to deal with a multiscale problems, e.g., detection of cancer [117] and growth of tumor [75].

Two types of mathematical models, namely, observation based and physics based, are used to formulate the real world problems in to mathematical forms [39]. The starting point of observation based model formulation is the measurement of experimental data. These types of models are generally empirical in nature. On the contrary, the physics based models are formulated by using universal physical laws which explain the presumed physical facts. After the formulation of the physics based model, experiments need to be performed to validate the model. Preference is given to use of observation based models when the mechanism of model formulation is not well defined. However, observation based models do not provide much insight of the formulation. On the other hand, physics based models are generally preferred for predictive models in those areas which are not related to foods, for example, aeronautics [40].

The second most important thing needs to be focussed during model formulation is the number of parameters in the model. A model generally fit well to experimental data if the number of parameters in the model increases, but the uncertainty in the parameters estimation also increases, which is undesirable. Therefore, attention should be given during model formulation in such a way that the number of parameters in a model are less and the model still gives an acceptable fit.

1.5.1 Strain Energy Function

When an externally applied force causes a material to deform, energy must be introduced into the system. This energy is called strain energy. Strain energy is an important mechanical parameter for elastic solids; because it can be converted into mechanical energy to elastically restore an object to its original shape and orientation when an external force is removed. In other words, strain energy is the energy stored within a material as it is loaded.

The existence of strain energy, which allows the strained continuum to regain its initial state after the removal of the load, is the defining property of an elastic continuum. The mathematical expression of this physical entity is defined as a strain energy function [161]. During the impact on the food products, work is done by the normal contact force which caused compression in the products. During compression, normal contact force deforms the product and raises the internal energy. When the contact force/load is removed, the absorbed energy during compression is recovered and this part of energy is known as elastic strain energy [31].

The susceptibility of food products to mechanical damage depends on the mechanical properties of food materials. Traditionally, in most of the techniques for evaluation of food mechanical properties, it is assumed that the food behaves as a continuum material in which the mechanical properties essentially do not depend on the spatial scale. However, foods consist of different tissues, which in their turn form a complex conglomerate of cells [6]. It is apparent from literature [49–52] that the tissues of apple and potato can be assumed as hyperelastic material and hence strain energy function can be used to analyze and understand the mechanical properties of these two foods.

1.5.2 Constitutive Equations

Materials for which the constitutive behavior is only a function of current state of deformation are known as elastic. The objective of the constitutive theories is to develop mathematical models for representing the real behavior of materials to determine material response. A constitutive equation describes a physical property of a material under specific conditions of

interest. Nonlinear constitutive theory is suitable for hyperelastic materials, which can undergo large reversible deformations. Since, the physical phenomena representation should be the observer independent, therefore in model formulation, physical quantities are expressed in such a way that they are independent of coordinate systems. Hence, a constitutive equation must be a tensor equation. Every term in the equation must be a tensor of the same rank. It can be used to describe the mechanical behavior of any continuum, as an example, the generalized constitutive equation has been used to study the effects of secondary flow on the rate of deformation tensors, pressure and velocity components [25]. In the continuum mechanics theory, the material behavior of solids and fluids can be described by a set of field equations [155].

1.5.3 Stress, Strain and Deformation

Mathematical models play the vital role to predict the stress and to gain further insight of important aspects in biological materials when experimental measurement of stress is difficult [9]. Change in the material body is termed as deformation, under applied certain external forces. The deformation in the body can be produced by the application of normal and/or tangential components of force.

For the study of finite deformation of membrane or cell-wall, the deformation should be described in terms of 'stretch ratios' (ratios of final lengths to initial lengths) at the place of strains, because a stretch ratio depends only on the state of strain and not on the choice of reference axis [18]. The deformation of the body can be described mathematically by labeling the particles of the body under some specific method and the position of each material particle can be specified before and after the deformation. The region occupied by the material particles at any time before deformation is termed as reference configuration and after deformation it is called deformed/current configuration. Suppose that a material particle X, whose rectangular Cartesian coordinates are (X_1, X_2, X_3), occupies the position $\mathbf{X}$ before deformation. After the application of load, the geometric shape of the body changes and assumes a new configuration called deformed configuration. Now, let the particle X occupies the new position $\mathbf{x}$ in the deformed configuration. The deformation of the body may be described by

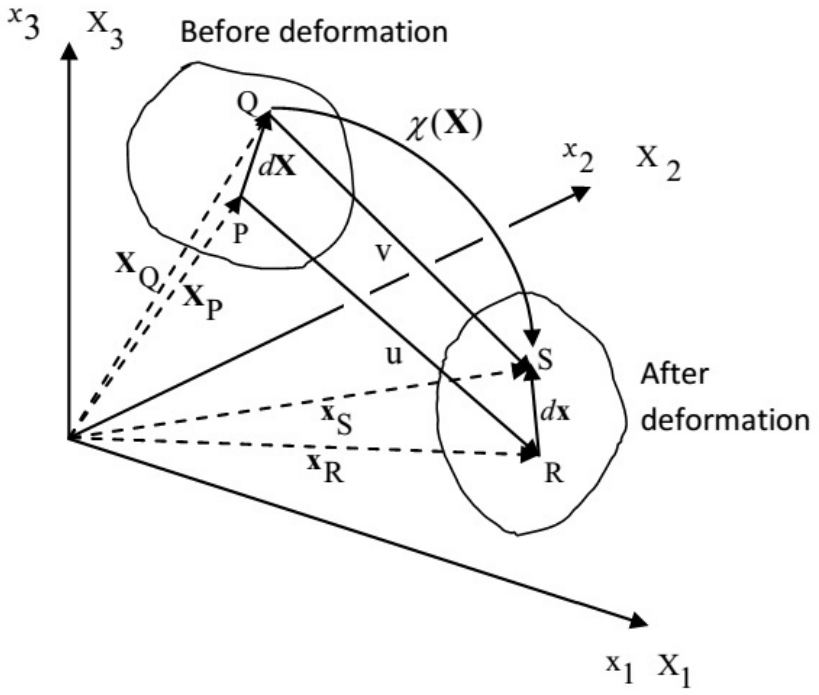

Figure 1.6: In the undeformed configuration, points P and Q, separated by $d\mathbf{X}$, takes the position R and S, respectively, in the deformed configuration where they are separated by $d\mathbf{x}$.

a map $\chi(\mathbf{X})$, called deformation map, which takes the position vector $\mathbf{X}$ from reference configuration and places the same point in the deformed configuration as $\mathbf{x} = \chi(\mathbf{X})$. Under the applied load on the body, the material element $d\mathbf{X}$ in reference configuration is transformed into a material element $d\mathbf{x}$ in the deformed configuration (Fig. 1.6). The tensor which gives the relationship between $d\mathbf{X}$ and $d\mathbf{x}$ is defined as deformation gradient, and given as

$$d\mathbf{x} = \mathbf{F} \cdot d\mathbf{X} = d\mathbf{X} \cdot \mathbf{F}^T \qquad \text{or} \qquad \mathbf{F} = \left(\frac{\partial \mathbf{x}}{\partial \mathbf{X}} \right)^T . \tag{1.3}$$

More explicitly, we have

$$\mathbf{F} = \begin{bmatrix} \frac{\partial x_1}{\partial X_1} & \frac{\partial x_1}{\partial X_2} & \frac{\partial x_1}{\partial X_3} \\ \frac{\partial x_2}{\partial X_1} & \frac{\partial x_2}{\partial X_2} & \frac{\partial x_2}{\partial X_3} \\ \frac{\partial x_3}{\partial X_1} & \frac{\partial x_3}{\partial X_2} & \frac{\partial x_3}{\partial X_3} \end{bmatrix} . \tag{1.4}$$

According to the polar decomposition theorem, the deformation gradient tensor can be written as

$$\mathbf{F} = \mathbf{R} \cdot \mathbf{U} = \mathbf{V} \cdot \mathbf{R}, \tag{1.5}$$

where $\mathbf{U}$ and $\mathbf{V}$ are the positive-definite symmetric right and left stretching tensor, respectively and $\mathbf{R}$ is the orthogonal rotation tensor. Two more measures of the stretching of the deformation is introduced as the right and left Cauchy-Green deformation tensor and defined by

$$\mathbf{C} = \mathbf{F}^T \cdot \mathbf{F} \qquad \text{and} \qquad \mathbf{B} = \mathbf{F} \cdot \mathbf{F}^T. \tag{1.6}$$

The tensors $\mathbf{B}$ and $\mathbf{C}$ are related to $\mathbf{V}$ and $\mathbf{U}$ by $\mathbf{B} = \mathbf{V}^2$ and $\mathbf{C} = \mathbf{U}^2$. Since $\mathbf{F}^T \cdot \mathbf{F}$ is real and symmetric, therefore, there exists an orthogonal matrix $\mathbf{A}$ that transforms $\mathbf{F}^T \cdot \mathbf{F}$ into a diagonal matrix, i.e.,

$$\mathbf{U}^2 = \mathbf{F}^T \cdot \mathbf{F} = \mathbf{C} = \mathbf{A} \begin{bmatrix} \lambda_1^2 & 0 & 0 \\ 0 & \lambda_2^2 & 0 \\ 0 & 0 & \lambda_3^2 \end{bmatrix} \mathbf{A}^T, \tag{1.7}$$

where λ_1, λ_2 and λ_3 are the eigenvalues of $\mathbf{U}$ (or $\mathbf{V}$) which are called principal stretches and the corresponding orthogonal eigenvectors are called the principal directions. Throughout the thesis as otherwise stated, we assume that the material under consideration is incompressible, which leads to the condition $det\ \mathbf{F} = 1$, where det means the determinant.

1.5.4 Levenberg-Marquardt Method

To solve the non-linear least squares problems, a standard technique Levenberg-Marquardt method is frequently employed. This curve-fitting method is a combination of the Gauss-Newton and gradient descent minimization method. The non-linear least square problems, generally, comes into the picture when a parameterized function, non-linear in parameters,

fitted to a set of measured data points by minimizing the sum of squares of the errors between the function and data points. Therefore, let a parameterized function $f(x,\mathbf{p})$ is fitted to a data set of n points (x_i, y_i). Then, the aim is to find the value of parameter $\mathbf{p}$ such that the sum of square of the errors between the measured data $y(x_i)$ and the fitting function $f(x_i,\mathbf{p})$ is minimum, i.e.,

$$S = \sum_{i=1}^{n} [y(x_i) - f(x_i,\mathbf{p})]^2 \tag{1.8}$$

is minimum. Since, the model function $f(x,\mathbf{p})$ is nonlinear in parameter $\mathbf{p}$, therefore, minimization of S with respect to $\mathbf{p}$ is carried out iteratively. The aim of every iteration is to calculate the perturbation $\mathbf{h}$ in the parameter $\mathbf{p}$ that reduces S. Therefore, according to the Levenberg-Marquardt method (if there is no error in measuring the data set)

$$[\mathbf{J}^T\mathbf{J} + \lambda\mathbf{I}]\mathbf{h}_{lm} = \mathbf{J}^T(\mathbf{y} - \mathbf{f}(\mathbf{p})), \tag{1.9}$$

where $\mathbf{J} = \frac{\partial \mathbf{f}(\mathbf{p})}{\partial \mathbf{p}}$ is the Jacobian matrix, $\mathbf{J}^T$ is the transpose of Jacobian matrix, $\mathbf{I}$ is the identity matrix, λ is the (non-negative) damping factor. For small value of λ, this technique reduces to Gauss-Newton method

$$[\mathbf{J}^T\mathbf{J}]\mathbf{h}_{gn} = \mathbf{J}^T(\mathbf{y} - \mathbf{f}(\mathbf{p})). \tag{1.10}$$

According to the Gauss-Newton method, sum of the squared errors is reduced by assuming the least squares function as locally quadratic, and finding the minimum of the quadratic. For large values of λ, this technique reduces to gradient descent method

$$\mathbf{h}_{gd} = \alpha\mathbf{J}^T(\mathbf{y} - \mathbf{f}(\mathbf{p})), \tag{1.11}$$

where the positive scalar α determines the length of the step in the steepest-descent direction. Further, in the gradient descent method, the sum of the squared errors is reduced by updating the parameters in the direction of the greatest reduction of the least squares objective.

The steepest-descent procedure is expected to converge for poor starting values but requires a lengthy solution time. On the other hand, the Gauss Newton method will converge rapidly for good starting estimates. Thus, in the Levenberg-Marquardt procedure, the initial values of λ are large and will decrease to zero as the optimum is approached.

1.6 Review of Literature

Study of texture of fruits and vegetables is important as it is used to fix the quality attributes of these products. Texture can be determined by the macroscopic mechanical properties of soft tissues, which is generally affected during harvesting, packaging, transportation and storage. The macroscopic mechanical properties of the tissue are, thus, determined by various microscopic cellular and histological features, such as cell size, intercellular space, turgor pressure, mechanical properties of the cell-wall and middle lamella. A micromechanical approach is therefore preferable to understand the relative importance of these features on the overall mechanical behaviour of foods [108].

A great amount of literature has been published on the mechanical properties of biological tissues and development of constitutive relation for plant materials [3], soft tissues [43] and arterial tissues [66]. The main focus has been given to study the relation between stress and strain in the tissues. Under low stress levels, soft biological tissues deform finitely. Therefore, the infinitesimal elasticity cannot be used to study the finitely deforming incompressible biological material [143]. To get rid of this problem, several researchers have used the same approach as has been adopted to develop constitutive law for rubber-like materials. Numerous strain energy functions for rubber-like materials [53, 59, 110], elastic and hyperelastic material [104, 136, 170], red blood cell membranes [160], axial plant growth [97] and porous hyperelastic materials [36] exists in the literature. Silber et al. [154] used a constitutive modeling method to describe the elastic properties of soft foams and demonstrated the applicability of strain energy function for finite hyperelasticity. Liepsch [86] discussed the importance of biofluid mechanics for future cell research in basic biology. Apart from above

studies, a concise list of strain energy functions for tissues is provided in Table (1.2). However, in this thesis we have restricted our attention to those strain energy functions which were developed to characterize mechanical properties of agricultural products.

A large body of literature (discussed in the present paragraph) has been published related to different types of properties of apple and potato. But a very few number of papers [49–52] are available which discussed mechanical properties of apple and potato tissues by using mathematical models. Bruce [18] reported that the mechanical properties of cell-wall can be delineated by using theory developed for continuum isotropic materials. Under a uniform load, Pitt [119] developed a mechanics model for the cellular structure and obtained the relationship between cell-wall stress, applied external stresses and cell turgidity. In addition, a probability model was developed to discuss the failure process in vegetative tissues. The effects of body accelerations on fluid flow [27] and pulsatile flow of fluid through a tube [26] have been studied, and the variation of wall shear stress in tube was obtained. The tissue stiffness and stress-strain failure properties of vegetative tissue were investigated by developing a mathematical model for the cellular structure under a uniform load [121]. Apart from these properties, physico-chemical composition of apple [157] and physic-chemical characteristics & chipping performance of potatoes [133] were investigated. In addition, Chopra and Singh [32] extended their studies for the extraction of pulp from apple fruits. A compression test was performed by Holt and Schoorl [64] on apple and potato and obtained the fracture properties of these products. When an external load, such as compression, is applied to apple and/or potato, the energy is stored elastically and recovered on the release of the load [64]. Elastic-plastic bending of shallow shells is presented by Mazumdar et al. [96]. Pitt [120] performed an experiment and developed a statistical model to determine the failure characteristic of potato tissues under cyclic loading. Mijovic and Liepsch [102] studied the fluid flow in an elastic Y-model experimentally and concluded that the model wall elasticity also influences the flow behavior. Walsh et al. [174] estimated the wall shear stress experimentally and validated the results with numerically predicted results. Hepworth and Bruce [62] measured the deformation of tissue and individual cells within tissues using light microscopy and image analysis during potato tissue compression. A relationship between deformation

of global tissue and cells was found. Sharma et al. [149] studied the temperature distribution in living biological tissues with different heating methods by means of mathematical modeling. Further, thermal and temperature dose response of tumor tissues were investigated by Sharma et al. [150] during hyperthermia treatment.

Gupta et al. [57] & Gupta and Sowokinos [56] studied the kinetic and physicochemical properties of those factors whose biochemical and molecular mechanisms involved in regulating the sweetening in potato tubers during cold storage. However, Brusewitz et al. [19] determined the effect of storage time and static preloading on cell-wall stress-strain relation, cell turgor pressure and tissue stiffness in potato. It was found that the cell turgor pressure decreases in starting of storage and latter it increases. The sugar content in potato is developed when the tubers exposed to temperatures below 10^oC in the cold storage [98].

It is worth mentioning that the mechanical properties of tissues depend on temperature and turgor pressure, and these parameters can change the fracture properties of tissues. Therefore, Zdunek et al. [182] applied mechanical test and used the acoustic emission method to analyze the change in fracture properties of potato tissues. Elnajjar et al. [44] studied the heat transfer characteristics of multi-walled carbon nanotubes. It was reported by Mernone and Mazumdar [100] that the mathematical model can help in a better way to understand the physiological characteristics of fluid flow being modeled. Lin and Pitt [87] performed experiments on apple and potato and discussed the effect of strain rate and turgor pressure on failure mode, failure stress, failure strain and tissue stiffness. It was noticed that with higher level of cell-wall stretch, the cell-wall stiffness in apple and potato parenchyma increases, which indicates the non-validity of Hook's law for cell-wall material. Further, the mode of tissue failure was dependent on cell turgor, for example, tissue under high turgor failed by cell-wall rupture, while tissue under low turgor failed by cell separation. Kilani et al. [74] studied the blood flow in a Screw-Type Blood Pump.

It is evident that turgor pressure is an important mechanical property of apple and potato cells. The effect of turgor pressure on other properties of foods and food quality has been investigated by several researchers as discussed below. The differences of mechanical properties of potatoes were examined during storage for one and ten months [146], and the loss of

water in the cells was compensated by adjusting turgor pressure. Bajema et al. [12] studied the tuber tissue behavior under natural turgor reduction through slight dehydration. Also, the failure properties of potato tuber tissue were investigated under axial compression by adjusting the turgor pressure using mannitol solution. Cellular structure and intracellular pressure play a significant role in determining the mechanical properties of apple and potato tissues. Potato tissue cracking is greatly influenced by cell size and turgor pressure. Oey et al. [109] investigated the influence of turgor pressure on micromechanical properties of apples tissue during cellular deformations and recorded ripening stage.

During the storage of apple and potato, water loss is responsible for decrease in turgor pressure which results the mechanical resistance reduction in tissues. These tissues are more prone to debonding of the cells, changes in cell shapes, cell-wall cracking and leakage of intercellular liquids through the cell-walls [77]. Water loss from apple and potato is the serious problem during storage. Rapid water loss, specially from potato, can take place at harvest and during first weeks of storage. Dehydration in tubers can be increased during transportation in open air vehicles and harvesting the tuber in low relative humidity. During the harvest and storage of the tuber, more moisture can be lost due to greater vapor pressure deficit. During the early storage season, higher storage temperature, higher transpiration and higher tuber respiration rate results the greater shrinkage loss [21].

It is evident that the requirement of drying of fruits and vegetables is due to the increasing demand of dry foods. The most important aim of drying is the reduction of moisture content to a required level for allowing safe storage, to prevent growth of mould, microbes, microbial and other harmful reactions [147]. In the food industry, drying of food is a crucial aspect of the production of various types of foods. This process is very challenging. However, using a mathematical modeling, a new dryer can be developed, the appearance of the product can be enhanced, flavor can be encapsulated and nutritional value can be maintained [33].

Many foods have a cellular solid structure or alternatively can be considered to have a porous structure [131]. The quality of these food products is determined by the porous characteristics of these food products. Explicitly, porosity is a direct consequence of air bubble formation during the production of the food products and has a dramatic and important effect

on textural quality [138]. Quality and texture of food products can be characterized by their structural properties during dehydration without affecting their taste and appearance. The dehydration process is frequently used to extend shelf-life by increasing stability of food products during storage, since it decreases extensively the water activity of the material and minimizes physical changes [95].

Several physical and structural changes can be seen in food materials due to moisture removal during drying process [76]. Ratti [132] modified the transport property and dimensions of individual particles during drying, that caused changes in shape and size of food materials. Numerous studies are available in literature which investigated these physical and structural changes in various foodstuffs. Among the diverse-studied properties for different drying methods, some of the properties are listed in Table (1.3) for selected fruits and vegetables. Quevedo et al. [124] and Gibson et al. [54] reported that the mechanical properties of food material are effected by the presence of pores and the degree of porosity. The application of channel flow through porous medium is discussed by Sharma and Sharma [151] in the field of agriculture engineering. The porosity of apple and potato mainly depends on the temperature, moisture contents, humidity, air velocity, drying method and initial porosity [78, 111, 129].

Drying of apple and potato can result the significant microstructural deformations that may be responsible for change in physical properties and bulk level deformation of these food products. The structure of many hydroscopic materials, such as food products, is basically an array of cells [30]. Cellular fruit's tissues are taken as a combination of cell body, cell membrane, cell-wall and intercellular spaces. Intercellular spaces (pores) are randomly distributed among the cells and diverse in different foods [147]. For example, in apple tissue pores are large and interconnected, while in potato, they are thin and isolated [134].

1.7 Objective of the Study

Due to the increasing demands of fresh and damage free food products, the study of mechanical and structural properties of foods is an important topic of research. From above literature

review, it is clear that most of the previous works, related to apple and potato properties, have been done experimentally. To study the mechanical properties of apple and potato tissues, very few models are available, but there is an ambiguity to use an appropriate mathematical model. The relationship between turgor pressure and stretch ratio is not developed yet. Further, the effect of pressure and initial porosity on current porosity in apple and potato has not been investigated mathematically so far. Apart from this, the dependence of structural properties of apple and potato on drying time has not been studied previously. Therefore, the objectives of this thesis are:

- To propose a new strain energy function, and use this function to develop a suitable constitutive relationship between cell-wall tension and stretch ratio for apple and potato tissues.
- To develop a mathematical relationship between stretch ratio and turgor pressure for apple and potato tissues.
- To examine the effect of pressure and initial porosity on the current porosity in apple and potato by means of mathematical modeling.
- To propose a drying model for apple and potato, and use this model to analyze structural properties with respect to drying time.

Table 1.2: The various strain energy functions discussed for tissues.

Authors	**Developed relation**	**Developed relation for**	**Expression**
Gou [55]	Strain energy function	Biological tissues	$W = c\left[e^{kI_1(I_1^2-3I_2)}-1\right]$
Tong and Fung [168]	Pseudo-strain energy function	Skin	$W = \frac{1}{2}(\alpha_1 e_1^2+\alpha_2 e_2^2+\alpha_3 e_{12}^2+2\alpha_4 e_1 e_2)+\frac{1}{2}cexp(a_1 e_1^2+a_2 e_2^2+a_3 e_{12}^2+2a_4 e_1 e_2+\gamma_1 e_1^3+\gamma_2 e_2^3+\gamma_4 e_1^2 e_2+\gamma_5 e_1 e_2^2)$
Fung [48]	Stress-Strain Relationship	Soft tissues	$S_{ij}=\frac{\partial \rho_0 W}{\partial E_{ij}}(i,j=1,2,3)$
Zulliger et al. [185]	Strain energy function	Arterial wall	$W=\frac{c}{2}(I_1-3)+\frac{k_1}{k_2}\left(\frac{1}{2}(exp[k_2(I_4-1)^2]-1)+\frac{1}{2}(exp[k_2(I_{4'}-1)^2]-1)\right)$
Rigbi and Hiram [135]	Strain energy function	Membranes	$W=\int(\lambda_1^2+\lambda_2^2+\lambda_1^{-2}\lambda_2^{-2}-3)IdI$
Skalak et al. [160]	Strain energy function	Red blood cell membranes	$W=\frac{B}{4}\left(\frac{1}{2}I_1^2+I_1-I_2\right)\frac{C}{8}I_2^2$
Zhu and Melrose [183]	Pseudo-strain energy function	Plant and vegetative tissues	$W=C_1[(k_1(\lambda_1^2-\ln\lambda_1^2)+k_2(\lambda_2^2-\ln\lambda_2^2)+k_3(\lambda_3^2-\ln\lambda_3^2)-(k_1+k_2+k_3))+\alpha\{k_1(1/\lambda_1^2+\ln\lambda_1^2)+k_2(1/\lambda_2^2+\ln\lambda_2^2)+k_3(1/\lambda_3^2+\ln\lambda_3^2)-(k_1+k_2+k_3)\}]$

Table 1.3: Various examined parameters in different drying experiments for various foodstuffs.

Examined parameters	**Examined Products**	**Drying Methods**	**References**
Porosity, Moisture content	Apple	Air drying	Lozano et al. [88]
Porosity, Shrinkage, Density	Potato, Carrot, Garlic, Pear, Sweet potato	Air drying	Lozano et al. [89]
Porosity, Density, Shrinkage	Apple, Potato, Carrot	Air drying	Zogzas et al. [184]
Porosity, Structure, Density	Potato	Air drying	Wang and Brennan [176]
Porosity, Density, Specific surface area, Pore size, Pore size distribution	Apple, Potato Cabbage, Carrot	Air and Freeze drying	Karathanos et al. [72]
Porosity, Density, Specific Volume	Apple, Potato, Banana, Carrot	Conventional, Vacuum, Osmotic, Microwave, Freeze Drying	Krokida and Maroulis [81]
Porosity, Density, Specific volume, Moisture Contents, Pressures	Apple, Potato, Banana, Carrot	Vacuum dehydration	Krokida et al. [83]
Porosity, Shrinkage, Moisture contents	Potato	Air drying	McMinn and Magee [99]
Porosity, Shrinkage, Density, Moisture contents	Apple	Osmotic drying	Mavroudis et al. [92]
Porosity, Density, color and viscoelastic behavior	Apple, Potato, Banana, Carrot	Microwave and Microwave-vacuum drying	Krokida and Maroulis [82]
Porosity, density	Apple, Potato, Abalone, Sates	Freeze drying	Sablani and Rahman [139]

Chapter 2

A New Strain Energy Function to Characterize Apple and Potato Tissues

2.1 Introduction

Several constitutive laws have been developed by researchers to understand the mechanical properties of agricultural products. Initially in this process, Nilsson et al. [107] developed a linear elastic constitutive model by assuming cells as fluid filled, cell-wall as thin and cell conglomerate obeys Hooke's law on a gross level. By using Nilsson's model, Murase et al. [105] developed a model to analyze the effect of Young's modulus of potato tissue. By considering cell conglomerate as two dimensional, Pitt [119] developed an elasticity model for vegetative tissues, which predicts that the stiffness in the tissues increases but decreases both the stress and strain at which cell-wall failures are initiated, as initial turgor pressure increases, Pitt and Chen [121] developed a mathematical model for individual plant cells to relate the externally applied stress and strain to the cell-wall stresses, cell viscoelastic properties and cell turgor pressure. Pitt and Davis [122] modeled the parenchyma cells as the thin-walled fluid-filled sphere, and used the finite-element technique to analyze the response of cells to external compressive load. Gates et al. [52] developed an elastic cell-wall constitutive law for large strains. Gao et al. [50] developed a constitutive model to analyze the elastic properties of cellular materials (e.g., apple and potato). Another nonlinear constitutive

law was introduced by Gao et al. [51] to describe the data for apple parenchyma. Zhu and Melrose [183] developed a mechanics model for plant and vegetable tissues by considering tissues as a lattice of three dimensional hexagonal cells. The effect of microfibrillar stiffening factors was also investigated.

Mechanical damage to the soft tissues of apple and potato is amenable to reduce the quality of these products [122]. External loads damage 50% of the edible tissues of apple and potato during harvesting, handling, transportation and storage. Lin and Pitt [87] studied the effect of turgor pressure and strain rate on tissue stiffness, failure stress and failure strain of the apple and potato tissues. It was noticed that under constant strain rate and uniaxial compressive loading, fruit or vegetable tissues may fail either by cell rupture or cell debonding. Gao and Pitt [49] reported that the intercellular bonding and cell orientation affect the stress-strain properties of cellular structure. Further, they found the relationship between micromechanical properties of individual cells and macroscopic properties of whole tissue.

Investigations were carried out by researchers to study the deformation of soft tissues of apple and potato by assuming cell shape as spherical. Most of the studies concentrated on the individual cell deformation. Experiments have been performed [50, 87] on different varieties of apple and potato cultivars, in which mechanical properties of tissues, such as cell turgor pressure, cell-wall stiffness and cell-wall stress-strain relations were examined. To reveal some of the above properties of tissues mathematically, different models [50–52], shown in Table (2.1), have been developed for different experimental data. These models are product specific i.e. one model can not be used to study mechanical properties of other variety. Therefore, there is an ambiguity, which model should be considered to study the mechanical properties of apple and potato tissues for a particular data. To overcome this problem, in the present chapter, our aim is to propose a new strain energy function and use this function to develop a suitable mathematical model which is appropriate to the all experimental data [50, 87] of apple and potato.

Table 2.1: Various constitutive models, strain invariants, stretch-tension relations and calculated material constants for apple and potato tissues.

		Gates et al. [52]	Gao et al. [50]	Gao et al. [51]
Model	Apple	$W = \frac{B}{4}\left[\frac{I_1^2}{2} + 2(I_1 - I_2)\right] + \frac{C}{4\alpha}[\exp(\alpha I_2) - (\alpha I_2)]$	$W = \frac{1}{8}C_1 I_1^4 + \frac{1}{4}C_2 I_2^2$	$W = \frac{C_e}{4}\left[2\beta\left(I_1^2 + \frac{1-\nu}{1+\nu}I_2\right) + I_1^4\right]$
	Potato		$W = \frac{B_1}{2}\left[\frac{1}{2}I_1^2 + 2(I_1 - I_2)\right] + \frac{B_2}{2}\int \frac{I_0^\alpha + (I_2 - I_0)\lvert I_2 - I_0\rvert^{\alpha-1}}{\sqrt{I_2+1}} dI_2$	
Strain invariants		$I_1 = \lambda_1^2 + \lambda_2^2 - 2, \quad I_2 = \lambda_1^2\lambda_2^2 - 1$	$I_1 = \lambda_1^2 + \lambda_2^2 - 2, \quad I_2 = \lambda_1^2\lambda_2^2 - 1$	$I_1 = \lambda_1 + \lambda_2 - 2, \quad I_2 = (\lambda_1 - \lambda_2)^2$
Stretch-tension relation	Apple	$T = \frac{C}{2}[\lambda^2 \exp\{\alpha(\lambda^4 - 1)\} - 1]$	$T = C_1(2\lambda^2 - 2)^3 + C_2\lambda^2(\lambda^4 - 1)$	$T = \frac{C_e}{\lambda}[8(\lambda - 1)^3 + 2\beta(\lambda - 1)]$
	Potato		$T = B_2[I_0^\alpha + (I_2 - I_0)\lvert I_2 - I_0\rvert^{\alpha-1}]$	
Material constants	Apple	$C = 0.1831$ MPa, $\alpha = 6.89$	$C_1 = 9.06$ MPa, $C_2 = 0.552$ MPa	$C_e = 106.5$ MPa, $\beta = 0.0104, \nu = 1/3$
	Potato	$C = 0.0268$ MPa, $\alpha = 8.02$	$\beta_2 = 0.290$ MPa, $I_0 = 0.327, \alpha = 0.435$	

2.2 Mathematical Formulation

Deformation of any agricultural product is directly related to the deformation of individual cells in the tissue and vice versa. Therefore, it is appropriate to study either individual cell deformation or the cell conglomerate (tissue) deformation. When an external load is applied on any agricultural product, its tissues deform and the shape of product changes. Due to this deformation, damage occurs in agricultural products. Earlier, most of the studies have been done by considering individual cell deformation rather than the deformation of tissue.

In the present chapter, a section of soft tissues is assumed as an array of homogeneous cells of identical size, shape and properties. We have focused on a conglomerate of cells in the form of a cubic slice of unit volume. Suppose the cubic slice is cut from apple or potato and a load (or force f_1, f_2, f_3) is applied on this cubic slice. The slice deflects in the direction of applied load, and after deformation, it takes the new shape as shown in Fig. (2.1)

Here we have considered the homogeneous deformation that can be classified as pure homogeneous strain (when a strain occurs such that the unit cube transformed into a rectangular parallelepiped having three unequal edge lengths, then this type of strain is known as pure homogeneous strain). The rectangular Cartesian coordinates (X_1, X_2, X_3) identify material particles in the reference configuration, while (x_1, x_2, x_3) are the corresponding coordinates after deformation with respect to the same axes (Fig. 2.1). The principal axes of the deformation coincide with the Cartesian coordinate directions.

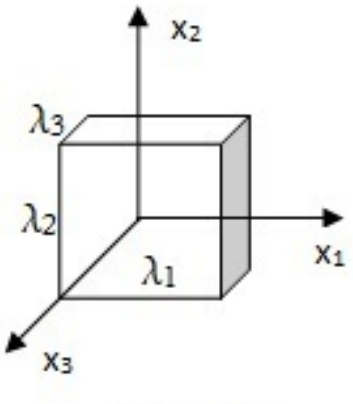

Figure 2.1: Strained state of the cubic slice.

The following assumptions are made in the present study:

- The material of tissues is isotropic, incompressible and homogeneous.
- The material of tissues shows hyperelastic behavior.
- The slice, considered for the deformation, is very thin.

Let three principal stresses are acting in the direction parallel to the principal axes of strain. The stresses can be defined in two ways: true stresses and nominal stresses. True stresses are defined as forces per unit strained area and are denoted by t_1, t_2 and t_3, whereas nominal stresses are defined as forces per unit unstrained area and are denoted by f_1, f_2 and f_3. Principal stretch ratios are denoted by λ_1, λ_2 and λ_3 corresponding to stresses t_1, t_2 and t_3, applied on the tissues. By considering the form of unit volume, it is supposed that the force f_1 (in the direction of x_1) acts on the area $\lambda_2\lambda_3$ measured in the strained state (Fig. 2.1). Therefore, the corresponding true stress is given by

$$t_1 = \frac{f_1}{\lambda_2\lambda_3} = \lambda_1 f_1, \tag{2.1}$$

where (incompressibility condition)

$$\lambda_1\lambda_2\lambda_3 = 1. \tag{2.2}$$

Similarly, we can find t_2 and t_3 ($t_2 = \lambda_2 f_2$ and $t_3 = \lambda_3 f_3$).

2.2.1 Strain Energy Function (SEF)

The study of mechanical behavior of soft tissues is based on the suitable choice of the SEF. To formulate the SEF, there are two approaches, namely, microstructural and phenomenological [68]. In the microstructural approach, the geometrical and mechanical properties of individual tissue components are measured directly. Then, with assumptions pertaining to the interactions between these components, a macroscopic constitutive relation for the complex tissue is derived by first principle. Whereas, in the phenomenological approach,

construction of SEF depends on an iterative process [143, 163]. It was mentioned by Gao et al. [50] that for the development of constitutive law, it is necessary to hypothesize the model first and then validates it with the experimental data. The model, which provides the best fit with the experimental data, is considered as a valid function. At the present time, phenomenological approach is used widely to obtain the SEF [37]. Hereof, due to the relative simplicity and consistency within a continuum framework, in our study, we have focused on the phenomenological approach to construct the SEF.

Fung [47] proposed a SEF (Eq. 2.3) to describe the elasticity properties of soft biological tissues in simple elongation. The SEF was based on the fact that in simple elongation, the tensile stress is nearly an exponential function of the strain in the lower strain range. This model consists of first strain invariant I_1 only, which is responsible for capturing the stiffness at lower strain.

$$W = \frac{G}{2b}\left(e^{b(I_1-3)} - 1\right), \tag{2.3}$$

where the dimensionless constant $b > 0$ is stiffening parameter and $G > 0$ is the shear modulus for infinitesimal deformations. When a load is applied to the tissues of apple or potato, tissues do not deform in one direction. Furthermore, it is possible that a large strain, up to 50%, can be imposed on potato tissues during loading [52]. Consequently, this model (Eq. 2.3) is not able to characterize the mechanical behavior of apple and potato tissues. Therefore, we proposed an extended form of this SEF (Eq. 2.3) by adding a term of second strain invariant I_2. The basic idea of adding this term in the expression of W (SEF) is that this term provides a better sensitivity to the rapid stiffening characteristic at large stretches of tissues. Another reason of adding this term in the existing model is that the new model shows the better fit with tension-stretch data for the apple and potato tissues in comparison of the previously established models.

Further, we also keep in the mind that the proposed SEF satisfies necessary conditions [37], which are as follows:

1. The strain energy function must be non-negative for all deformations.

2. The strain energy function must be invariant under coordinate transformations.

3. The strain energy function must be a function of either stretch or strain invariants. Furthermore, because of isotropy, the strain energy function is symmetrical with respect to the principal stretches.

4. The strain energy function must have a zero value at the undeformed state.

A SEF (W), which satisfies all above conditions, is given by the following equation:

$$W = \frac{C_1}{2b}[\exp(b(I_1-3))-1] + \frac{C_2}{2}(I_2-3)^2, \tag{2.4}$$

where b, C_1 and C_2 are material constants. The Fung [47] model can be obtained by substituting $C_2 = 0$ in Eq. (2.4).

2.2.2 Constitutive Equation

For the study of tissue deformation, we have followed the Cauchy-Green deformation criterion, according to which strain invariants I_1 and I_2 are given as

$$I_1 = \lambda_1^2 + \lambda_2^2 + \lambda_3^2, \qquad I_2 = \lambda_1^2\lambda_2^2 + \lambda_2^2\lambda_3^2 + \lambda_3^2\lambda_1^2. \tag{2.5}$$

Since, we have assumed that the material of tissues is incompressible; therefore, only two stretches can be varied independently. For this reason, it is appropriate to use the incompressibility condition (Eq. 2.2) to express the SEF as a function of two independent stretches. As a result, we can get

$$W = \frac{C_1}{2b}\left[\exp\left(b\left(\lambda_1^2+\lambda_2^2+\frac{1}{\lambda_1^2\lambda_2^2}-3\right)\right)-1\right] + \frac{C_2}{2}\left(\lambda_1^2\lambda_2^2+\frac{1}{\lambda_1^2}+\frac{1}{\lambda_2^2}-3\right)^2. \tag{2.6}$$

Now, forces can be determined by the equation which equates the change in SEF with respect to stretch ratios to the work done by applied forces. There are different methods to obtain the tension-stretch relation for the study of deformation of tissues. Most of the researchers (e.g., [50–52]) considered the soft tissues as a two-dimensional array of cells for

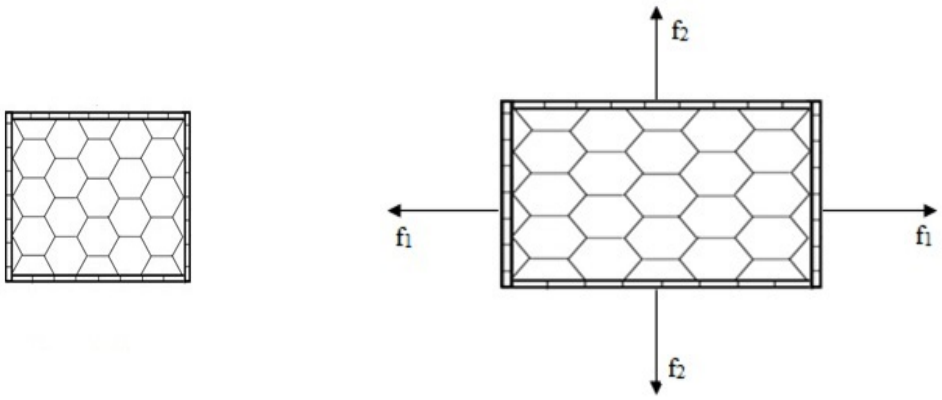

(a) (b)

Figure 2.2: Two dimensional arrangement of cells: (a) undeformed state, and (b) deformed state.

the convenience of analysis. To obtain the tension-stretch relation, we have used the method mentioned by Treloar [169]. When a load is applied to a thin slice of cells, then a plane stress condition occurs, and we may set $f_3 = t_3 = 0$, i.e. the stress normal to the plane of the slice. Now, let us consider that only two forces f_1 and f_2 are applied in the direction of λ_1 and λ_2 on the conglomerate of cells (Fig. 2.2). Suppose these forces f_1 and f_2 are applying such that the extension in the direction of λ_1 is increased by the amount $d\lambda_1$, while λ_2 held constant, the only work done by applied forces is that done by the force f_1. Therefore,

$$dW = f_1 d\lambda_1, \tag{2.7}$$

also, from Eq. (2.6)

$$dW = \frac{\partial W}{\partial \lambda_1} d\lambda_1. \tag{2.8}$$

On combining Eqs. (2.1), (2.7) and (2.8),

$$t_i = \lambda_i \frac{\partial W}{\partial \lambda_i} \qquad (i = 1, 2). \tag{2.9}$$

(Note that in Eq. (2.9), there is no summation over the repeated index i)

When tissues are assumed to be the three-dimensional elastic continuum, $W(\lambda_1, \lambda_2)$ denotes the strain energy per unit initial volume [164]. The relation between stress t_i and tension T_i can be derived from SEF as

$$T_i = \frac{h}{\lambda_1 \lambda_2} t_i \qquad (i = 1, 2), \tag{2.10}$$

where h is the thickness of tissues.

When the tissues are treated as a two-dimensional elastic continuum (considering h very small in comparison to other dimensions), $W(\lambda_1, \lambda_2)$ denotes the strain energy per unit initial area [165]. Therefore,

$$T_i = \frac{1}{\lambda_1 \lambda_2} t_i \qquad (i = 1, 2). \tag{2.11}$$

From Eqs. (2.6), (2.9) and (2.11), we can get

$$\begin{aligned} T_1 &= C_1 \left(\frac{\lambda_1}{\lambda_2} - \frac{1}{\lambda_1^3 \lambda_2^3} \right) \exp\left(b \left(\lambda_1^2 + \lambda_2^2 + \frac{1}{\lambda_1^2 \lambda_2^2} - 3 \right) \right) \\ &+ 2C_2 \left(\lambda_1 \lambda_2 - \frac{1}{\lambda_1^3 \lambda_2} \right) \left(\lambda_1^2 \lambda_2^2 + \frac{1}{\lambda_1^2} + \frac{1}{\lambda_2^2} - 3 \right), \end{aligned} \tag{2.12}$$

$$\begin{aligned} T_2 &= C_1 \left(\frac{\lambda_2}{\lambda_1} - \frac{1}{\lambda_1^3 \lambda_2^3} \right) \exp\left(b \left(\lambda_1^2 + \lambda_2^2 + \frac{1}{\lambda_1^2 \lambda_2^2} - 3 \right) \right) \\ &+ 2C_2 \left(\lambda_1 \lambda_2 - \frac{1}{\lambda_1 \lambda_2^3} \right) \left(\lambda_1^2 \lambda_2^2 + \frac{1}{\lambda_1^2} + \frac{1}{\lambda_2^2} - 3 \right). \end{aligned} \tag{2.13}$$

Due to the availability of data for an isotropic condition only, here we are more concern with isotropic deformation of tissues so that we can compare our results with the previous results. Hence for isotropy, $(\lambda_1 = \lambda_2 = \lambda)$, $T_1 = T_2 = T$ and Eqs. (2.12) or (2.13) reduces to

$$\begin{aligned} T &= C_1 \left(1 - \frac{1}{\lambda^6} \right) \exp\left(b \left(2\lambda^2 + \frac{1}{\lambda^4} - 3 \right) \right) \\ &+ 2C_2 \left(\lambda^2 - \frac{1}{\lambda^4} \right) \left(\lambda^4 + \frac{2}{\lambda^2} - 3 \right). \end{aligned} \tag{2.14}$$

Table 2.2: Estimated values of material constants in our model for various experimental data.

Data	**Product**	b	C_1**(MPa)**	C_2**(MPa)**
Lin and Pitt [87]	Ida red apple	1	0.5764	11.5541
	Idaho potato	1	0.2405	1.4305
Gao et al. [50]	Empire apple	1	0.3524	6.4440
	Russet Burbank potato	1	0.0283	3.0118

2.3 Results and Discussion

In the present chapter, material constants are estimated by the correlation between predicted values and various experimental values of apple as well as potato tissues. Due to the availability of data for isotropic stretch only, constitutive law (Eq. 2.14) is written in terms of isotropic tension caused by a uniform isotropic stretch. For regression analysis, Levenberg-Marquardt algorithm is used to fit the model with available experimental data, and the values of b, C_1 and C_2 are obtained for the best fit of the model to the experimental data. The values of estimated constants are written in Table (2.2).

Results obtained by our model are compared with the results of four different models; one model of Gates et al. [52] (GPRC = Gates-Pitt-Ruina-Cooke), two models of Gao et al. [50] (GPBa = Gao-Pitt-Bartsch model for apple and GPBp = Gao-Pitt-Bartsch model for potato), and one model of Gao et al. [51] (GPR = Gao-Pitt-Ruina) for distinct experimental data, which are shown in the form of tables as well as in figures.

2.3.1 Comparison of Our Model with the GPRC Model

We have calculated material constants by regression procedure from the experimental data of Lin and Pitt [87] for Ida red apple and Idaho potato. Comparisons are made between our model and GPRC model on the basis of coefficient of determination (R^2) and standard deviation (SD) for both apple and potato, and are shown in Table (2.3). The obtained curve between tension (T) and stretch ratio (λ) are shown in Figs. (2.3) and (2.4) for apple and potato, respectively. Both the curves demonstrate concave-upward profile attribute of tissues.

Table 2.3: Comparison between our model and GPRC model on the basis of a coefficient of determination (R^2) and standard deviation (SD).

	GPRC model	**Our model**
Ida red apple		
R^2	0.991	0.996
SD	0.009	0.0045
Idaho potato		
R^2	0.958	0.986
SD	0.026	0.0020

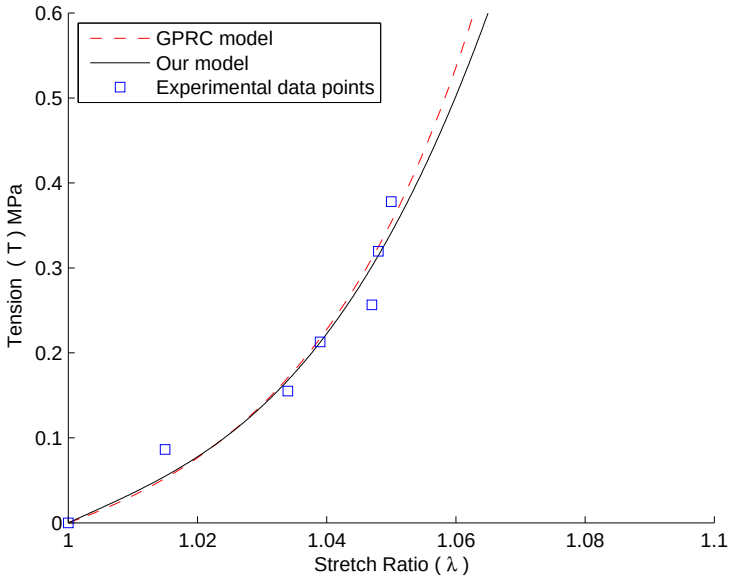

Figure 2.3: Isotropic tension versus isotropic stretch ratio. Comparison of our model with GPRC model for the experimental data of Lin and Pitt [87] for Ida red apple.

Now, the obtained results are summarized as follows:

- Figure (2.3) depicts the nonlinear variation in cell-wall tension with respect to stretch ratio in apple tissues.

- The nonlinear relation in tension-stretch shows that Hook's law is invalid to characterize the mechanical properties of apple and potato tissues, as also mentioned by Gates et al. [52], but the contrary of the result of Lin and Pitt [87] for Ida Red apple which

mentioned that Hook's law is valid for this commodity.

- The tension in the tissues increases exponentially as λ increases, which agreed the experimental observation of Lin and Pitt [87]. This indicates that the stiffness of the cell-wall material (the slope of the graph) increases sharply as the stretch ratio increases.

- For apple data, Fig. (2.3) shows that our model is very close to the GPRC model. Therefore, it is clear that our model can describe similar material properties as the GPRC model.

- It is clear from Fig. (2.3) that from $\lambda = 1$ to $\lambda = 1.04$, the value of T for our model is identical to the value of T for the GPRC model and after $\lambda = 1.04$, T is increasing slowly in our model than the GPRC model as λ increases.

- Figure (2.4) presented the graph between cell-wall tension and stretch ratio, and the comparison of our model with GPRC model for potato data.

- For the GPRC model, initially T increases slowly as λ increases and when λ crossed the value 1.06, T started to increase rapidly, while in our model, the tension in the tissues increases monotonically as λ increases.

- However, the point of inflection seems at the value $\lambda = 1.082$ in the experimental data point. The possible reason of this behavior of tension may be due to the turgor pressure on the cell-wall caused by fluid inside the cell. When the tissue is compressed, fluid inside the cells generates the pressure (turgor pressure) on the cell-wall which results the stretching in the cell-wall material. After a certain limit, turgor pressure produces less effect on the cell-wall; therefore, the rate of increment of tension become slower.

- For the potato data, tension-stretch graph depicts a difference between our model and the GPRC model (Fig. 2.4). The reason is the previous study (with GPRC model) was done by excluding last two data points, whereas our model shows good agreement with all data points.

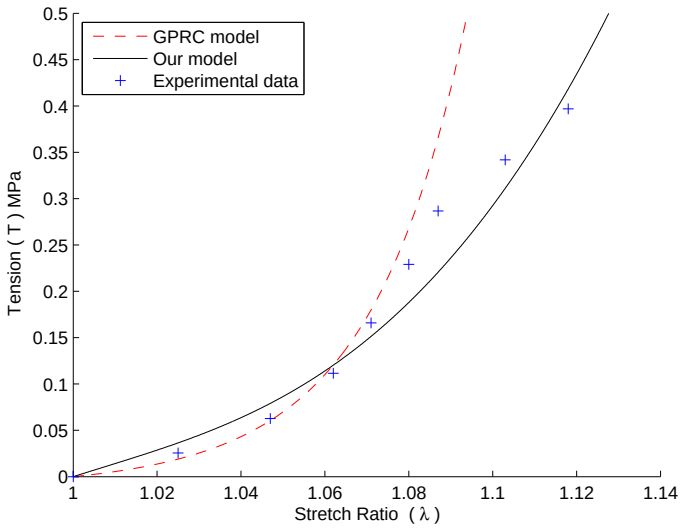

Figure 2.4: Isotropic tension versus isotropic stretch ratio. Comparison of our model to GPRC model for the experimental data of Lin and Pitt [87] for Idaho potato.

- It is clear from Fig. (2.4) that the stiffness in the cell-wall increases rapidly up to $\lambda = 1.082$.
- Values of R^2 and SD for our model are better than the values of R^2 and SD for the GPRC model (Table 2.3).

2.3.2 Comparison of Our Model with GPBa, GPR and GPBp Models

Due to the repeatedly applied loads on the tissues, increment in stiffness may enhance the rupturing of the cell-wall. As a result, tissues can be broken structurally and texturally by a loss of firmness [120], and this diminish the apparent freshness of the product. Further, the obtained results are summarized as follows:

- Material constants b, C_1 and C_2 are calculated from the experimental data of Gao et al. [50] for the Empire apple and Russet Burbank potato tissues.
- The results of our model are compared with the results of two models of Gao et al. [50] (GPBa and GPBp models) and one model of Gao et al. [51] (GPR model) in respect of R^2 and SD (Table 2.4).

Table 2.4: Comparison between our model, GPBa, GPBp and GPR models on the basis of a coefficient of determination (R^2) and standard deviation (SD).

	GPB model	**GPR model**	**Our model**
Empire Apple			
R^2	0.920	0.920	0.940
SD	0.054	0.054	0.030
Russet Burbank Potato			
R^2	0.964		0.965
SD	0.022		0.004

- Plotted graph between T and λ for apple and potato are shown in Figs. (2.5) and (2.6), respectively.

- Both the graphs manifest a sharply increasing slope in the tension-stretch curve with the increasing stretch. The stiffness in cell-wall increases exponentially with the increment in stretch ratio.

- Figure (2.5) depicts the graph between cell-wall tension and stretch ratio for GPBa, GPR and our model for experimental data of apple [50].

- Graph of our model is tantamount to the graph of GPBa and GPR model. This demonstrates that our model can describe the same material properties, for apple tissues, as the GPBa and GPR models. However, the rate of increasing T with respect to λ is slow in our model as compare to GPBa and GPR model. This situation also agreed by experimental values.

- The advantage of our model over the GPBa and GPR model is that our model is better in respect of R^2 and SD, and also closer to the experimental values. Therefore, for the better description of the mechanical properties of apple and potato tissues, our model is appropriate.

- The comparison of our model with GPBp model is presented in Fig. (2.6) for the experimental data (Gao et al. [50]) of potato.

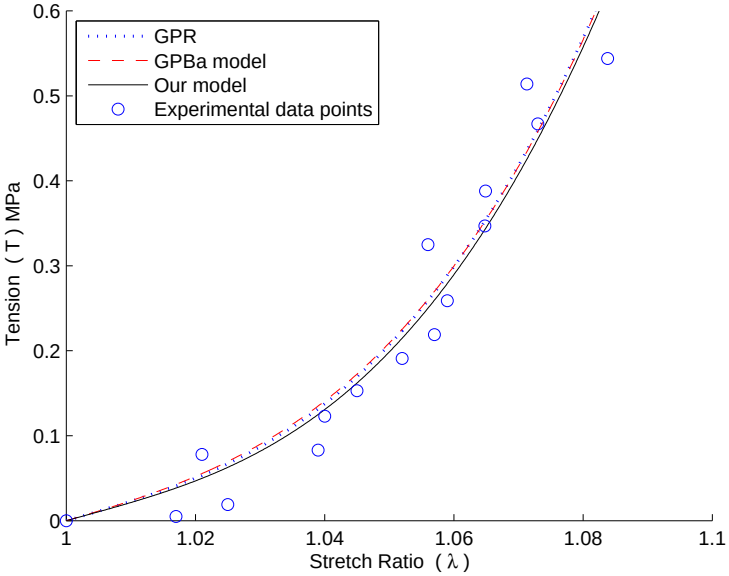

Figure 2.5: Isotropic tension versus isotropic stretch ratio. Comparison of our model with GPR and GPBa model for apple data (Gao et al. [50]).

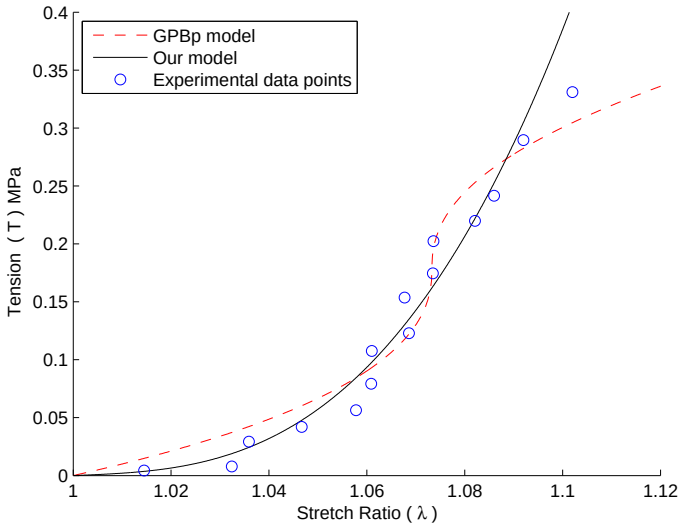

Figure 2.6: Isotropic tension versus isotropic stretch ratio. Comparison of our model with GPBp model for potato data (Gao et al. [50]).

- For our model, T increases exponentially as λ increases, while for the GPBp model, it showed ***S*** type shape (Fig. 2.6). The reason for this behavior during deformation is as follows [50]: the embedded microfibrils in a potato cell-wall are elastic. So, during the infinitesimal deformation of the cell-wall of potato tissues, these microfibrils undergo elastic extension. For finite deformation, the pectin matrix deforms causing rapid slippage between microfibrils; therefore, large cell-wall deformations are plastic and have a different stress-strain slope.

- However, in Fig. (2.6), the experimental values of tension are seemed to increase exponentially as stretch ratio increases. Furthermore, the values of R^2 and SD for our model is better than the GPBp model (Table 2.4); therefore, it is clear that our model is more appropriate to describe mechanical characteristics of potato tissues.

2.4 Conclusions

By comparing the results of our model with the GPRC, GPBa, GPBp and GPR models, it can be concluded that our model performs better than these models. Our model satisfies similar material properties and has better values of the coefficient of determination (R^2) and less value of standard deviation (SD) as compared to the previous models. The benefit of our model, over the previous models, is that our model can incorporate those mechanical properties of apple and potato tissues for which various models were developed previously. However, due to unavailability of the experimental setup, our model could not be validated by own experimental data, although it presented good agreement with experimental material behavior, and better performance than previous models. At this stage, to use the model in industrial applications, parameters C_1 and C_2 should be previously calibrated experimentally. From the present study, it is also clear that analysis either of a single cell or a conglomerate of cells does not make much difference in tissue properties during deformation. In this study, following points are of consideration:

- A SEF is proposed to study the mechanical properties of apple and potato tissues.

- By using this SEF, a tension-stretch relation is developed for finite deformation of cell conglomerate.
- Model is fitted to the various experimental data of apple and potato. Results showed good agreement between predicted values and experimental values.
- The resulting models facilitate our understanding of the tissue's function and provide an insight into the tissue's response to a given deformation.
- Obtained results are compared to the results given in literature. It is noticed that our results are better in respect of R^2 and SD than the previous results.

Chapter 3

Analytical Study of Turgor Pressure in Apple and Potato Tissues

3.1 Introduction

A large percentage of water is contained in apple and potato which is responsible for turgidity in the soft tissues. To determine the quality of these products, it is important to understand the effect of turgor pressure in the cells. Initially, the study of turgor pressure for tissues was provided by Nilsson et al. [107], who derived the relationship between tissue rigidity and turgor pressure for infinitesimal deformation. The influence of turgor pressure was found on the failure strain, failure stress, tissue stiffness and failure mode in soft tissue by performing experiments on apple and potato samples [87] and apple samples [121]. Under constant uniaxial loading, potato tissues decrease the failure susceptibility [106] and reduce its strength at high turgor pressure [63].

Turgor pressure and temperature influence the mechanical properties of apple and potato tissues. Bajema et al. [13] investigated the effect of turgor pressure and temperature on the failure properties of potato tissues. Zdunek et al. [182] analyzed the potato tissues, and observed that failure mode of the tissues between cell-wall rupturing and cell-cell debonding can be changed by changes in turgor pressure and temperature. Turgor pressure and cell size have a great effect on the wall elasticity of plant cells and potato tissue cracking. So, an

acoustic emission method was used to analyze failure conditions [77] and fracture properties [182] of potato tissues with different turgor pressure and cell size distribution.

In many studies, turgor pressure was adjusted by soaking potato tissues [8, 12, 146], apple and potato tissues [87] and tomato tissues [71] in mannitol solutions of various concentrations. Further, the influences of turgor pressure on pear tissues [41] and apple tissues [5, 108] were investigated during tensile and compression test. It was adduced that macroscopic mechanical behavior of apple and potato depends on microscopic properties. Oparka and Wright [112] analyzed the effect of cell turgor pressure on sucrose partitioning in potato tuber tissues during storage. Increment in turgor pressure reduces the failure stress and strain under axial compression of apple and potato tissues [12].

To study the effect of turgor pressure on cellular structure of apple and potato tissues, most of the work have been done experimentally. A very less number of studies are available which deal with the problem mathematically. Therefore, the aim of the present chapter is to develop a mathematical relationship between turgor pressure and stretch ratio by using strain energy function for apple and potato tissues . Further, a generalized form of the strain energy function is proposed, which can be used in future studies to investigate the mechanical properties of hyperelastic tissues.

3.2 Materials and Methods

3.2.1 Experiments

The tissues considered in the present study are from ‘Ida Red’ apples and ‘Idaho’ potatoes. In this chapter, experiments conducted by Lin and Pitt [87] on apple and potato tissues have been used for validation of the results. Apples and potatoes were kept in cold storage before testing. Both the products were divided into sections and then cylindrical samples were cut from the flesh side of the sections. Cell turgor pressure was manipulated by soaking the cylindrical samples into mannitol solutions of concentrations from 0.0 to 0.8 M for apple and 0.0 to 0.5 M for potato. An Instron Universal testing machine was used for the compression test of apple and potato (for more details, see Lin and Pitt [87].

3.2.2 Mathematical Formulation

For the mathematical modeling, it is assumed that the tissues of apple and potato are composed of identical parenchyma cells which are uniform in thickness and mechanically homogeneous. Therefore, when a uniform compressive stress is applied to the tissues, each cell in the tissues is subjected to an equal load [121]. Consequently, the fluid inside the cell generates the pressure (turgor pressure) on the cell-wall. Further, as stress increases, turgor pressure increases within the cell and cell-walls start to stretch. In more turgid cells, if the external stress on the cellular conglomerate increases slightly, the cell-wall stretching exceeds its strength and cell-wall rupture occurs [35, 121].

3.2.2.1 Generalization of Strain Energy Function

The study of mechanical properties of hyperelastic material has been a topic of interest for many decades. Numerous strain energy functions have been developed for the characterization of hyperelastic materials (Tables 1.2 and 2.1). In this context, a new strain energy function (Eq. 2.4) has been introduced in Chapter 2 and a mechanical model has been developed to present the relation between cell-wall tension and stretch ratio for apple and potato tissues. A more general form of this strain energy function are proposed as

$$W = \left(\frac{A}{b}\right)[\exp(b(I_1-3))-1] + \left(\frac{B}{m}\right)(I_2-3)^m, \tag{3.1}$$

where A and B are the material constants, which can be determined by experimental data, and m is any natural number. This generalized form can be used in further studies for investigating mechanical properties of hyperelastic material (for example, biological tissues). This function satisfies the necessary requirement of normalization conditions [65], which states that W (SEF) should vanish in the reference configuration where $I_1 = I_2 = 3, I_3 = 1$ i.e. $W(\mathbf{I}) = 0$; and W increases with deformation i.e. $W \geq 0$.

On expanding the exponential term, Eq. (3.1) can be written as

$$W = \left(\frac{A}{b}\right)\left[\sum_{n=1}^{\infty}\left(\frac{b^n}{n!}\right)(I_1-3)^n\right] + \left(\frac{B}{m}\right)(I_2-3)^m. \tag{3.2}$$

Table 3.1: Reduced form of strain energy function (Eq. 3.1) and/or (Eq. 3.2) into several well known strain energy functions.

Values of m and n	Reduced strain energy function	Reduced strain energy function is equivalent to strain energy function of
$m \to \infty$	$W = (A/b)[\exp(b(I_1-3))-1]$	Fung [47]; Humphrey and Yin [69]
$m \to \infty, n = 1$	$W = A(I_1-3)$	Neo-Hookeano model (Rivlin [136])
$m \to \infty, n = N$	$W = (A/b)\sum_{n=1}^{N}(b^n/n!)(I_1-3)^n$	Yeoh [181]
$m = 1$	$W = (A/b)[\exp(b(I_1-3))-1]+B(I_2-3)$	Veronda and Westmann [173]
$m = 2$	$W = (A/b)[\exp(b(I_1-3))-1]+\frac{B}{2}(I_2-3)^2$	Chapter 2
$m = 1, n = 1$	$W = A(I_1-3)+B(I_2-3)$	Mooney [104]
$m = 1, n = 2$	$W = A(I_1-3)+(Ab/2)(I_1-3)^2+B(I_2-3)$	Isihara et al. [70]
$m = 1, n = 3$	$W = A(I_1-3)+(Ab/2)(I_1-3)^2+(Ab^2/6)(I_1-3)^3+B(I_2-3)$	Biderman [16]

Now, we are in the position where several strain energy functions can be acquired from Eqs. (3.1) and/or (3.2). For the different values of m and n, Eqs. (3.1) and/or (3.2) can be reduced into several previously developed strain energy functions. A concise list is given in Table (3.1).

3.2.2.2 Constitutive Equation

Several strain energy functions have been reported in the literature for characterization of biological tissues. To study the mechanical properties of apple and potato tissues, however, as shown in Chapter 2, the more appropriate form of strain energy function can be procured from Eq. (3.1) corresponding to $m = 2$. In the present chapter, therefore, we have modeled our problem by considering the following form of strain energy function

$$W = \left(\frac{A}{b}\right)[\exp(b(I_1-3))-1]+\left(\frac{B}{2}\right)(I_2-3)^2, \tag{3.3}$$

where $A = C_1/2$ and $B = C_2$.

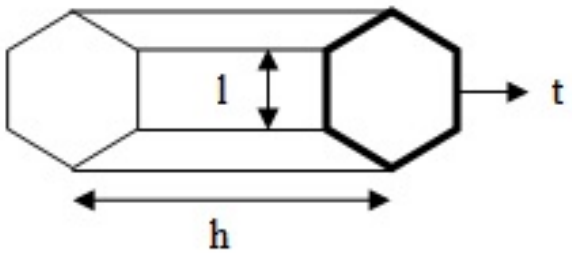

Figure 3.1: A typical hexagonal cell structure with l as edge length of hexagonal section, t as thickness of cell-wall and h as height of the prisms.

Furthermore, the principal components of Cauchy stress are written as

$$\tau_i = -p + 2\left[\lambda_i^2\left(\frac{\partial W}{\partial I_1}\right) - \lambda_i^{-2}\left(\frac{\partial W}{\partial I_2}\right)\right], \quad i = 1, 2, 3 \tag{3.4}$$

where τ_i are principal components of Cauchy stress, λ_i are the eigenvalues of left Cauchy-Green tensor, and scalar p introduced as an indeterminate Lagrange multiplier analogous to a hydrostatic pressure (for more details, see Holzapfel [65]).

For the study of plant vegetative tissues, a remarkable study was done by Zhu and Melrose [183]. In this context, we have considered apple and potato tissues as having hexagonal cellular structure (Fig. 3.1). In the assumed hexagonal cellular structure, let us consider that l denotes the edge length of the hexagonal section, t denotes the thickness of the cell-wall and h denotes the height of the prisms. The principal stretch ratios of the cell-wall are defined as

$$\lambda_1 = \frac{l}{l_0}, \quad \lambda_2 = \frac{h}{h_0}, \quad \lambda_3 = \frac{t}{t_0}, \tag{3.5}$$

where l_0, t_0 and h_0 are the initial dimensions at turgor pressure $p_c = 0$. The cell-wall volume fraction (the cell-wall volume over the tissue volume) is

$$v_0 = \frac{2t_0}{\sqrt{3}l_0}. \tag{3.6}$$

Further, as mentioned by Zhu and Melrose [183], Cauchy stresses can be derived by the

force equilibrium and given by

$$\tau_1 = \left(\frac{\sqrt{3}lp_c}{t}\right) - p_i, \qquad \tau_2 = \left(\frac{\sqrt{3}lp_c}{2t}\right) - p_i, \qquad \tau_3 = -p_i, \tag{3.7}$$

where $p_i = p_c + p_0$, p_0 is external atmospheric pressure.

Stresses are indeterminate to the amount of an uninformed hydrostatic pressure (p) due to the assumption of incompressibility of material. Merely, the differences between any two of the principal stresses are determinate [169]. By calculating the difference of the stresses therefore the effect of hydrostatic stress will be removed. Consequently, from Eqs. (3.5 – 3.7), we can get the difference in the stresses as

$$\tau_1 - \tau_3 = \frac{2\lambda_1^2\lambda_2 p_c}{v_0}, \tag{3.8}$$

$$\tau_2 - \tau_3 = \frac{\lambda_1^2\lambda_2 p_c}{v_0}. \tag{3.9}$$

Furthermore, from Eq. (3.4), we can obtain

$$\tau_1 - \tau_3 = 2(\lambda_1^2 - \lambda_3^2)\left(\frac{\partial W}{\partial I_1} + \lambda_2^2\frac{\partial W}{\partial I_2}\right), \tag{3.10}$$

$$\tau_2 - \tau_3 = 2(\lambda_2^2 - \lambda_3^2)\left(\frac{\partial W}{\partial I_1} + \lambda_1^2\frac{\partial W}{\partial I_2}\right), \tag{3.11}$$

where $\partial W/\partial I_i, i = 1, 2$ are calculated from Eq. (3.3). After equating Eq. (3.8) to (3.10) and (3.9) to (3.11), and making use of incompressibility condition i.e. $\lambda_1\lambda_2\lambda_3 = 1$, we obtain the following relations

$$\begin{aligned}\frac{\lambda_1^2\lambda_2 p_c}{v_0} &= (\lambda_1^2 - \lambda_1^{-2}\lambda_2^{-2})\left[(C_1/2)\exp(b(\lambda_1^2 + \lambda_2^2 + \lambda_1^{-2}\lambda_2^{-2} - 3))\right. \\ &+ \left. C_2\lambda_2^2(\lambda_1^2\lambda_2^2 + \lambda_1^{-2} + \lambda_2^{-2} - 3)\right],\end{aligned} \tag{3.12}$$

$$\begin{aligned}\frac{\lambda_1^2\lambda_2 p_c}{v_0} &= (\lambda_2^2 - \lambda_1^{-2}\lambda_2^{-2})\left[C_1\exp(b(\lambda_1^2 + \lambda_2^2 + \lambda_1^{-2}\lambda_2^{-2} - 3))\right. \\ &+ \left. 2C_2\lambda_1^2(\lambda_1^2\lambda_2^2 + \lambda_1^{-2} + \lambda_2^{-2} - 3)\right].\end{aligned} \tag{3.13}$$

Here, Eqs. (3.12) and (3.13) are symmetric in λ_1 and λ_2, therefore, we can find the relationship between p_c and λ either from Eq. (3.12) or from Eq. (3.13). Therefore, from Eq. (3.13)

$$\begin{aligned} p_c &= (\lambda_2\lambda_1^{-2} - \lambda_1^{-4}\lambda_2^{-3})\left[\alpha\exp(b(\lambda_1^2+\lambda_2^2+\lambda_1^{-2}\lambda_2^{-2}-3))\right. \\ &+ \left. 2\beta\lambda_1^2(\lambda_1^2\lambda_2^2+\lambda_1^{-2}+\lambda_2^{-2}-3)\right], \end{aligned} \tag{3.14}$$

where

$$\alpha = C_1\nu_0, \quad \beta = C_2\nu_0. \tag{3.15}$$

The appropriateness of the study required that the validation of the proposed relation should be explored in the light of experimental observations. Since, the experimental data is available only for the isotropic stretch (i.e. stretching in the cell-wall is same in all directions), therefore $\lambda_1 = \lambda_2 = \lambda$, and Eq. (3.14) reduced to

$$p_c = (\lambda^{-1} - \lambda^{-7})[\alpha\exp(b(2\lambda^2+\lambda^{-4}-3)) + 2\beta\lambda^2(\lambda^4+2\lambda^{-2}-3)]. \tag{3.16}$$

This is the required relation between turgor pressure and stretch ratio.

3.3 Results and Discussion

In the present chapter, we have developed a relationship between turgor pressure and cell-wall stretch ratio for apple and potato tissues. The experimental data is used from literature [87] for validation of the obtained relation. The experimental data for apple and potato tissues is available only for an isotropic condition; therefore, the final expression of turgor pressure is written in terms of the isotropic stretch ratio. The constants (α and β) of turgidity are calibrated by correlating the predicted and experimental values of turgor pressure and stretched ratio for 'Ida Red' apple and 'Idaho' potato tissues. The Levenberg-Marquardt algorithm is employed for regression analysis to fit the model with experimental data. The fitted curve is satisfactory with a coefficient of determination of 98.02 % and a standard

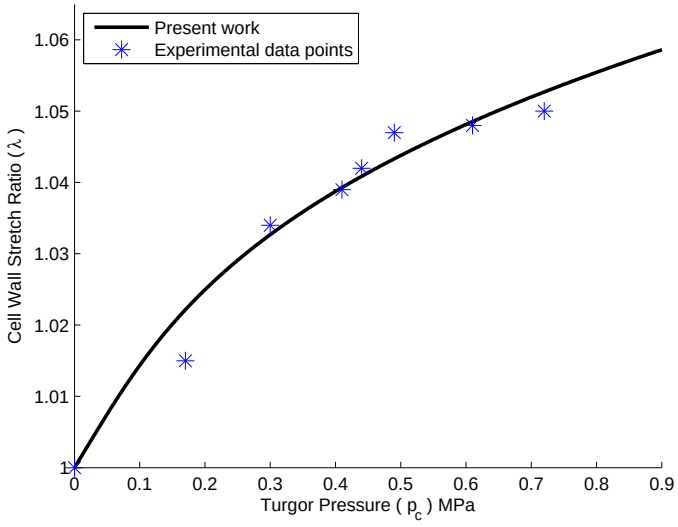

Figure 3.2: Graph between cell-wall stretch ratio and turgor pressure for Ida Red Apple (Experimental data from Lin and Pitt [87]).

deviation about the regression line of 0.017 for apple, and a coefficient of determination of 98.0 % and a standard deviation about the regression line of 0.019 for potato.

For the calibration of material constants α and β, experimental data of Lin and Pitt [87] is used for apple and potato tissues. The calibrated values of material constants are $\alpha = 1.1170$ MPa and $\beta = 23.4504$ MPa for apple and $\alpha = 0.5532$ MPa and $\beta = 2.7060$ MPa for potato. Further, the results obtained in this chapter are summarized as follows:

- The acquired graphs between stretch ratio and turgor pressure are shown in Figs. (3.2) and (3.3) for apple and potato, respectively.

- For each product, stretch ratio increases nonlinearly as turgor pressure increases. This result is supported by previous study [87].

- Further, it can be seen from the figures that at starting values of turgor pressure (approximately, upto $p_c = 0.3$ for apple (Fig. 3.2) and $p_c = 0.25$ for potato (Fig. 3.3)), the rate of increment of the stretch ratio is faster than the latter values of turgor pressure. After these values, as the turgor pressure increases, stretching in the cell-wall increases gradually. This behavior of stretch ratio is also confirmed by the experimental values.

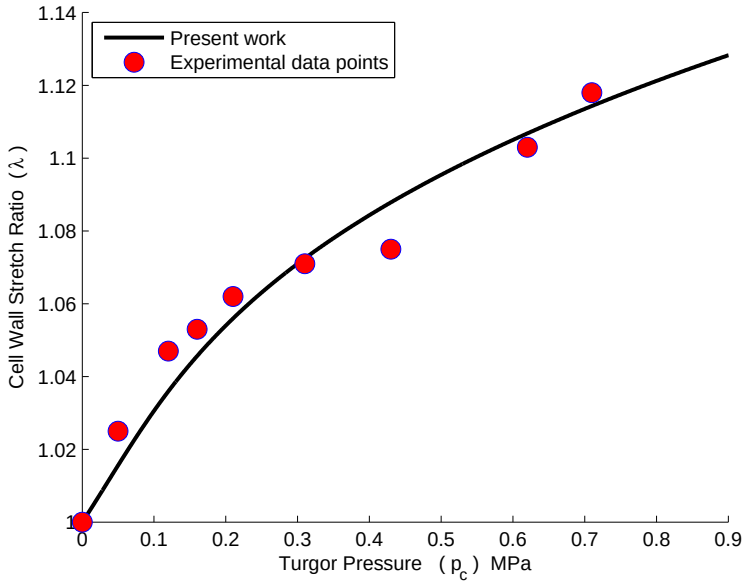

Figure 3.3: Graph between cell-wall stretch ratio and turgor pressure for Idaho Potato (Experimental data from Lin and Pitt [87]).

- Initially, when there is no stress applied to the apple tissues, i.e. turgor pressure (p_c) is zero, consequently, no stretching in the cell-wall, which implies $\lambda = 1$ (Fig. 3.2). Similar behavior can be seen for potato tissues (Fig. 3.3).

- When a load is applied to the tissues, stress is generated in the cell and fluid inside the cell generates the pressure (turgor pressure) on the cell-wall. With the enhancement of turgor pressure, stretching in the cell takes place, which results in the stiffness in the cell-wall. Also, tissues stiffness increases as turgor pressure increases.

- At higher turgor pressure, the unruptured cells provide greater resistance to applied load. In fresh tissues, when cell-walls are in greater turgid condition, less force or deformation can induced failure in tissues.

- From Figs. (3.2) and (3.3), it can be seen that, initially up to $p_c = 0.4$, the rate of enhancement of the stretch ratio is much faster than the latter values of turgor pressure.

- Both the products (apple and potato) show similar behavior for stretch in the cells for applied stress, albeit stretch in the potato cells is greater than the stretch in the

apple cells for same value of turgor pressure. For example, the stretch ratio is 1.05 corresponding to turgor pressure 0.72 in apple cells (Fig. 3.2); whereas, the stretch ratio is 1.118 corresponding to turgor pressure 0.71 in potato cells (Fig. 3.3). This demonstrates that potato cells (or tissues) can sustain more pressure than apple tissues.

Cell-walls are an important component in the construction of fruits and vegetables tissues. Strength of the cell-wall is the main property which characterize texture and quality of these products. During the compression of fresh tissues, pre-stressing of the cell-wall by water uptake leads to sufficient stiffness in the tissues. Stiffness of the cell-wall in tissues increases as stretch increases [87]. The effect of turgor pressure on the tissue stiffness is noticed during loading. There is a strong relationship between tissue stiffness and cell-wall stiffness [87, 119, 122]. Since at the higher stretch (i.e. higher turgor pressure) cell-walls become very stiff, this may lead to an unruptured cell-wall volume which will not increase further. Beyond this limit, further increment in turgor pressure may result in rupture of cell-walls, and hence, fluid inside the cell starts to move out. However, this situation is not seen in the presented graphs.

3.4 Conclusions

In the present work, a generalized form of a strain energy function is proposed. With the help of an appropriate form of this proposed strain energy function, a mathematical relationship between turgor pressure and stretch ratio is developed for apple and potato tissues. The validity of the relation is checked and found in good agreement with experimental values. Further, the influences of turgor pressure on the cell-walls of apple and potato tissues are discussed. Higher turgor pressure ruptures the cell-walls in these products, which is responsible for damage of cells and reduction in the quality of the products. The results obtained in the present study are sufficiently close to the experimental results. A good agreement between predicted and experimental results is obtained with the coefficients of determination being 98.02 % for apple and 98.0 % for potato. From the results of Chapters 2 and 3, it is clear that the cell-wall tension is affected by turgor pressure, i.e., as turgor pressure increases, stretches

in cell-wall increases, which is responsible for increment in cell-wall tension. Therefore, the quality and freshness of apple and potato are affected by turgor pressure also. In further studies, this mathematical relation may be helpful in understanding the mechanical properties and influences of turgor pressure on soft biological tissues, especially, apple and potato.

Chapter 4

Mathematical Modeling to Study the Influence of Porosity on Apple and Potato during Dehydration

4.1 Introduction

For the quality characterization of dehydrated food products, the study of structural properties, such as density and porosity, is important. These properties have profound effects on other properties, namely, permeability, diffusivity and thermal conductivity [78]. Among various changes, the most significant change in food products is the reduction of its external volume, which occurs during drying. The change in microstructure, i.e., shrinkage and formation of pores is the consequence of water loss and heating, that causes stress in cellular material [95]. Bai et al. [11] studied the structural changes in apple rings during convective drying. They observed that the removal of water leads to cell rupture and the formation of cracks in the inner structure, which is caused due to microstresses in the cell-wall during dehydration process. Further, Sinha [158] reported that during dehydration, the more the water loss, the more the contraction stresses are originated in the material, that generates the pressure outward on the cavity (pores) surfaces. As a result, pores of different size and shape build up in food products [94], that increase the porosity in food products.

Numerous studies are available in the literature [72, 93, 99, 125, 126, 176], which reported that the formation of pores is the consequence of evaporation of water from cellular products during dehydration. Further, it is also reported that the development and increment of pores in foods during drying is strongly affected by initial porosity, initial material moisture content, relative humidity, composition, drying methods and drying conditions [184].

Rahman [126] mentioned that the factors which affect the development of pores can be grouped as (i) extrinsic and (ii) intrinsic factors. Relative humidity, temperature, gas atmosphere, pressure, electromagnetic radiation and air circulation are including in extrinsic factors, whereas the intrinsic factors are: initial structure and chemical composition. During drying, the shrinkage is considered as ideal if the decrease in volume of material is proportional to the loss of mass. On the other hand, porosity comes into the view if the volume reduction of material is lesser than volume of water loss [90].

As drying process proceeds and temperature increases, the moisture content in apple and potato decreases. Consequently, internal pressure in these products generated by water vapor, which is responsible for pore formation. The most common terminology used for characterizing pores is porosity (volume fraction of pores) [125]. For the prediction of porosity during dehydration, therefore, the aim of this chapter is (i) to develop a mathematical relationship between porosity (volume fraction of pores) and pressure (a contraction stress generated in the cells due to water removal during dehydration) with the help of strain energy function for apple and potato; and (ii) to examine porosity behavior with respect to pressure and initial porosity.

4.2 Mathematical Medeling

4.2.1 Problem Formulation

Natural solid foodstuffs constitute systems of cellular tissues, and therefore, may be regarded as peculiar porous systems [99]. Rahman [125] described various factors (such as surface tension, pore pressure, structure, environment pressure, and mechanisms of moisture transport) that play important role in explaining the pore formation during drying of food

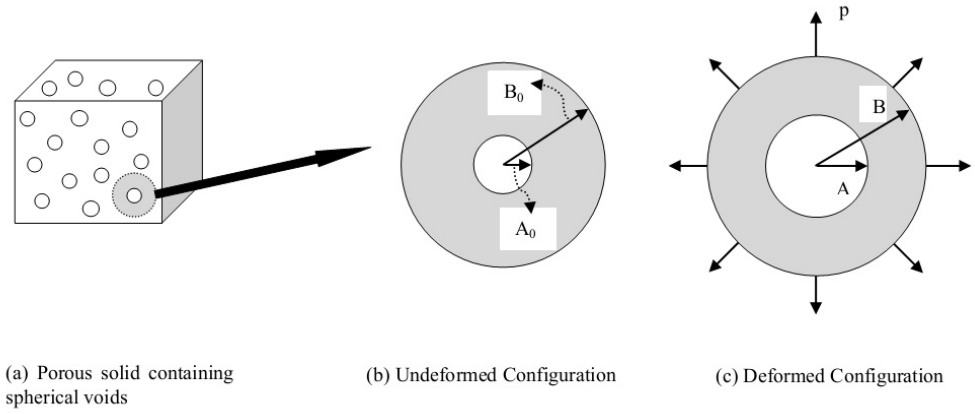

Figure 4.1: The structure of porous material (a) cubic porous solid containing spherical voids (b) undeformed configuration (c) deformed configuration.

products. Further, Rahman [125] hypothesized that the capillary force is the main force responsible for collapse, so counterbalancing this force causes formation of pores and lower the shrinkage. The counterbalancing forces are results of generation of internal pressure due to vaporization of water or other solvents, variation in moisture transport mechanism and pressure outside the material. It is also reported in literature [132] that food products undergo deformations that can be characterized by changes in volume, shape, porosity, density, shrinkage, and collapse phenomena during drying.

To study the porosity behavior and deformation of porous material (apple and potato), let us consider an arbitrary small cubic volume element containing pores distributed in it (Fig. 4.1a). For the mathematical analysis, it is assumed that every pore in the cubic volume element surrounded by a spherical surface, which is lying completely in the material matrix at every instant. Suppose that this porous material is subjected to the pressure, that is responsible for counterbalancing forces and generated on the surface of porous matrix, as depicted in Fig. 4.1 (c). Therefore, the problem under consideration is the study of deformation of a sphere consisted of spherical pore, and the analysis of growth of the pore (i.e. void or cavity) in deforming material. Due to spherical symmetry, the pressure on the surface of porous matrix prescribed radial deformation of the spherical solid element enclosing pore. Fig. 4.1(b and c) depicts the undeformed and deformed configurations of the spherical material, respectively. Suppose that in the undeformed configuration, the radius of a spherical

void cell is denoted by A_0 (inner radius) and that of the bulk material by B_0 (outer radius), while in the deformed configuration, the radius of the void cell and material are denoted by A (inner radius) and B (outer radius), respectively. Using spherical polar coordinates, the position $\mathbf{x}$ of a particle is denoted by (R,Θ,Φ) in the undeformed configuration, and after deformation, suppose it takes the new position $\mathbf{y}$ and is denoted by (r,θ,ϕ). For the study of cavitations in porous hyperelastic solid, the radial symmetric deformation ([15, 67, 159]) is defined as

$$\mathbf{y} = \frac{F(R)}{R}\mathbf{x}, \tag{4.1}$$

where $\mathbf{y} = (y_1, y_2, y_3)$, $\mathbf{x} = (x_1, x_2, x_3)$, $R = |\mathbf{x}| = \sqrt{\left(x_1^2 + x_2^2 + x_3^2\right)}$ and $F(R)$ is a function of R, which will be determined.

Since deformation is radially symmetric; therefore,

$$r = |\mathbf{y}| = F(R), \quad \Theta = \theta, \quad \Phi = \phi. \tag{4.2}$$

Deformation gradient tensor $\mathbf{F}$ (defined in Eq. 1.3) associated with deformation (Eq. 4.1) is given by

$$\mathbf{F} = \frac{\partial \mathbf{y}}{\partial \mathbf{x}} = \left[\frac{\partial y_i}{\partial x_j}\right], \tag{4.3}$$

where

$$\frac{\partial y_i}{\partial x_j} = \frac{x_i x_j}{R^2}\left(F'(R) - \frac{F(R)}{R}\right) + \frac{F(R)}{R}\delta_{ij}, \quad \text{for all } i,j = 1,2,3 \tag{4.4}$$

where $F'(R)$ is derivative of $F(R)$ and δ_{ij} is Kronecker delta. By the assumption of incompressibility, we have

$$det(\mathbf{F}) = 1 \ \text{ and also } \ B^3 - A^3 = B_0^3 - A_0^3. \tag{4.5}$$

On solving Eqs. (4.3) and (4.5) (with the help of Eq. (1.4) and (4.4), and after some simplification), we obtain

$$det(\mathbf{F}) = F'(R)\left(\frac{F(R)}{R}\right)^2. \tag{4.6}$$

By using incompressibility condition, $det(\mathbf{F}) = 1$, Eq. (4.6) is solved to obtain

$$F(R) = \left(R^3 + C\right)^{1/3}, \tag{4.7}$$

where C is constant of integration.

During deformation, the point $R = A_0$ deformed into the point $r = F(R) = A$, therefore, Eq. (4.7) reduced to

$$F(R) = \left(R^3 + A^3 - A_0^3\right)^{1/3}. \tag{4.8}$$

If $A = A_0$, Eq. (4.8) implies that $r = R$, i.e., no deformation in the solid matrix.

4.2.2 Constitutive Relation

To study the mechanical properties of apple and potato tissues, we have proposed a strain energy function in Chapter 2. By using this strain energy function, the influence of turgor pressure on apple and potato tissues, as a function of stretch ratio, has been discussed in Chapter 3. In the present chapter, therefore, we have considered this strain energy function (Eq. 2.4) to obtain the desired mathematical relation for prediction of porosity in apple and potato.

In Eq. (2.4), strain invariants I_1 and I_2 are defined as

$$I_1 = tr\mathbf{B} \quad \text{and} \quad I_2 = \frac{1}{2}\left[(tr\mathbf{B})^2 - tr(\mathbf{B})^2\right], \tag{4.9}$$

where $\mathbf{B}$ is the left Cauchy-Green deformation tensor calculated from $\mathbf{B} = \mathbf{F}\cdot\mathbf{F}^T = \mathbf{V}^2$, $\mathbf{F}$ is given by Eq. (4.3) (for more details, see subsection 1.5.3 in Chapter 1). Principal stretches

$\lambda_r, \lambda_\theta$ and λ_ϕ (i.e. eigenvalues of $\mathbf{V}$) are given by

$$\lambda_r = F'(R), \quad \lambda_\theta = \lambda_\phi = \frac{F(R)}{R}. \tag{4.10}$$

Using incompressibility condition (Eq. 2.2), $\lambda_r \lambda_\theta^2 = 1$, Eq. (4.9) can be written as

$$I_1 = \lambda_r^2 + \frac{2}{\lambda_r} \text{ and } I_2 = \frac{1}{\lambda_r^2} + 2\lambda_r, \tag{4.11}$$

where

$$\lambda_r = F'(R) = \left(1 + \frac{A^3 - A_0^3}{R^3}\right)^{-2/3} = \left(1 - \frac{A^3 - A_0^3}{r^3}\right)^{2/3}, \tag{4.12}$$

$$\lambda_\theta = \left(1 + \frac{A^3 - A_0^3}{R^3}\right)^{1/3} = \left(1 - \frac{A^3 - A_0^3}{r^3}\right)^{-1/3}. \tag{4.13}$$

For the isotropic, incompressible and hyperelastic material, Cauchy stress tensor [65] is defined as

$$\tau = -\rho + 2\frac{\partial W}{\partial I_1}\mathbf{B} - 2\frac{\partial W}{\partial I_2}\mathbf{B}^{-1}, \tag{4.14}$$

where ρ is hydrostatic pressure. From Eq. (4.14), the principal components of Cauchy stress can be obtained as

$$\tau_{rr} = -\rho + 2\lambda_r^2 \left(\frac{\partial W}{\partial I_1}\right) - \frac{2}{\lambda_r^2}\left(\frac{\partial W}{\partial I_2}\right), \tag{4.15}$$

$$\tau_{\theta\theta} = -\rho + 2\lambda_\theta^2 \left(\frac{\partial W}{\partial I_1}\right) - \frac{2}{\lambda_\theta^2}\left(\frac{\partial W}{\partial I_2}\right). \tag{4.16}$$

4.2.3 Equilibrium Equation

During deformation, the stress distribution within the material can be solved with the help of equilibrium equation. For the radial deformation, the equilibrium equation [24, 67, 123] can

be written as

$$\frac{d\tau_{rr}}{dr}+\frac{2}{r}(\tau_{rr}-\tau_{\theta\theta})=0\ . \tag{4.17}$$

4.2.4 Boundary Conditions

The pressure, p, developed on the surface of the porous sphere (which is responsible for counterbalancing force in formation of pores) based on deformed configuration is related to radial stress [24, 123] by the relation

$$\tau_{rr}=p\left(\frac{B_0}{B}\right)^2 \quad \text{at } r=B$$

or by using Eqs. (4.5) and (4.13) (i.e. substituting value of $B^3-B_0^3$ from Eq. (4.5) into Eq. (4.13), then at $r=B$, $\lambda_\theta=(B_0/B)^{-1}$), τ_{rr} can be rewritten as

$$\tau_{rr}=\frac{p}{\lambda_\theta^2} \quad \text{at } r=B\ . \tag{4.18}$$

It is also assumed that the cavity surface is traction free, which gives

$$\tau_{rr}=0 \quad \text{at } r=A\ . \tag{4.19}$$

4.2.5 Final Desired Relation

The difference between τ_{rr} and $\tau_{\theta\theta}$ can be calculated from Eqs. (4.15) and (4.16) as

$$\tau_{rr}-\tau_{\theta\theta}=-2\left(\frac{1-\lambda_r^3}{\lambda_r}\right)\left(\frac{\partial W}{\partial I_1}+\frac{1}{\lambda_r}\frac{\partial W}{\partial I_2}\right). \tag{4.20}$$

Hence, the problem in hand is to solve the Eq. (4.17) with boundary conditions (4.18) and (4.19). Therefore,

$$\frac{d\tau_{rr}}{dr}=\frac{4}{r}\left(\frac{1-\lambda_r^3}{\lambda_r}\right)\left(\frac{\partial W}{\partial I_1}+\frac{1}{\lambda_r}\frac{\partial W}{\partial I_2}\right). \tag{4.21}$$

On integrating Eq. (4.21) from $r = A$ to $r = B$, we get

$$\tau_{rr}(B) - \tau_{rr}(A) = 4\int_A^B \left[\left(\frac{1-\lambda_r^3}{\lambda_r}\right)\left(\frac{\partial W}{\partial I_1} + \frac{1}{\lambda_r}\frac{\partial W}{\partial I_2}\right)\right]\frac{dr}{r}. \tag{4.22}$$

By using boundary conditions (4.18) and (4.19), and change the variable of integration from r to λ_r with the help of Eq. (4.12), we obtain

$$p = 2\bar{\lambda}_\theta^2 \int_{\bar{A}}^{\bar{B}} \left[\left(\frac{1+\lambda_r^{3/2}}{\lambda_r^{1/2}}\right)\left(\frac{\partial W}{\partial I_1} + \frac{1}{\lambda_r}\frac{\partial W}{\partial I_2}\right)\right] d\lambda_r, \tag{4.23}$$

where $\bar{A}, \bar{B}$ (with initial porosity $f_0 = (A_0/B_0)^3$ and current porosity $f = (A/B_0)^3$) and $\bar{\lambda}_\theta$ (λ_θ at $r = B$) are given by

$$\bar{A} = \left(\frac{f_0}{f}\right)^{2/3},\ \bar{B} = (1+f-f_0)^{-2/3},$$

and

$$\bar{\lambda}_\theta = \left(\frac{B_0^3 + A^3 - A_0^3}{B_0^3}\right)^{1/3} = (1+f-f_0)^{1/3}. \tag{4.24}$$

On using Eq. (2.4) with (4.11), Eq. (4.23) reduced to

$$\begin{aligned} p &= 2\bar{\lambda}_\theta^2 \int_{\bar{A}}^{\bar{B}} \left[\left(\frac{1+\lambda_r^{3/2}}{\lambda_r^{1/2}}\right)\left\{\frac{C_1}{2}\exp\left(b\left(\lambda_r^2 + \frac{2}{\lambda_r} - 3\right)\right)\right.\right. \\ &+ \left.\left.\frac{C_2}{\lambda_r}\left(\frac{1}{\lambda_r^2} + 2\lambda_r - 3\right)\right\}\right] d\lambda_r. \end{aligned} \tag{4.25}$$

With the use of Eq. (4.24), Eq. (4.25) gives the desired relation between current porosity and pressure in terms of initial porosity during dehydration in apple and potato.

4.3 Porosity Measurement Methods

Porosity plays an important role in characterizing the quality and the texture of dry and intermediate moisture foods. It has significant effect on the physical (such as thermal conductivity, thermal diffusivity and diffusion coefficient), textural and mechanical properties of foods [125]. Porosity is defined as the volume fraction of the air or the void fraction in the sample, and expressed as:

$$\text{Porosity} = \frac{\text{Void volume}}{\text{Total volume}}.$$

Various methods, that can be used for porosity measurement of food products, were reported by Sahin and Sumnu [144], and are summarized as follows:

- **Direct method:** This method is used to determine the porosity by calculating the difference of bulk volume of a sample of porous material and the volume measured after destruction of all voids by compression. The porosity of very soft material can be determined by using this method.

- **Optical method:** In this method, porosity is determined from the microscopic view of a section of the porous medium. This method is appropriate if the porosity is uniform throughout the sample.

- **Density method:** In this method, porosity is measured from the densities of materials as:

  $$\text{Porosity} = 1 - \frac{\text{Bulk Density}}{\text{Particle Density}},$$

  where bulk density and particle density can be measured by the methods given in the literature [81]. In another way, if the densities data of the material are not available then porosity can be calculated from its pore volume. Liquid or gas displacement method [144] can be used for pore volume measurement.

- **Gas pycnometer method:** In this method, air comparison pycnometer is used to measure the porosity by measuring the volume fraction of air.

- **Using porosimeters:** Mercury porosimetry can be used to determine the porosity, pore's characteristics and pore size distribution. Porosimeters are based on the principle of either liquid extrusion from the pores or liquid intrusion into pores. In liquid intrusion method, liquid (such as oil, mercury or water) is forced into the pores by applying pressure and intrusion volume is measured. On the other hand, in extrusion porosimetry, pores in the porous materials are filled by wetting liquids and pressure is applied to displace the liquid from the pores. Further, change in volume of extruded liquid is measured with pressure.

Among these methods for porosity measurement, density method was used extensively by researchers to measure the porosity of apple, carrot and potato [184], potato [176] and apple, banana, carrot and potato [81, 83]. However, Gas pycnometer and porosimeters method was used for corn, wheat and sorghum kernels [23], apple, potato, cabbage and carrot [72] and apple [129]. These methods can also be used to measure porosity of food products before and after drying process. In the present chapter, the data used for porosity is measured by density method. The details of density method can be found in literature [81, 83, 176, 184] for the experimental measurement of porosity of apple and potato.

4.4 Results and Discussion

4.4.1 Analysis of Cavity Growth

To discuss the growth of cavity (pores) during dehydration in apple and potato, we have considered two possible cases for the value of A (i.e. growth of cavity). It may be possible that either $A = A_0$ or $A > A_0$.

(i) When $A = A_0$

It is evident from literature [93, 178] that the fresh apple and potato contains certain amount of arbitrarily distributed voids/pores in it. However, the cavities are small as

compared to the whole structure of the product. For instance, if we assume that initial porosity in these products is zero (i.e. $A_0 = 0$) which leads to $A = 0$, the Eqs. (4.2) and (4.8) describes a trivial deformation in which the body remains undeformed. Also, the value $A = 0$ contradicts the results regarding pores formation during dehydration, which have been reported in several experimental studies [83, 88, 129]. Therefore, the assumption $A_0 = 0$ is not valid and hence $A_0 > 0$. Again, if $A = A_0 > 0$, then Eqs. (4.2) and (4.8) describes a trivial deformation.

(ii) When $A > A_0$

In this case, cavity formation and size of cavity depends on the values of A_0. If we assume that $A_0 = 0$ (i.e. absence of initial porosity), then the value of p calculated from Eq. (4.25) is very large for formation of pores in drying products. Practically, no such large pressure can be generated during dehydration in these products. Therefore, it is reasonable to consider some positive value of initial pore radius (i.e. $A_0 > 0$). Also the value of A depends on p that should not exceed a suitable limit. The case $A = A_0$ is not possible as discussed above. The only possibility remains is $A > A_0$. For practically valid situations, we have explored all possible conditions for A. During dehydration when amount of water in apple and potato decreases, internal pressure in cells increases, consequently radius of cavity (A) increases.

4.4.2 Numerical Solution

Equation (4.25) presents the relationship between current porosity and pressure (in kPa), which is (responsible for counterbalancing force in formation of pores) developed on the surface of spherical elements containing pores formed by water evaporation during dehydration. The integral in Eq. (4.25) is evaluated numerically by using Gauss-Legendre quadrature rule. The values of constants, $b = 1$, $C_1 = 0.3524$ (MPa), $C_2 = 6.4440$ (MPa) for apple and $b = 1$, $C_1 = 0.0283$ (MPa), $C_2 = 3.0118$ (MPa) for potato, are taken from Chapter 2. The obtained relation (Eq. 4.25) is used to predict the porosity variation in apple and potato for varying pressure values during drying.

4.4.3 Experimental Data

For various drying methods and temperature, experimental works had been carried out for diverse food products (for example, apple, banana, carrot and potato) by several researchers [79, 80, 82], and a relationship between moisture content and maximum stress and maximum strain was reported in dehydrated products. This stress is analogy to the pressure generated on the cell-wall, or in other words, on the surface of spherical elements containing pores. The values of pressure generated on the spherical surface are varying in different drying methods; therefore, a range (from minimum value to maximum value) for pressure is considered in the present work. In the acquired range of pressure, we have done our calculation and obtained a range for porosity. This range of porosity is recumbence in between the range (values of porosity) which is given in literature. For different experimental studies, the values of initial porosity for apple and potato are presented in the Table (4.1).

Krokida and Maroulis [78] & Oikonomopoulou and Krokida [111] collected data of porosity for various foodstuffs, temperature, conditions and drying methods from literature. It was observed that porosity is varying from 0.1 to 0.92 and 0.03 to 0.89 for apple and potato, respectively. In the present study, for the applicability of the developed mathematical relation, data have been extracted from the experimental works [81, 176, 184] for apple and

Table 4.1: Initial porosity of apple and potato.

Product	**Initial porosity**	**References**
Apple	0.15	Krokida and Maroulis [81]
	0.182	Lozano et al. [88]
	0.194	Sablani and Rahman [139]
	0.20	Mavroudis et al. [92]; Rahman [128]
	0.22	Rahman et al. [129]
Potato	0.03	Mavroudis et al. [92]
	0.04	Lozano et al. [89]
	0.05	Suzuki et al. [162]; Zogzas et al. [184]
	0.08	Krokida and Maroulis [81]

potato.

4.4.4 Model Validation

The relationship between porosity and pressure, developed in the present work, is based on the strain energy function (Eq. 2.4). To study the mechanical properties of apple and potato, the adequacy of this strain energy function is described well in Chapter 2 and Chapter 3. The developed model has been validated with the help of existing experimental data. A good agreement has been obtained between predicted values and experimental data. It has been reported that this strain energy function is appropriate to study the mechanical properties of apple and potato. Therefore, in the present chapter, the strain energy function given in Eq. (2.4) has been used for the development of the desired relation. Further, by considering the range of pressure given in literature [79, 80], the values of porosity are calculated for various drying methods. The obtained values of porosity are checked and found in the range which is given in literature [81, 176, 184]. Therefore, it can be concluded that the relation developed in the present chapter is appropriate for the study of porosity behavior as a function of pressure.

4.4.5 Porosity Variation in Different Drying Methods

By using Eq. (4.25), values of current porosity are calculated for the different values of pressure. For various drying methods, the effects of pressure and initial porosity on the current porosity are plotted in the Figs. (4.2–4.6) for apple and Figs. (4.7–4.11) for potato. Before starting the drying process, when there is no moisture loss, the porosity (i.e. the initial porosity) is shown in Figs. (4.2–4.11) corresponding to pressure $p = 0$. During dehydration, as moisture content decreases in apple and potato samples, air fill the space left by the water. Increasing volume of air put the pressure on the cell-wall, as a result cell shrinks which causes increment in the porosity. Further, during dehydration, it can be seen that the current porosity increases as initial porosity increases.

4.4.5.1 Porosity Variation in Apple

The variations in current porosity with respect to pressure and initial porosity are presented in Figs. (4.2–4.6) for apple in various drying methods. The main results are summarized as follows:

- Figure (4.2) depicts the porosity variation as a function of pressure and initial porosity during freeze drying of apple.
- Due to continuous process of drying, moisture loss from the sample increases, which causes increment in pressure, consequently current porosity increases in the sample. Pressure and initial porosity has significant effects on the current porosity.
- The current porosity increment is depending on the initial porosity and it is higher for the greater value of the initial porosity. For any particular fixed value of pressure, significant increment in current porosity is observed corresponding to greater value of initial porosity. For example, in freeze drying for $p = 10$, the value of current porosity is 0.445 corresponding to initial porosity 0.15, whereas current porosity is 0.651 corresponding to initial porosity 0.22 (Fig. 4.2).
- Further, initial porosity has considerable effect on pressure. It is observed that for the high value of initial porosity, less amount of pressure is sufficient to attain the maximum value of current porosity. For example, in freeze drying, for initial porosity 0.15, maximum value of current porosity (0.9357) is achieved for $p = 53.2578$, whereas for initial porosity 0.22, maximum value (0.9357) is achieved for $p = 24.7555$ (Fig. 4.2).
- Figure (4.3) displays the effect of the pressure and the initial porosity on the current porosity for vacuum drying of apple. Graphs are plotted for different values of the initial porosity (0.15, 0.182, 0.194, 0.2, 0.22).
- From Fig. (4.3), it can be observed that the current porosity increases as pressure increases. That is, at the initial drying stage, moisture removes rapidly from the sample, which causes the rapid increment in pressure, consequently, current porosity increases swiftly. However, the increment of porosity become slow for latter drying stages.

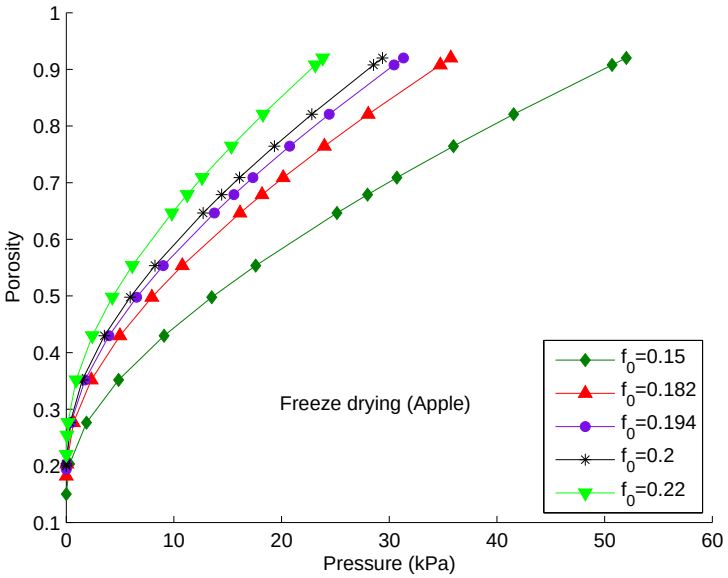

Figure 4.2: Porosity variation with respect to initial porosity and pressure developed due to water removal during freeze drying of apple.

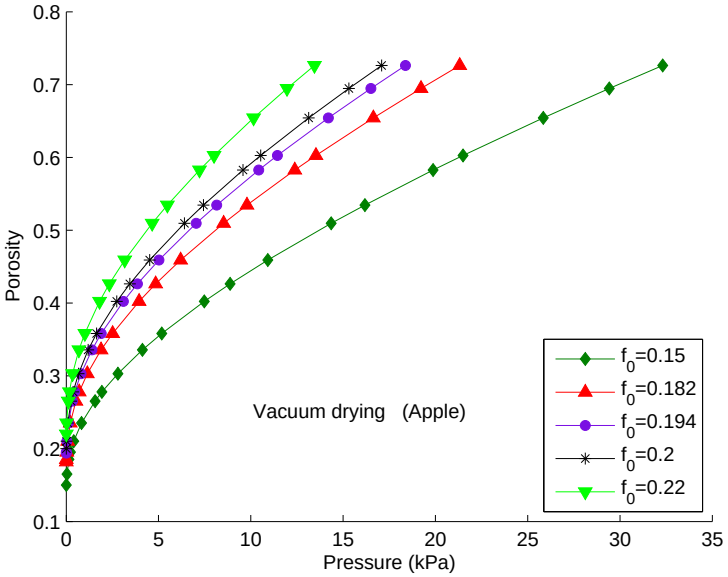

Figure 4.3: Porosity variation with respect to initial porosity and pressure developed due to water removal during vacuum drying of apple.

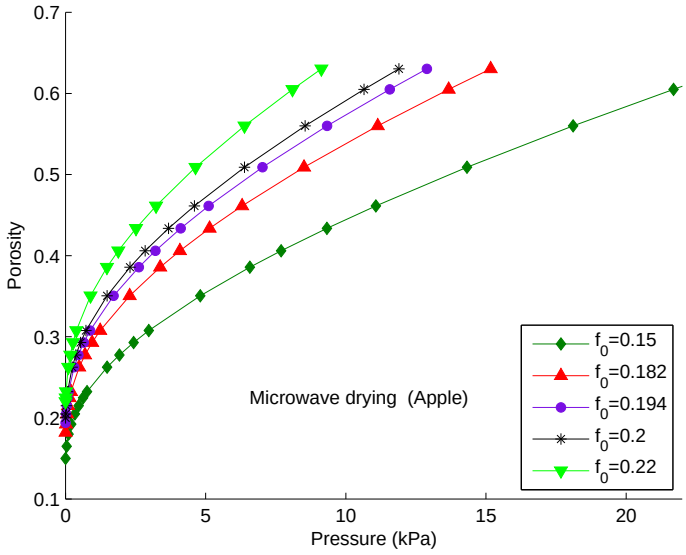

Figure 4.4: Porosity variation with respect to initial porosity and pressure developed due to water removal during microwave drying of apple.

- In the vacuum drying, values of pressure and current porosity are less as compare to freeze drying for the same value of initial porosity (Fig. 4.3).

- Figures (4.4 and 4.5) illustrate the current porosity variation with respect to pressure and initial porosity for microwave and convective drying, respectively. Again, current porosity increases as pressure increases.

- In microwave and convective drying, similar effects of the initial porosity, as in freeze and vacuum drying, are observed on current porosity and pressure. When the value of initial porosity is low, the highest value of current porosity is achieved at large amount of pressure, whereas corresponding to higher value of initial porosity, highest value of current porosity is achieved at lower amount of pressure.

- In the microwave and convective drying, the values of pressure and current porosity are less as compare to vacuum drying (Figs. 4.3 and 4.5).

- For the osmotic dehydration of apple sample, the dependence of current porosity on pressure and initial porosity is presented in Fig. (4.6).

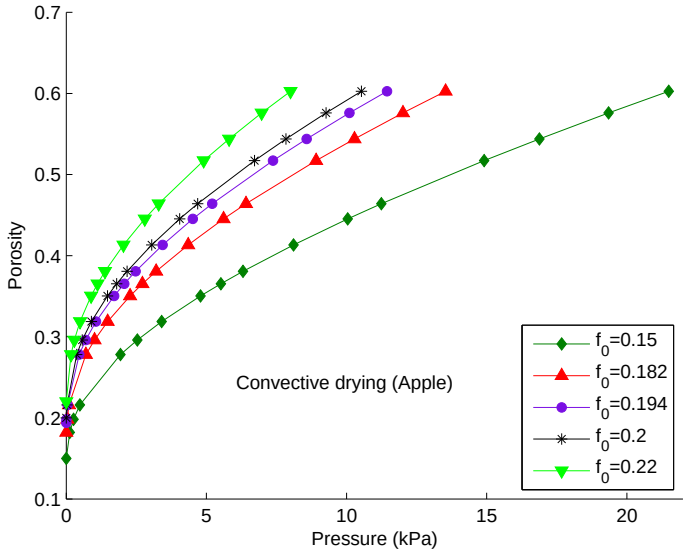

Figure 4.5: Porosity variation with respect to initial porosity and pressure developed due to water removal during convective drying of apple.

- Current porosity is increasing with pressure, which favour the physical phenomenon of food dehydration. Further, current porosity and generated pressure depends on the initial porosity. For lower values of initial porosity, higher value of pressure causes porosity increment, while for higher value of initial porosity, lower value of pressure causes porosity increment.

- In case of osmotic dehydration, the values of pressure and current porosity are less as compare to microwave and convective drying (Fig. 4.6).

- Figures (4.2–4.6) illustrate that the current porosity varies from 0.15 to 0.93, 0.72, 0.63, 0.60 and 0.54 in the cases of freeze drying, vacuum drying, microwave drying, convective drying and osmotic dehydration, respectively. These range of porosity for apple are supported by experimental results [78, 111] for different drying methods.

- Current porosity is the highest in freeze drying (Fig. 4.2), whereas it is the lowest in osmotic dehydration (Fig. 4.6). The high porosity in freeze drying of foodstuffs is the consequence of absence of capillary forces during sublimation of the frozen solvent [90].

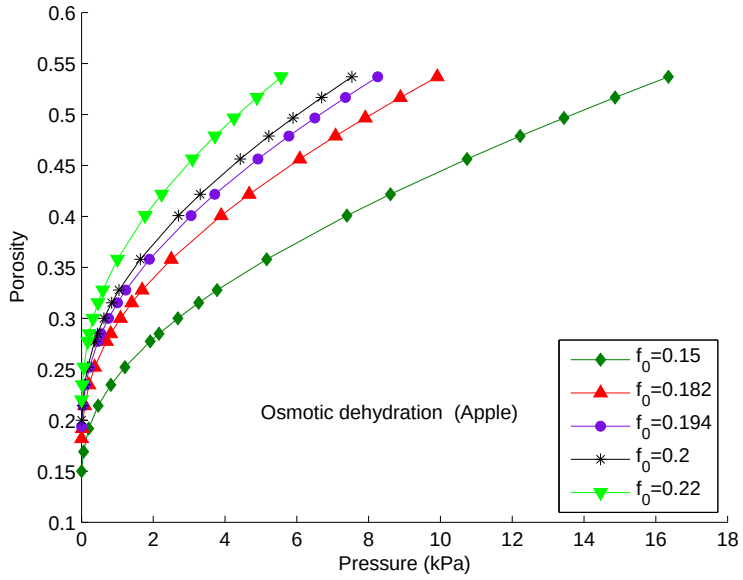

Figure 4.6: Porosity variation with respect to initial porosity and pressure developed due to water removal during osmotic dehydration of apple.

- In the different drying methods, greatest value of pressure is different (Figs. 4.2–4.6). It is maximum in freeze drying whereas minimum in osmotic dehydration.

In the early stage of drying, the porosity increases rapidly for all values of the initial porosity and after that its increasing rate became slow. The open space in the structure formed by the water evaporation is caused of the incapability of structure to collapse perfectly as water evaporated [72]. The cause for collapse may be the interfacial tension of tissue's walls filled with water.

4.4.5.2 Porosity Variation in Potato

The current porosity and generated pressure are shown in Figs. (4.7–4.11) for various drying methods and different values of initial porosity in potato. Further, following results are observed:

- Figure (4.7) depicts the effects of pressure and initial porosity on current porosity for freeze drying of potato. It is observed that the current porosity increases as pressure increases.

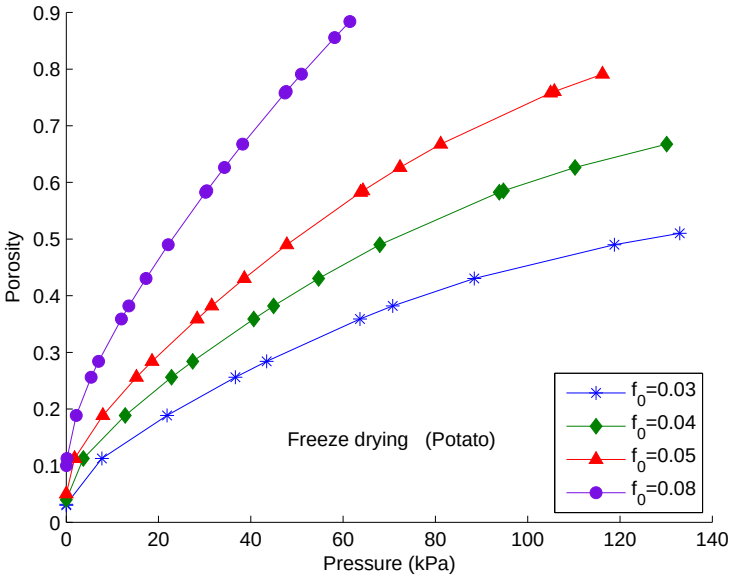

Figure 4.7: Porosity variation with respect to initial porosity and pressure developed due to water removal during freeze drying of potato.

- Further, current porosity depends on the initial porosity. For any fixed value of pressure, the higher value of current porosity is observed corresponding to greater value of initial porosity.

- Pressure is also affected by initial porosity. For less values of initial porosity, large amount of pressure generated in potato cells. However, for greater value of initial porosity, lesser amount of pressure are generated which is responsible for porosity.

- Similar types of behavior of porosity and pressure are recorded for microwave drying of potato (Fig. 4.8).

- Figures (4.7) and (4.8) display that the high pressure is generated in potato cells. The possible explanation of high pressure in these drying methods are as follows: in freeze drying method large crystal of ice form, which is responsible for high pressure. Whereas, in microwave drying electromagnetic waves are used to generate the heat inside the material, which causes the high pressure.

- The current porosity variation, in terms of pressure and initial porosity, are presented

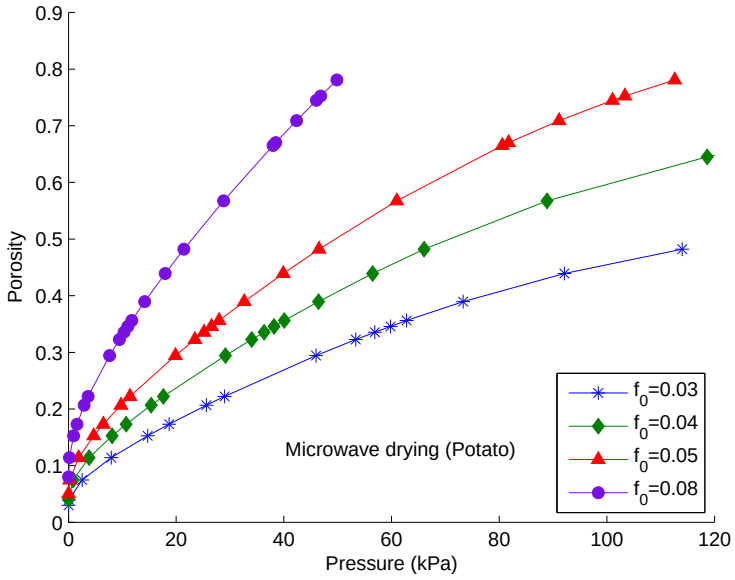

Figure 4.8: Porosity variation with respect to initial porosity and pressure developed due to water removal during microwave drying of potato.

in Figs. (4.9–4.11) for vacuum drying, drying at 70^oC and convective drying, respectively. Similar trends of current porosity, as for freeze and microwave drying, are observed for these drying methods.

- The value of current porosity is the highest in freeze drying (Fig. 4.7), whereas it is the lowest in convective drying (Fig. 4.11).

- The current porosity increases rapidly in starting drying hours of potato in case of vacuum drying, convective drying and drying at temperature 70^oC for initial porosities 0.05 and 0.08, whereas the value of current porosity is lower in these cases for initial porosities 0.03 and 0.04.

- The values of porosity and pressure are higher in vacuum drying than the convective and drying at 70^oC but lower than the freeze and microwave drying.

- The porosity characteristics presented the nonlinear variation with respect to pressure, as expressed, in the form of Eq. (4.25). Further, it can be seen from Figs. (4.7–4.11) that the current porosity increases rapidly for slight changes in initial porosity.

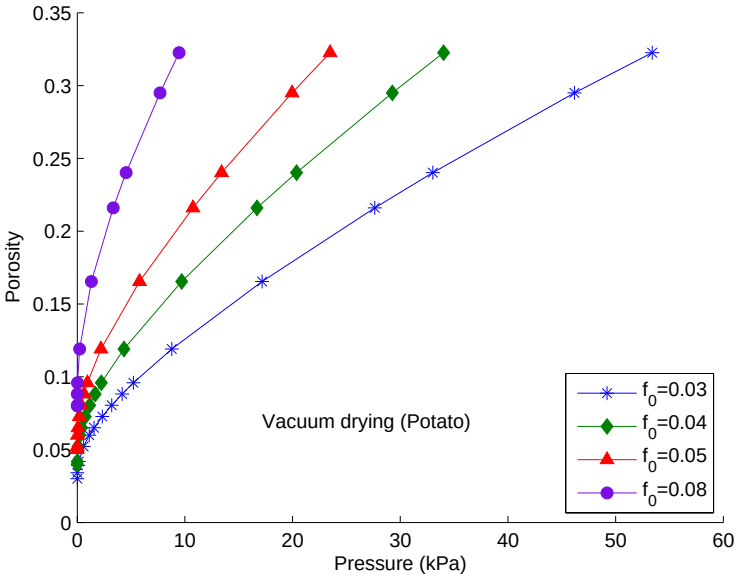

Figure 4.9: Porosity variation with respect to initial porosity and pressure developed due to water removal during vacuum drying of potato.

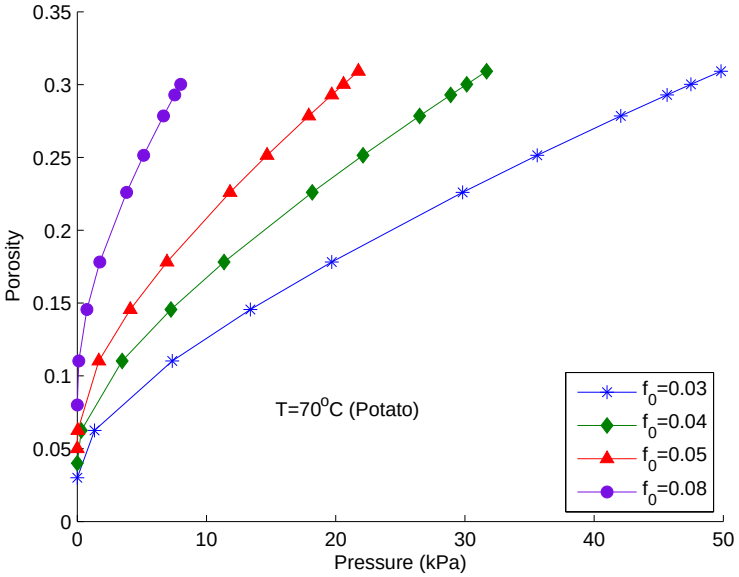

Figure 4.10: Porosity variation with respect to initial porosity and pressure developed due to water removal during drying potato at 70^oC.

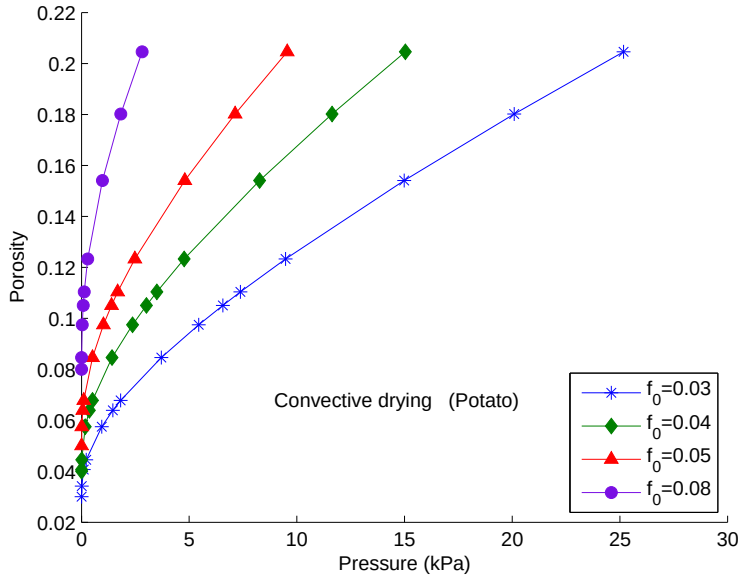

Figure 4.11: Porosity variation with respect to initial porosity and pressure developed due to water removal during convective drying of potato.

- For potato (Figs. 4.7–4.11), current porosity varies from 0.03 to 0.88, 0.78, 0.32, 0.31, 0.20 in case of freeze drying, microwave drying, vacuum drying, drying at temperature 70^oC and convective drying, respectively, for the given values of pressure. These range of porosity for potato are supported by experimental results [78, 111] for different drying methods.

- It is also observed that potato is more sensitive against drying temperature than the apple. The rate of porosity increment in potato drying is high as compare to apple drying.

- Ultimately, the increasing porosity affects the shrinkage properties of apple and potato predominantly.

The possible reason of the formation of porosity in foodstuffs explained by Krokida et al. [83] is given as: in the initial drying hours, cellular tissues are sufficiently elastic to shrink into the space left by the evaporated water. As the drying process proceeds, the water is replaced by air, and hence, structural changes occur in the tissue that results in a more rigid

skeleton, that favoring the development of porosity. Further, results obtained in this chapter are supported by experimental results of Krokida and Maroulis [81].

4.4.6 Comparison of Different Drying Techniques

Several drying methods are generally liable for formation of different porous micro and macro structures in a different way due to various process parameters. In the process of freeze drying of apple and potato, internal water from these products removed in two steps: firstly, the product is frozen by keeping pressure and temperature low, and secondly, the water is removed by sublimation. In the vacuum drying method, drying is performed using low temperature and different pressure. In the microwave drying method, heat inside the material is generated using electromagnetic waves. This method is applied by food industries to dry the products at the reduced drying time using dielectric heating with microwaves. Convective air drying is the most widely applied method for food dehydration. In this method, high temperature is applied for drying food products, and the moisture is removed from the center to the surface of the product. In the osmotic dehydration method, apple and potato is immersed in the concentrated solutions, as a result, products of intermediate moisture content obtain due to natural water removal. The details of various drying techniques can be found in literature [78, 111]. Drying methods have immeasurable influences on the porosity of apple and potato. Results of these methods can be compared as follows:

- The final porosity for apple is the highest (92%) in freeze drying (Fig. 4.2) and the lowest (54%) in osmotic dehydration (Fig. 4.6). The higher porosity value for apple means that the greater volume of pores is formed during freeze drying. The larger pores creation is the consequence of larger ice crystal development during freeze drying. The porosity of apple during other drying techniques, such as vacuum drying, microwave drying and convective drying are 73%, 63% and 60%, respectively.

- It is clear that the microwave dried apple developed lower porosity than vacuum dried apple and greater porosity than convective dried apple (Figs. 4.3–4.5). Similar results for porosity of apple were reported by Krokida and Maroulis [82].

- In the case of potato drying, the freeze dried potato (Fig. 4.7) developed the highest porosity (89%), whereas the lowest porosity (21%) is obtained in convective drying (Fig. 4.11). These results are agreed with those obtained by Krokida and Maroulis [82] and Zogzas et al. [184]. For the other drying methods, for example, microwave drying, vacuum drying and air drying at temperature 70^oC, the porosity of potato is 78%, 33% and 31%, respectively.

- The porosity of vacuum dried potato is greater than the porosity of air dried potato and lower than the porosity of microwave dried potato (Figs. 4.8–4.10). Similar results were reported by Krokida and Maroulis [78, 82] for porosity of potato.

It is evident from results, discussed above for porosity of apple and potato, that the dried apple developed higher porosity than the dried potato in freeze drying, vacuum drying and convective drying. This means that the apple is more capable to shrink as compare to potato. These results may be helpful for food drying industries to choose an appropriate drying technique to obtain the desired quality, appearance and texture of final product.

4.5 Conclusions

In the present chapter, a mathematical relation, for the prediction of porosity (volume fraction of pores) variation in apple and potato, is developed as a function of initial porosity and pressure which is (responsible for the counterbalancing forces) developed on the surface of porous spherical structure during dehydration. Current porosity is largely depended on the initial porosity. For the different values of initial porosity, the effect of pressure on the current porosity is obtained. The obtained porosity range for apple and potato is satisfactory and agreed by the previously published experimental observations. It is evident from practical situations that the contraction stress (pressure) increases in cells of apple and potato due to water removal. Therefore, the present study justifies the physical behavior of apple and potato in respect of change of porosity and pressure during dehydration. Additionally, due to close resemblance between experimental and theoretical results, the developed mathematical relation is appropriate for the study of porosity behavior of apple and potato. This

relation may be helpful in food industries for choosing the suitable drying process according to requirement of final dried product. Also, it can be used in further studies for the calculation of porosity and structural properties of apples and potatoes. Eventually, the use of this mathematical relation can be extended to examine the porosity behavior for other fruits and vegetables during dehydration.

Chapter 5

Modeling of Time Based Variation of Moisture Content, Density, Porosity and Specific Volume during Drying of Apple and Potato

5.1 Introduction

Among various fruits and vegetables, apple and potato are the most widely used foods for consumption. These are frequently used in different forms, processed and unprocessed. Fresh apple and potato contains a large percentage of water, which should be removed to obtain long time preservable processed products. Water removal from apple and potato is the main factor responsible for changing their physical properties during dehydration. It is a very crucial and complex process. The applications of food drying techniques are very common to improve food stability and minimize chemical and physical changes during storage [95]. Drying is the most extensively used technique for food preservation [45, 53, 171]. This process is often used in food industries to maintain the quality, nutrition values and extend the shelf-life of foods.

During drying, tension inside the cells of biological products (such as apple and potato)

reduces due to water removal which caused the amendment in cellular structure [153]. As a result, a considerable reduction in shape, size, mass and volume of food products occurs that influences their structural properties. Therefore, dehydrated food products have many benefits, such as convenience in use and minimize transportation, storage and packaging cost and time [141].

Structural properties, such as shrinkage, porosity, density (particle and bulk) and specific volume generally characterize the structure of dried apple and potato. These properties are immensely affected due to the water reduction, and play a crucial role in characterizing the quality of final dried product. These properties are also very essential in improvement of the quality of existing products, and in the development of new industrial products with specific desired properties. These structural properties have been investigated by several researchers by performing experiments on different fruits and vegetables. In this process, Lozano et al. [89] reported the data on bulk density, porosity and shrinkage as a function of moisture content by performing experiments on pears, carrots, potatoes, sweet potatoes and garlic. Porosity and density in drying starch materials were investigated by Marousis and Saravacos [91]. Further, a linear relationship between porosity and moisture content, and a polynomial function for density and moisture content were fitted with obtained data. For the prediction of structural properties as a function of moisture content, several researchers have proposed mathematical models for apple, banana, carrot and potato [81, 83], potato [176], apple, potato and carrot [184]. Al-Muhtaseb et al. [4] examined the shrinkage, bulk density, particle density and porosity with respect to moisture content variation of potato starch gel. Experimental data of various vegetables for apparent density, true density and porosity in terms of moisture content was correlated with a simple mathematical model [17]. Chemkhi and Zagrouba [29] experimentally determined the density and shrinkage of potato and correlated the data with density and shrinkage equations as a function of moisture content.

It is clear from above literature that the mathematical models, developed by several researchers to predict structural properties of various food products, are the function of moisture content solely. During dehydration, the effect of drying time on the structural properties has not been considered so far. The concept of structural properties in terms of drying time

may be interesting and give a new direction in further research to obtain a desired quality of dried food products. For industries point of view, variations in structural properties with respect to time are important for allocation and optimization of resources. Furthermore, to obtain the desired quality of dried food products, measurement of moisture content repeatedly is time consuming and may contain errors during the measurement process. Therefore, to resolve this problem, a mathematical model needs to be developed to predict moisture content as a function of drying time and then use of this model to predict structural properties in terms of drying time.

Mathematical modeling is an important tool to study the drying characteristics of fruits and vegetables under different drying conditions. It provides a platform where overall improvement in quality of the final products can be controlled. Mathematical models are generally used to describe the drying behavior and predict the quality of the dried products with the help of variables involved in the process. Several thin layer drying models are available in literature. These models are frequently used to describe the drying behavior of different agricultural products, for example, carrots [1], apple, potato and pumpkin [2], potato [14], sweet potato [42], black tea [115], apple [140, 171], pumpkin, green pepper, stuffed pepper, green bean and onion [180].

The thin-layer drying is defined by Akpinar [2] as to dry one layer of sample or slice of fruits or vegetables. The drying phenomenon of these products can be described by the thin-layer drying models that can be categories as theoretical, semi-theoretical and empirical [115]. The first category of thin-layer drying models is considered for study the internal resistance to moisture transfer, while other two categories are considered for study the external resistance to moisture transfer between air and product [61]. The theoretical models are derived from Fick's second law of diffusion [115], while semi-theoretical models are generally derived from Fick's second law by its modifications and from Newton's law of cooling [45].

Keeping above literature in mind, the overall objective of this chapter is to (i) propose a suitable drying model for moisture content as a function of drying time and use this model to study the drying characteristics of apple and potato; (ii) conduct experiments on one variety of apple and three varieties of potato at different drying temperature to validate the proposed

drying model; (iii) describe the influences of temperature on drying kinetics of apple and potato; and (iv) use of the proposed drying model for determining the structural properties of apple and potato with respect to drying time.

5.2 Mathematical Model

5.2.1 Drying Model

The concept of thin-layer drying models for characterizing the drying behavior was suggested, initially, by Lewis [85], who derived the semi-theoretical model from Newton's law of cooling for porous hygroscopic materials

$$MR = \frac{X - X_e}{X_0 - X_e} = \exp(-kt), \tag{5.1}$$

where MR is the moisture ratio, X, X_e and X_0 are the instantaneous, equilibrium and initial moisture contents (g water/g dry matter), respectively, k is the drying constant (m^{-1}), t is the time (min). After that, Page [114] modified the Lewis model by adding a dimensionless empirical constant (n) and used it for study the drying behavior of shelled corns

$$MR = \frac{X - X_e}{X_0 - X_e} = \exp(-kt^n). \tag{5.2}$$

Overhults et al. [113] modified the Page model and obtained the following equation (this model is known as Modified Page-I Model)

$$MR = \frac{X - X_e}{X_0 - X_e} = \exp(-kt)^n. \tag{5.3}$$

In addition, to describe the drying kinetics of soybeans, White et al. [179] introduced the following model (this model is known as Modified Page-II Model)

$$MR = \frac{X - X_e}{X_0 - X_e} = \exp(-(kt)^n). \tag{5.4}$$

Table 5.1: Semi-theoretical thin-layer drying models.

No.	Model Name	Model equation	References
1	Lewis (Newton)	$MR = \exp(-kt)$	Lewis [85]
2	Page	$MR = \exp(-kt^n)$	Page [114]
3	Modified Page-I	$MR = \exp(-kt)^n$	Overhults et al. [113]
4	Modified Page II	$MR = \exp(-(kt)^n)$	White et al. [179]
5	Modified Page equation- II	$MR = \exp(-k(t/l^2)^n)$	Diamante and Munro [42]
6	Midilli et al.	$MR = a\exp(-kt^n) + bt$	Midilli et al. [101]
7	Two term exponential	$MR = a\exp(-kt) + (1-a)\exp(-kat)$	Sharaf-Eldeen et al. [148]
8	Modified Two-Term Exponential	$MR = a\exp(-kt) + (1-a)\exp(-gt)$	Verma et al. [172]
9	Approximation of Diffusion	$MR = a\exp(-kt) + (1-a)\exp(-kbt)$	Kaseem [73]; Yaldýz and Ertekýn [180]
10	**Our model**	$MR = \exp(-(kt)^n) - akt$	**Present work**

Except of these models, several other researchers have used Fick's second law of diffusion for derivation of thin-layer drying models for study of drying behavior of different agricultural products (a list is given in the Table 5.1).

The drying process of apple and potato is considered as the external resistance to moisture transfer between air and product. Therefore, the drying behavior of these products can be characterized by semi-theoretical thin-layer drying models. Various drying models were tested with measured experimental data for apple and potato. Some of them were good, but others have shortcomings, such as they were failed to describe drying behavior of these products at the time $t = 0$. Also, during the initial hours of drying, some models under predict the drying behavior, while they over predict the drying behavior during the later stages of drying. Further, the number of parameters should be less in a model to be estimated adequately and fit the model to experimental data. In this context, to overcome from the above-mentioned shortcomings, we proposed the following semi-theoretical model to study the drying kinetics of apple and potato

$$MR = \frac{X - X_e}{X_0 - X_e} = \exp(-(kt)^n) - akt, \tag{5.5}$$

where X, X_e and X_0 are the instantaneous, equilibrium and initial moisture contents (g water/g dry matter), respectively, k is the drying constant (m^{-1}), t is the drying time, n is the dimensionless empirical drying exponent and a is the empirical model constant (dimensionless).

The constant a is introduced for obtaining the best fit of the model to experimental data; whereas, the drying exponent n is introduced to obtain rapid drying behavior during the early stage of drying. The proposed model is the modification of the Modified Page-II model by adding a linear term. The linear term is added in this model to overcome the problem of over prediction drying behavior of apple and potato during last drying hours. The moisture ratio (MR) can be calculated from Eq. (5.6) instead of $(X - X_e)/(X_0 - X_e)$ due to the very small value of X_e as compare to X or X_0 ([140, 166])

$$MR = \frac{X}{X_0}. \tag{5.6}$$

Hence, Eq. (5.5) reduced to

$$MR = \frac{X}{X_0} = \exp(-(kt)^n) - akt. \tag{5.7}$$

The amount of the evaporated moisture with respect to time is termed as drying rate and can be expressed as

$$DR = \frac{X_{t+\Delta t} - X_t}{\Delta t}, \tag{5.8}$$

where DR is the drying rate (g water/g dry matter. min), X_t and $X_{t+\Delta t}$ are the moisture contents (g water/g dry matter) at the time t and $t + \Delta t$, respectively, t is the drying time (min).

The dependence of drying constant (k) on the drying temperature (T) is described by the exponential equation

$$k = C\exp(DT), \tag{5.9}$$

where C and D are constants.

5.2.2 Density, Porosity and Specific Volume Model

Several researchers (e.g., [82, 83, 184]) have performed experiments on apple, potato, banana and carrot to examine the density (particle and bulk), porosity and specific volume at various moisture contents. Further, to predict these properties, following mathematical models were proposed:

Particle density

$$\rho_p(X) = \frac{1+X}{\frac{1}{\rho_s} + \frac{X}{\rho_w}}, \tag{5.10}$$

Bulk density

$$\rho_b(X) = \frac{1+X}{\frac{1}{\rho_{b0}} + \frac{\beta' X}{\rho_w}}, \tag{5.11}$$

Porosity

$$\varepsilon(X) = 1 - \frac{\rho_b}{\rho_p}, \tag{5.12}$$

Specific volume

$$v(X) = \frac{1}{\rho_{b0}} + \frac{\beta' X}{\rho_w}, \tag{5.13}$$

where four parameters define as: the dry solid density ρ_s, the density of enclosed water ρ_w, the dry solid bulk density ρ_{b0}, and the volume shrinkage coefficient β'.

It is clear from the above equations that the structural properties are calculated as function of moisture content only. By using Eq. (5.7), these properties (particle density, bulk density, porosity and specific volume) can be calculated as a function of time. Therefore, substituting the value of X (moisture content) from Eq. (5.7) into Eqs. (5.10–5.13) and denoting $f = akX_0$, we obtain

Particle density

$$\rho_p(t) = \frac{1 + \{X_0 \exp(-(kt)^n) - ft\}}{\frac{1}{\rho_s} + \frac{\{X_0 \exp(-(kt)^n) - ft\}}{\rho_w}}, \tag{5.14}$$

Bulk density

$$\rho_b(t) = \frac{1 + \{X_0 \exp(-(kt)^n) - ft\}}{\frac{1}{\rho_{b0}} + \frac{\beta'\{X_0 \exp(-(kt)^n) - ft\}}{\rho_w}}, \tag{5.15}$$

Porosity

$$\varepsilon(t) = 1 - \frac{\rho_b(t)}{\rho_p(t)}, \tag{5.16}$$

Specific volume

$$v(t) = \frac{1}{\rho_{b0}} + \frac{\beta'\{X_0 \exp(-(kt)^n) - ft\}}{\rho_w}. \tag{5.17}$$

These are the desired equations for structural properties as function of drying time.

5.3 Material and Methods

5.3.1 Material

One apple variety (Fuji) was purchased at the local market in Shimla, Himachal Pradesh, India and kept at the room temperature until use. Further, three potato varieties, Kufri Chipsona-1, Kufri Himsona and Kufri Bahar, harvested in the month of March 2014 at Central Potato Research Institute Campus Modipuram, Uttar Pradesh, India, were used for the drying experiments. After harvesting, potatoes were stored at temperature 12^oC and humidity 90% until the drying experiments carried out. The experiments were conducted during the month of July 2014 in the PHT Laboratory of Central Potato Research Institute Shimla, Himachal Pradesh, India.

5.3.2 Sample Preparation

Before starting of each experiment, apple and potato were washed in running tap water, and cut into slices of 2 mm thickness by a mechanical slicer. Out of these slices, $20g$ sample was used from each variety for drying experiments. To calculate the initial moisture content, $100g$ sample of each variety was dried in an oven dryer at temperature 80^oC for 24 hours. The initial moisture content (wet basis) was found 85.45% of apple and 76.51%, 75.70% and 84.83% of Kufri Chipsona-1, Kufri Himsona and Kufri Bahar, respectively.

5.3.3 Experimental Procedure

The drying experiments were carried out using a tray dryer equipped with temperature controller, thermometer and multiple drying trays. From each apple and potato variety, $20g$ sample was placed in the tray dryer. Drying experiments were conducted at temperatures $60, 70$ and 80^oC. Each experiment was performed in five replications at each temperature and time to calculate the moisture contents.

Before placing samples in the dryer, the dryer was run for at least two hour to obtain steady temperature. Once the temperature had stabilized, the samples were placed on the tray and placed it in the dryer. A digital balance (SD Fine-Chem Limited, India EA-300, precision of $0.01g$) was used to determine the water loss from the samples by weighing the samples periodically during the drying process. The samples were weighted at every 30 minute time interval from starting to end of the process. The drying process was continued until the final moisture content of the samples reached approximately $3-5\%$ (dry basis) of each variety. The averages of five replications were calculated at each temperature and time in every experiment.

5.3.4 Statistical Analysis

A non-linear regression technique was employed for analysis of data measured during drying experiments. Among the various criterion of model fitting to experimental data, we used statistical test methods, such as chi-square (χ^2), coefficients of determination (R^2), and root

mean square error (RMSE), to evaluate the goodness of fit. The Levenberg-Marquardt (LM) algorithm was used for non-linear regression analysis. The higher values of R^2 and the lower values of RMSE and χ^2 were chosen as the criteria for goodness of fit.

5.4 Results and Discussion

5.4.1 Drying Properties

The dimensionless moisture content as a function of drying time is given by the Eq. (5.7). The moisture contents data, obtained in drying experiments, are fitted to drying model (Eq. 5.7) by employing non-linear regression technique. The calibrated values of model constants are written in the Table (5.2) for different drying temperature $(60, 70$ and $80^oC)$.

5.4.1.1 Fitting of the Drying Models

Several semi-theoretical drying models (Table 5.1) are fitted to the data of moisture content after converted it to moisture ratio (MR) by using the Eq. (5.6). The statistical results and comparison of models are shown in Tables (5.3 – 5.6) for apple, Kufri Chipsona-1, Kufri Himsona and Kufri Bahar, respectively.

Table 5.2: Estimated constants related to proposed model at different drying temperature for apple and potato.

Product	**Variety**	60^oC	70^oC	80^oC
Apple	Fuji	$k = 0.00761$ $n = 1.38951$ $a = 0.00455$	$k = 0.00941$ $n = 1.36380$ $a = 0.00254$	$k = 0.01283$ $n = 1.24917$ $a = 0.00061$
Potato	Kufri Chipsona-1	$k = 0.00523$ $n = 1.60203$ $a = 0.00644$	$k = 0.00655$ $n = 1.41921$ $a = 0.01038$	$k = 0.00834$ $n = 1.48259$ $a = 0.00618$
	Kufri Himsona	$k = 0.00549$ $n = 1.70892$ $a = 0.00202$	$k = 0.00714$ $n = 1.49928$ $a = 0.00560$	$k = 0.00886$ $n = 1.56078$ $a = 0.00324$
	Kufri Bahar	$k = 0.00570$ $n = 1.61507$ $a = 0.00280$	$k = 0.00696$ $n = 1.41448$ $a = 0.00930$	$k = 0.00851$ $n = 1.46990$ $a = 0.00716$

Table 5.3: Statistical results and comparison of various drying models at different temperature for apple.

		60^oC			70^oC			80^oC		
No.	**Model Name**	χ^2	R^2	*RMSE*	χ^2	R^2	*RMSE*	χ^2	R^2	*RMSE*
1	Lewis (Newton)	3.690E-3	0.9574	0.06073	2.580E-3	0.9777	0.05084	1.290E-3	0.9887	0.03589
2	Page	1.038E-4	0.9989	0.01019	1.434E-4	0.9988	0.01198	1.452E-4	0.9988	0.01205
3	Modified Page-I	3.690E-1	0.9709	0.06073	2.820E-3	0.9777	0.05310	1.430E-3	0.9987	0.03783
4	Modified Page II	9.506E-5	0.9992	0.00975	1.432E-4	0.9988	0.01197	1.451E-4	0.9988	0.01205
5	Modified Page equation- II	1.043E-4	0.9992	0.01021	1.582E-4	0.9988	0.01258	1.633E-4	0.9988	0.01278
6	Midilli et al.	9.919E-5	0.9993	0.00996	1.815E-4	0.9988	0.01347	1.840E-4	0.9988	0.01357
7	Two term exponential	3.690E-3	0.9709	0.06073	2.820E-3	0.9777	0.05310	1.430E-3	0.9887	0.03783
8	Modified Two-Term Exponential	1.230E-3	0.9911	0.03504	1.100E-3	0.9921	0.03318	4.577E-4	0.9968	0.02139
9	Approximation of Diffusion	1.976E-4	0.9987	0.01406	2.382E-4	0.9982	0.01543	1.603E-4	0.9989	0.01266
10	**Our model**	8.045E-5	0.9994	0.00897	1.407E-4	0.9990	0.01186	1.066E-4	0.9992	0.01033

Table 5.4: Statistical results and comparison of various drying models at different temperature for Kufri Chipsona-1.

		60^oC			70^oC			80^oC		
No.	**Model Name**	χ^2	R^2	*RMSE*	χ^2	R^2	*RMSE*	χ^2	R^2	*RMSE*
1	Lewis (Newton)	6.810E-3	0.9446	0.08255	4.480E-3	0.9626	0.06695	4.990E-3	0.9607	0.07064
2	Page	1.910E-4	0.9985	0.01382	2.000E-4	0.9984	0.01414	1.518E-4	0.9989	0.01232
3	Modified Page-I	7.270E-3	0.9446	0.08525	4.860E-3	0.9626	0.06968	5.540E-3	0.9607	0.07446
4	Modified Page II	1.889E-4	0.9985	0.01375	1.989E-4	0.9984	0.01411	1.513E-4	0.9989	0.01230
5	Modified Page equation- II	2.051E-4	0.9985	0.01432	2.203E-4	0.9984	0.01485	1.716E-4	0.9989	0.01310
6	Midilli et al.	2.121E-4	0.9986	0.01456	1.386E-4	0.9990	0.01177	1.722E-4	0.9990	0.01313
7	Two term exponential	7.270E-3	0.9446	0.08526	4.860E-3	0.9626	0.06968	5.550E-3	0.9607	0.07447
8	Modified Two-Term Exponential	3.470E-3	0.9735	0.05890	1.920E-3	0.9864	0.04383	2.100E-3	0.9867	0.04583
9	Approximation of Diffusion	7.391E-4	0.9947	0.02719	4.528E-4	0.9968	0.02128	4.602E-4	0.9971	0.02145
10	**Our model**	1.656E-4	0.9988	0.01287	1.304E-4	0.9991	0.01142	1.372E-4	0.9991	0.01171

Table 5.5: Statistical results and comparison of various drying models at different temperature for Kufri Himsona.

		60^oC			70^oC			80^oC		
No.	**Model Name**	χ^2	R^2	*RMSE*	χ^2	R^2	*RMSE*	χ^2	R^2	*RMSE*
1	Lewis (Newton)	7.420E-3	0.9406	0.08615	5.050E-3	0.9590	0.07108	5.860E-3	0.9555	0.07655
2	Page	3.431E-4	0.9974	0.01852	2.475E-4	0.9981	0.01573	2.108E-4	0.9985	0.01452
3	Modified Page-I	7.920E-3	0.9406	0.08898	5.470E-3	0.9590	0.07399	6.510E-3	0.9555	0.08070
4	Modified Page II	3.412E-4	0.9974	0.01847	2.455E-4	0.9981	0.01567	2.099E-4	0.9985	0.01449
5	Modified Page equation- II	3.696E-4	0.9974	0.01923	2.720E-4	0.9981	0.01649	2.386E-4	0.9985	0.01545
6	Midilli et al.	2.539E-4	0.9983	0.01594	2.634E-4	0.9983	0.01623	2.273E-4	0.9987	0.01508
7	Two term exponential	7.920E-3	0.9406	0.08899	5.480E-3	0.9590	0.07400	6.510E-3	0.9555	0.08070
8	Modified Two-Term Exponential	4.130E-3	0.9711	0.06426	2.350E-3	0.9838	0.04852	2.320E-3	0.9859	0.04817
9	Approximation of Diffusion	1.100E-3	0.9923	0.03317	6.075E-4	0.9958	0.02465	6.368E-4	0.9961	0.02523
10	**Our model**	2.119E-4	0.9985	0.01456	2.243E-4	0.9985	0.01498	1.254E-4	0.9992	0.01120

Table 5.6: Statistical results and comparison of various drying models at different temperature for Kufri Bahar.

		60^oC			70^oC			80^oC		
No.	**Model Name**	χ^2	R^2	*RMSE*	χ^2	R^2	*RMSE*	χ^2	R^2	*RMSE*
1	Lewis (Newton)	6.330E-3	0.9480	0.07958	4.340E-3	0.9640	0.06587	4.870E-3	0.9618	0.06976
2	Page	3.675E-4	0.9971	0.01917	2.755E-4	0.9979	0.01660	1.538E-4	0.9989	0.01240
3	Modified Page-I	6.760E-3	0.9480	0.08219	4.700E-3	0.9640	0.06856	5.410E-3	0.9618	0.07353
4	Modified Page II	3.660E-4	0.9971	0.01913	2.746E-4	0.9979	0.01657	1.533E-4	0.9989	0.01238
5	Modified Page equation- II	3.958E-4	0.9971	0.01990	3.027E-4	0.9978	0.01740	1.740E-4	0.9989	0.01319
6	Midilli et al.	4.501E-4	0.9970	0.02121	2.433E-4	0.9984	0.0156	1.614E-4	0.9991	0.01271
7	Two term exponential	6.760E-3	0.9480	0.08219	4.700E-3	0.9640	0.06856	5.410E-3	0.9618	0.07354
8	Modified Two-Term Exponential	3.580E-3	0.9742	0.05986	1.880E-3	0.9868	0.04336	2.090E-3	0.9868	0.04571
9	Approximation of Diffusion	9.549E-4	0.9931	0.03090	5.381E-4	0.9962	0.02320	4.609E-4	0.9971	0.02147
10	**Our model**	3.524E-4	0.9974	0.01877	2.052E-4	0.9985	0.01432	1.242E-4	0.9992	0.01115

Table 5.7: Statistical results for drying constant.

Equation	**Drying products**	**Coefficients**	χ^2	R^2	*RSME*
$k = C\exp(DT)$	Apple	$A = 0.00121, B = 0.02952$	1.917E-8	0.9988	1.384E-4
	Kufri Chipsona-1	$A = 0.00127, B = 0.02346$	1.902E-9	0.9996	4.362E-5
	Kufri Himsona	$A = 0.00135, B = 0.02356$	1.762E-8	0.9969	1.327E-4
	Kufri Bahar	$A = 0.00171, B = 0.02005$	1.431E-11	1	3.784E-6

To assess the better model, the comparison of models are made according to χ^2, R^2 and RMSE.

- It can be seen from Tables (5.3 – 5.6) that the values of R^2 are greater for our model than the corresponding values of other models.
- In addition, the values of χ^2 and RMSE are lower for our model than the corresponding values of other models. Accordingly, our model is better to characterize the drying behavior of apple and potato.
- Drying curves for our model, fitted to experimental data, are shown in Figs. (5.1 – 5.4) at different drying temperature.
- It can be seen from these figures that the proposed model provides a close relationship between the calculated and experimental moisture ratio. This reveals the aptness of the model for describing the drying characteristics of apple and potato.
- Further, the relationship between drying constant (k) and drying temperature (T), given by Eq. (5.9), is set up by using regression analysis and the statistical results are shown in the Table (5.7).

5.4.1.2 Effect of Temperature on Moisture Content

Drying curves for dimensionless moisture content (experimental and calculated) and drying time, for apple and potato dried at different temperatures, are shown in Figs. (5.1 – 5.4) for apple, Kufri Chipsona-1, Kufri Himsona and Kufri Bahar, respectively. It is apparent that

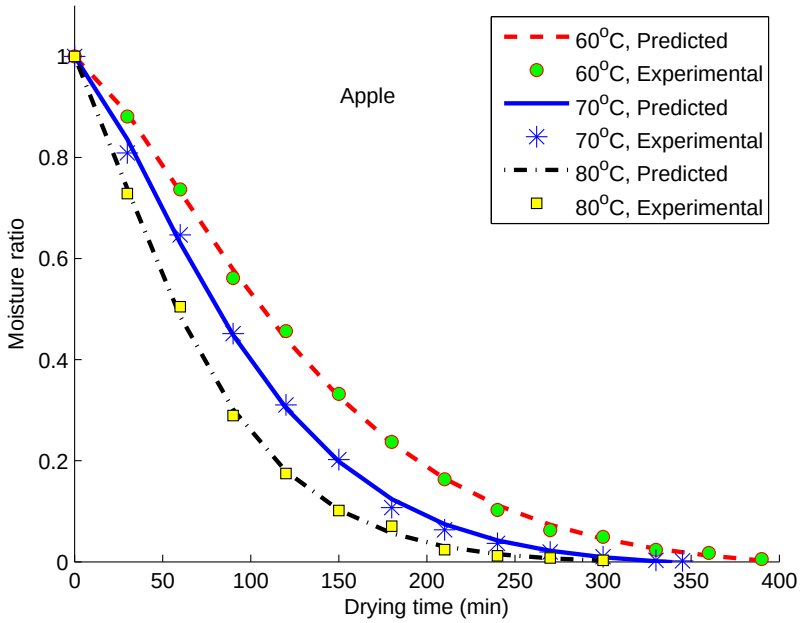

Figure 5.1: Moisture ratio variation with drying time at different temperature for apple.

the initial moisture content in samples are not same during each experiment. Therefore, to normalize the drying curves, and further, to minimize the effect of errors occurred during data measurement, graphs have been plotted for moisture ratio at place of moisture content with respect to time. Hence, plotted graphs are appearing similar in nature. Further, following results are observed from the study:

- Figure (5.1) depicts the moisture content variation with respect to drying time for apple.
- Figure (5.1) shows that the moisture content in apple decreases approximately exponentially as drying time increases. The moisture content decreases rapidly at the beginning of the drying process (approximately up to $t = 150$ min), whereas it decreases gradually at the end stage of drying (after $t = 150$ min). The reason of this behavior of moisture content is the excess of water in the sample in starting.
- As expected, drying temperature had a significant effect on moisture content and drying time. In other words, with the increase in drying temperature, drying curves became steeper and hence considerable decrease in drying time is noticed.

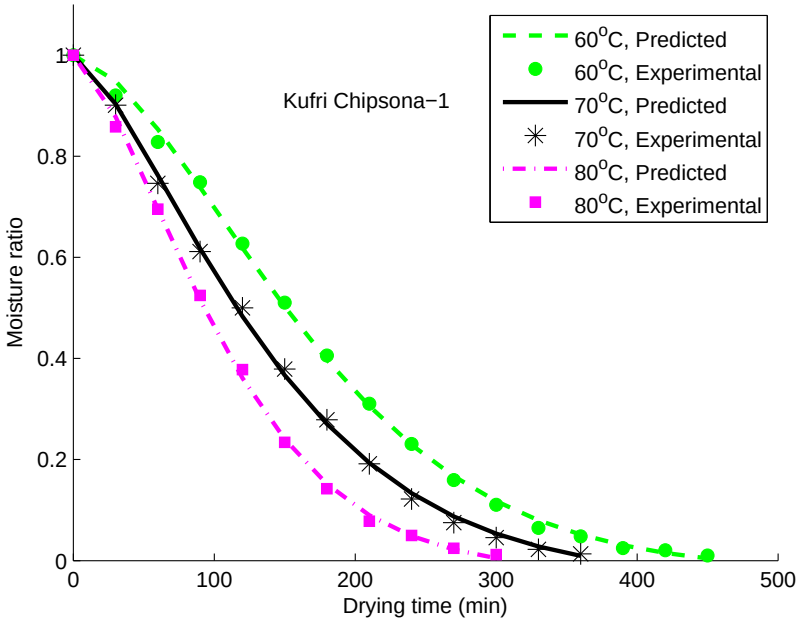

Figure 5.2: Moisture ratio variation with drying time at different temperature for Kufri Chipsona-1.

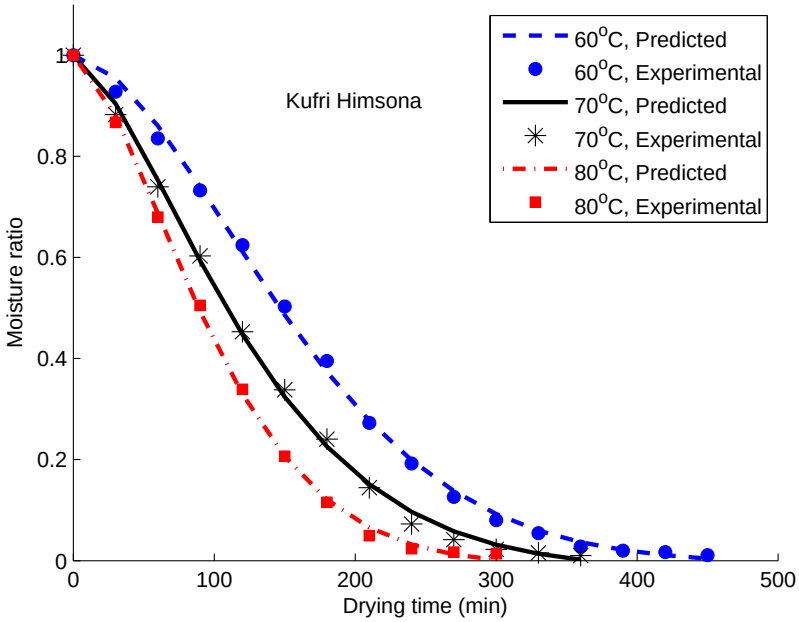

Figure 5.3: Moisture ratio variation with drying time at different temperature for Kufri Himsona.

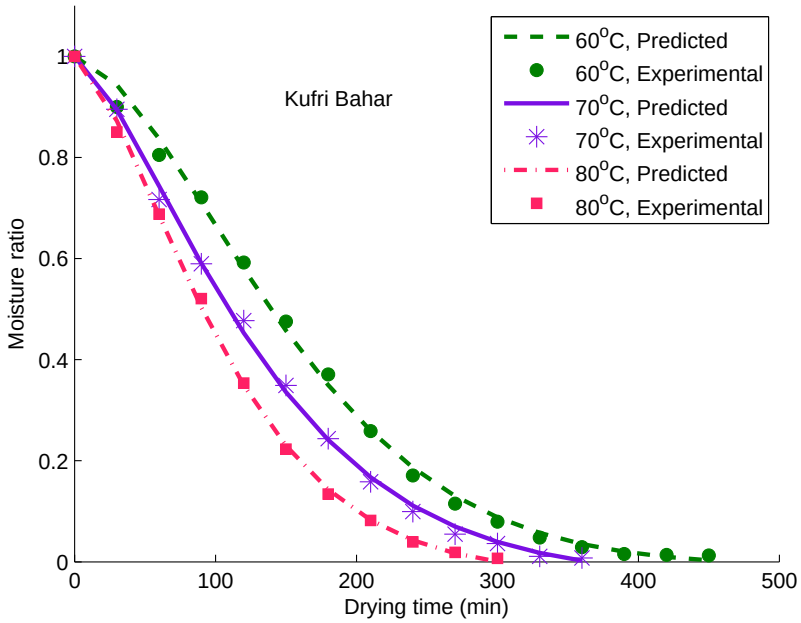

Figure 5.4: Moisture ratio variation with drying time at different temperature for Kufri Bahar.

- These effects of temperature on the time and moisture content are due to applying energy at a higher rate to drying samples and consequently increase in drying rate [28].
- Similar behavior of moisture content with respect to time and temperature are recorded for potato; Chipsona-1, Himsona and Bahar, Figs. (5.2 – 5.4), respectively.
- Figure (5.2) depicts the predicted and experimental moisture content variation with respect to drying time at different temperature for Chipsona-1.
- It is observed that moisture content decreases rapidly from sample during initial drying hours.
- Similar effect of drying time on moisture content variation for Himsona (Fig. 5.3) and Bahar (Fig. 5.4) is seen at different drying temperature.
- At the drying temperature $60, 70$ and 80^oC, the drying time were $390, 350$ and 300 min, respectively for apple, $450, 360$ and 300 min, respectively for potato to attain the final moisture content.

- The obvious decrease in drying time with the increase in drying temperature has also been observed by Aghbashlo et al. [1] for carrot, Bakal et al. [14] and Chayjan [28] for potato and Wang and Chao [175] for apple slices.

- It is also observed that apple sample requires less time to be dried as compare to potato sample.

5.4.1.3 Effect of Temperature on Drying Rate

The experimental and calculated drying rates as a function of time are shown in Fig. (5.5) for apple and in Figs. (5.6 – 5.8) for potato at different temperature.

- Figure (5.5) indicates that during the initial two hours of drying, drying rate is higher in apple than the latter hours of drying. Initially, the drying rate in apple is high due to the excess amount of water in the sample, and hereafter, as drying proceeds, amount of water in sample decreases gradually which results the decrease in drying rate.

- Further, it can be seen from the Fig. (5.6) that the drying rate for Chipsona-1 increases

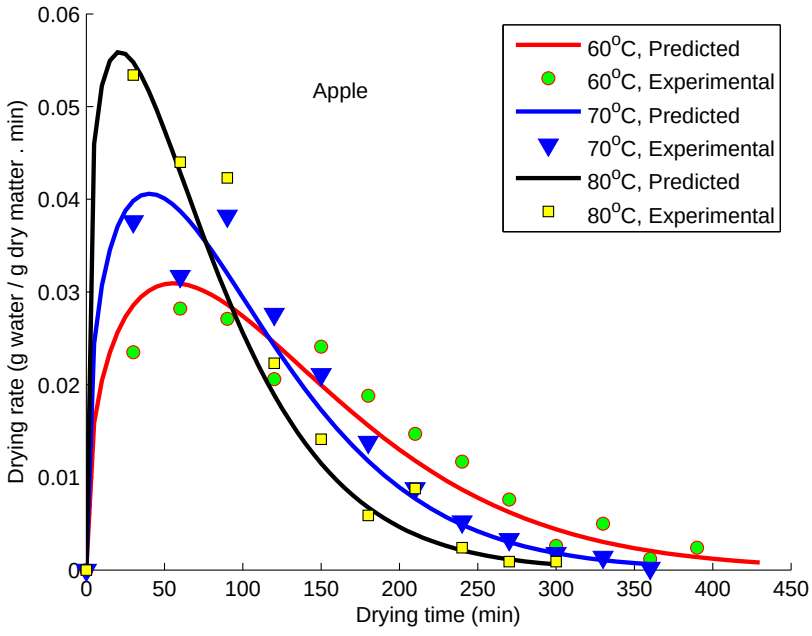

Figure 5.5: Changes of drying rate with time at different temperature for apple.

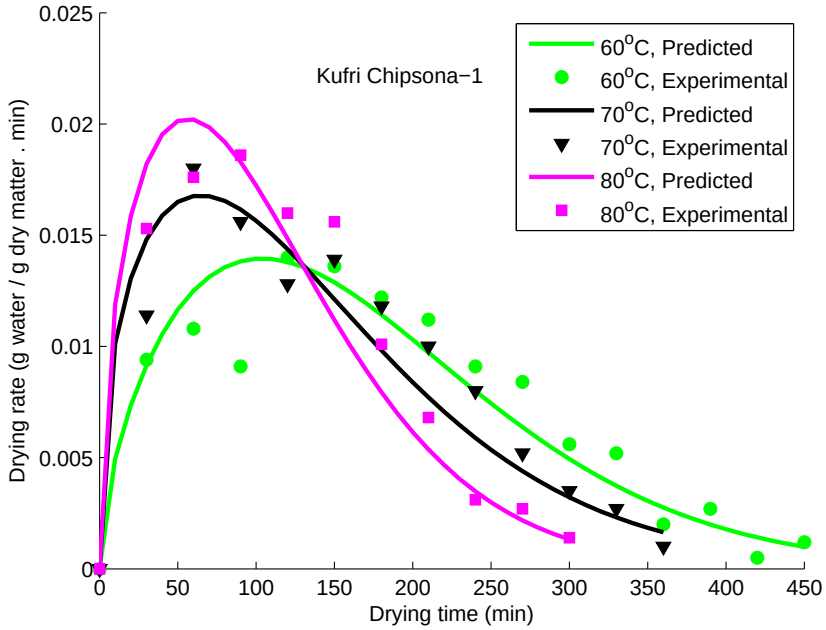

Figure 5.6: Changes of drying rate with time at different temperature for Kufri Chipsona-1.

rapidly in the initial drying hours and after reaching its maximum value, the drying rate decreases gradually as the sample approached the dried state. This means that the moisture loss rate in samples is more in starting drying hours as compare to the last drying hours.

- Similar behavior of the drying rate is observed for Himsona and Bahar, Figs. (5.7) and (5.8), respectively.

- The drying temperature has a great effect on the drying rate of apple and potato. In other words, a higher temperature resulted in a higher drying rate.

- Similar type of effect of drying temperature on the drying rate was also reported by Velić et al. [171] for apple and Darvishi et al. [38] for potato. Therefore, to reduce the drying time of apple and potato samples a higher drying rate can be produced by higher drying temperature.

- The main reason for increase the drying rate of apple and potato samples may be due to increase in heat transfer and acceleration of water migration between air and sample.

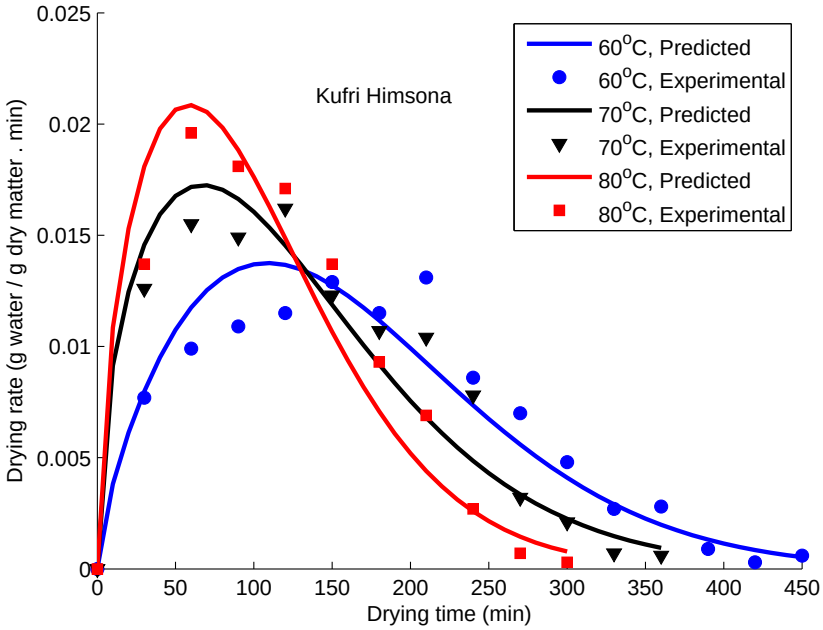

Figure 5.7: Changes of drying rate with time at different temperature for Kufri Himsona.

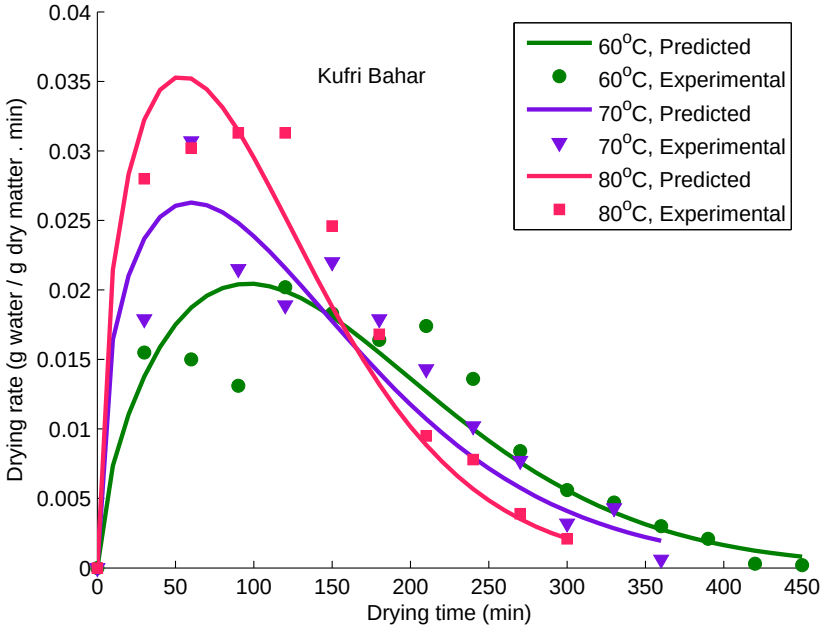

Figure 5.8: Changes of drying rate with time at different temperature for Kufri Bahar.

- From Figs. (5.5 – 5.8), it is also clear that the drying rate is greater in apple than potato.

- Additionally, Bahar has the greater drying rate than Chipsona-1 and Himsona, which is due to the fact of higher initial moisture content in Bahar than Chipsona-1 and Himsona. Hence, proposed model is able to predict the drying rate suitably for apple and potato.

5.4.2 Structural Properties

It is clear from subsections (5.4.1.1) and (5.4.1.2) that the proposed drying model is suitable to predict the moisture content variation with respect to drying time. Hence, during drying of apple and potato, we can calculate the drying time which may required to obtain a desired dried product. Therefore, we can use the proposed drying model for the prediction of structural properties of apple and potato with respect to time during drying. However, here we have discussed the structural properties of apple and Kufri Himsona at temperature 70^oC only. For other varieties and temperature, these properties can be discussed in similar way. Firstly, moisture content is calculated from Eq. (5.7) and then it is used to calculate structural properties. Further, the effect of drying temperature on structural properties can be determined by using Eq. (5.9) in Eqs. (5.14) – (5.17).

5.4.2.1 Particle and Bulk Density

The particle and bulk density, in terms of drying time, is given by Eqs. (5.14) and (5.15), respectively. Values of parameters ρ_s, ρ_{b0}, β' and ρ_w have been used from previous study [81] for drying of apple and potato at 70^oC. The variation of particle and bulk density with respect to time is presented in Figs. (5.9) and (5.10), respectively.

- Figure (5.9) shows the particle density with respect to moisture content for the existing model (Eq. 5.10) and the particle density with respect to moisture content calculated from drying model proposed in the present study for apple and potato.

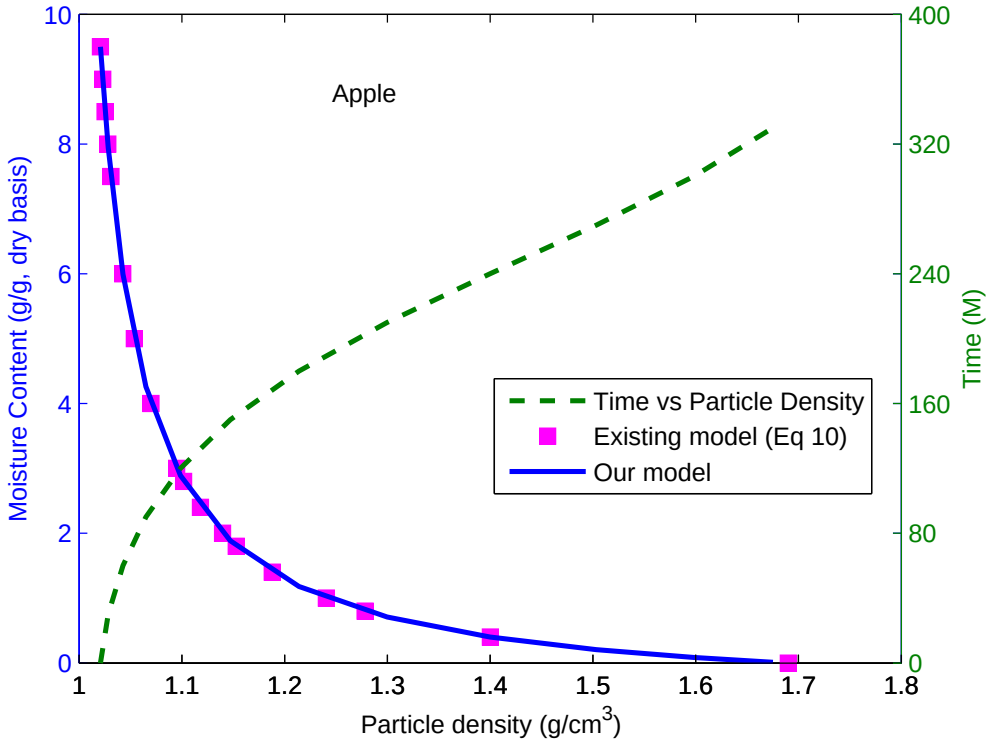

(a)

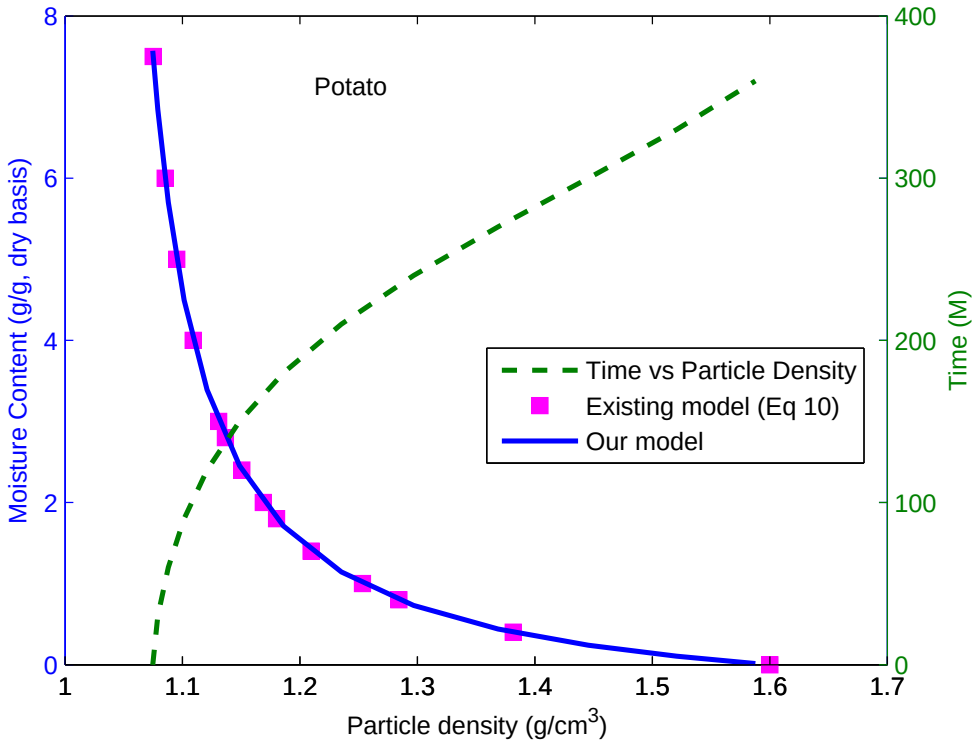

(b)

Figure 5.9: Variation of particle density with moisture content and drying time (a) apple (b) potato.

- It is clear from the figure that the particle density, in terms of moisture content, can be predicted well by using our model. Hence, these results confirm the use of Eq. (5.14) to obtain relationship between the particle density and drying time.

- Further, the particle density variation with respect to drying time is also presented in Fig. (5.9 a) for apple and Fig. (5.9 b) for potato.

- It can be seen from the Fig. (5.9) that the particle density increases as drying time increases.

- It is evident that as the drying process proceeds, moisture in the sample decreases, consequently, particle density increases. This should be expected because particle density ranges between water density ρ_w and density of dry solid ρ_s

- During the initial drying time (approximately up to $t = 150$ min), particle density increases slowly and after that it increases rapidly. The reason behind this behavior of particle density is the availability of high moisture content in the sample initially. Similar results were obtained by Krokida and Maroulis [81] for particle density of apple and potato.

- Furthermore, Fig. (5.10) presents the bulk density for apple and potato with respect to the moisture content for existing model (Eq. 5.11) and the bulk density with respect to moisture content calculated from drying model proposed in the present study.

- Fig. (5.10) shows close resemblance between both the results. Hence, the relationship (Eq. 5.15) between bulk density and drying time is admissible. In addition, bulk density ranges between density of water ρ_w and bulk dry solid density ρ_{b0} as expected.

- With the increase of drying time, moisture content in samples decreases, consequently, bulk density of potato increases. On the contrary, bulk density of apple decreases as drying proceeds.

- Initially (approximately up to $t = 150$ min), the rate of increment of bulk density is slow and after that as moisture in the sample reduced gradually, the bulk density of

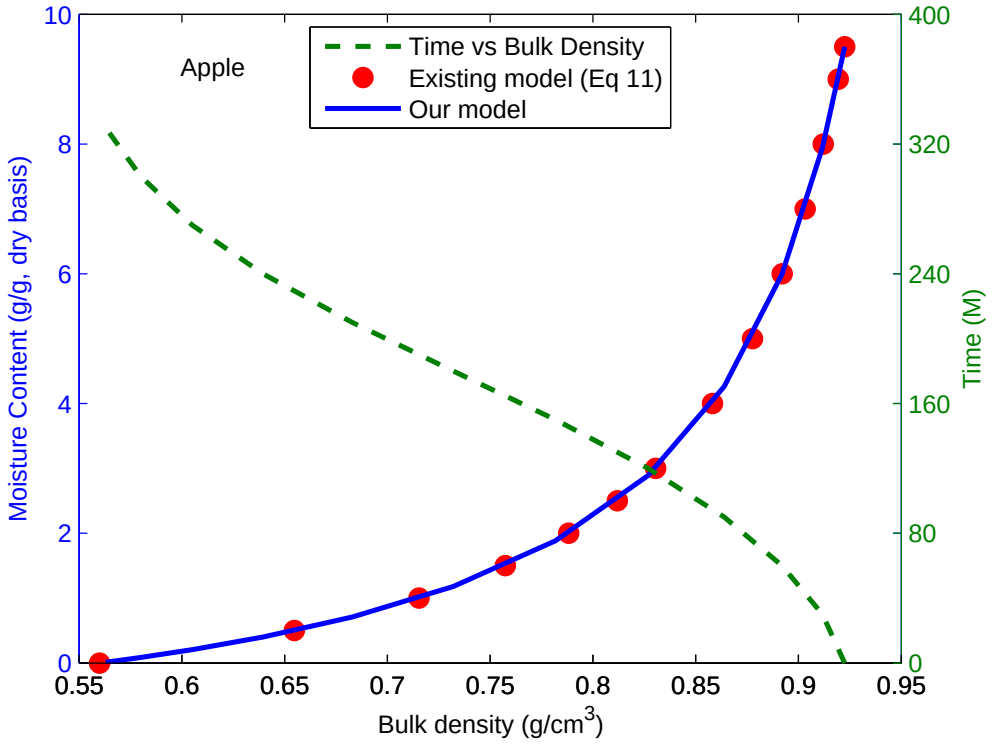

(a)

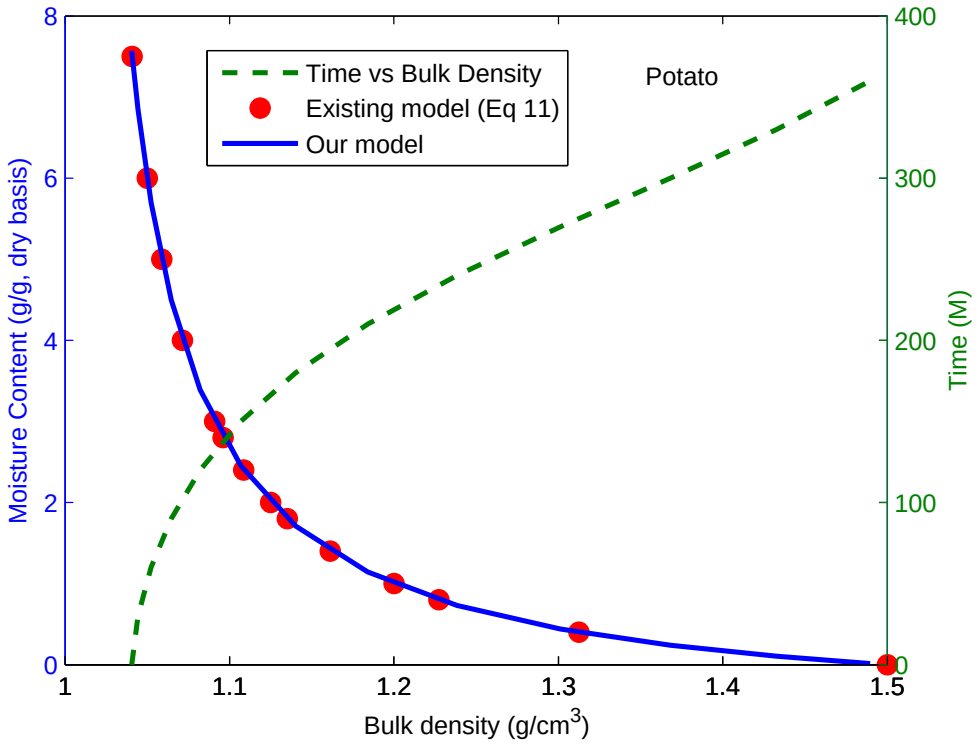

(b)

Figure 5.10: Bulk density variation with moisture content and drying time (a) apple (b) potato.

potato increases at a higher rate. While a reverse effect of drying time on the bulk density of apple is seen. These results are supported by experimental work of Krokida and Maroulis [81].

5.4.2.2 Porosity and Specific volume

Porosity is calculated from the Eq. (5.16) in terms of drying time. The expression of porosity is obtained by substituting the expression of particle density (Eq. 5.14) and bulk density (Eq. 5.15) into (Eq. 5.16). The suitability of the density equation is checked in subsection (5.4.2.1), therefore, the porosity of apple and potato can be calculated from Eq. (5.16).

- Figure (5.11) demonstrates the porosity variation of apple and potato with time and moisture content (existing and calculated in the present work). Similar to the density, our model is appropriately describing the porosity variation with respect to drying time.

- Initially, porosity is increasing at slow rate, and gradually, as drying time increases it appears to be increasing at a higher rate [81].

- Further, it can be seen from Fig. (5.11) that the porosity variation with respect to moisture content for existing model and our model presented very closely.

- Time dependent relation for specific volume is given by Eq. (5.17). Specific volume variation with respect to time and moisture content is depicted in Fig. (5.12) for apple and potato.

- During the initial drying hour, specific volume decreases at higher rate while after $t = 200$ min (approximately) it decreases at slower rate.

- Specific volume variation with moisture content seems linear, whereas it is seemed nonlinear with respect to drying time. The reason of this behavior of specific volume is the exponential reduction in moisture content during drying. In other words, as the drying process progressed, moisture content in the sample reduced in exponential fashion which is responsible for the reduction in the specific volume.

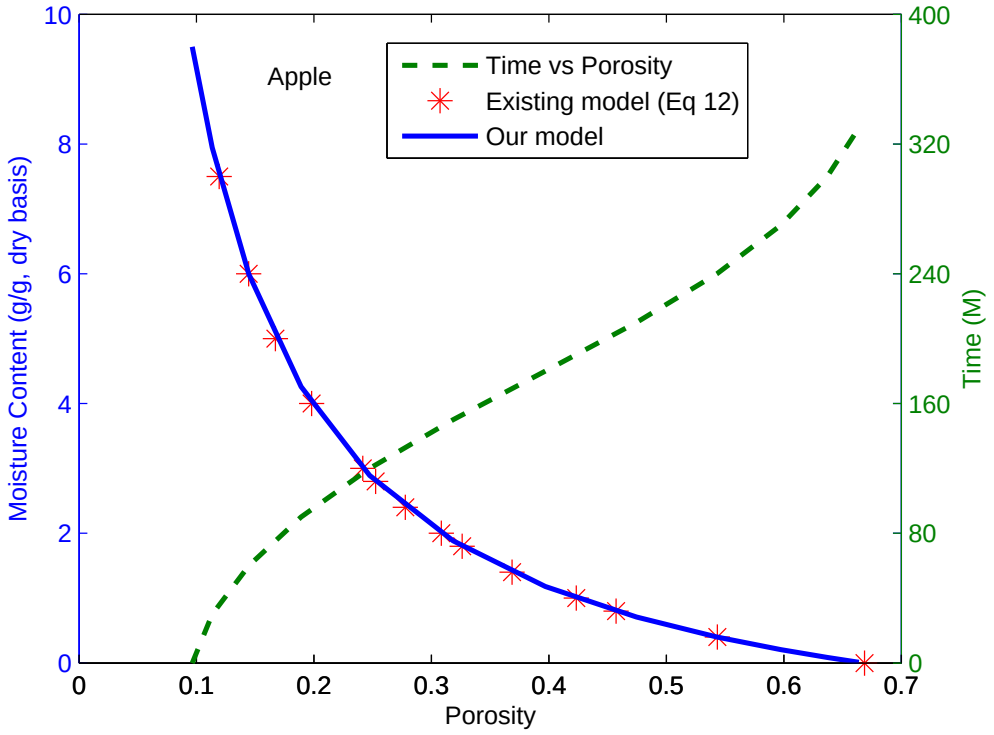

(a)

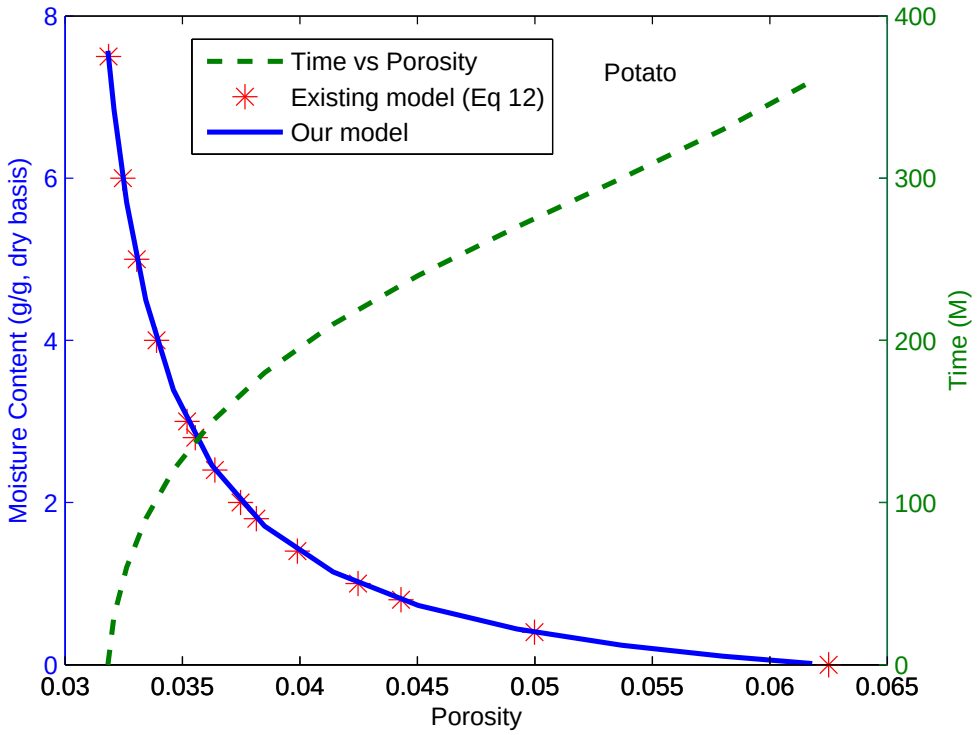

(b)

Figure 5.11: Porosity variation with moisture content and drying time (a) apple (b) potato.

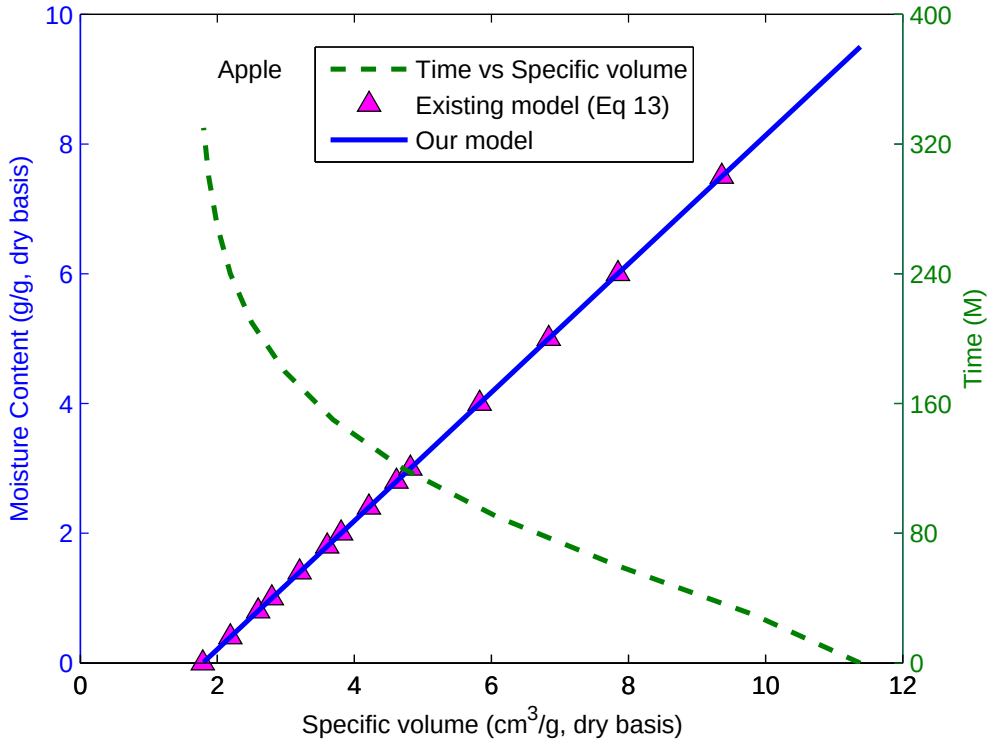

(a)

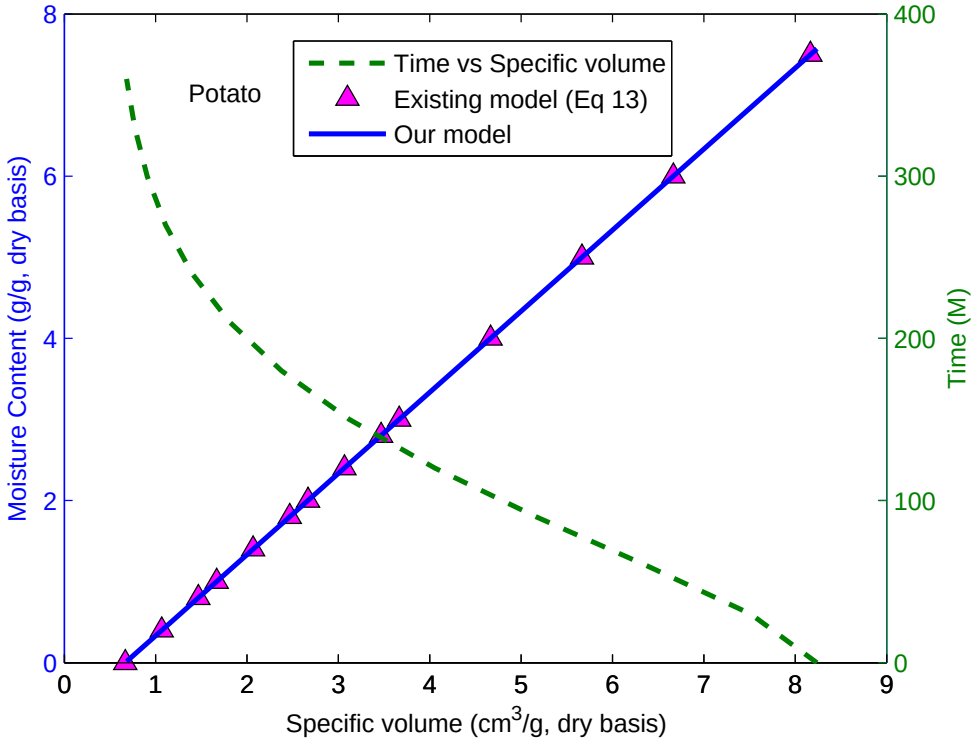

(b)

Figure 5.12: Specific volume variation with moisture content and drying time (a) apple (b) potato.

- Apple and potato shows similar pattern for specific volume variation with respect to drying time as well as moisture content, which is agreed by the literature [81].

5.5 Conclusions

A new drying model for prediction drying behavior of apple and potato is proposed and compared with several thin-layer drying models. The proposed model is validated with experimental data obtained from the experiments of one variety of apple and three varieties of potato at different temperature. There are close agreement between our model and experimental results, based on observations of the parameters studied in the present work, in comparison to the other models cited in literature. Our model is able to predict drying behavior suitably in the beginning ($t = 0$ min) of drying and in last drying hours when moisture content remains very less in samples. The drying constant (k) of our model can be predicted as a function of drying temperature from the exponential equation. The drying rate curves of apple and potato are produced and found falling drying rate period. Further, the drying model is used to predict structural properties, such as density, porosity and specific volume as a function of drying time. However, more experimental works need to be done to obtain data for structural properties in terms of drying time for other fruits and vegetables. Further, the proposed drying model can be used to predict the drying behavior and structural properties of other fruits and vegetables under different drying conditions, such as temperature, air velocity, humidity, and different sample geometry such as cubes, and various slice thickness. The use of the proposed model for commercialization will be a topic of further research.

Chapter 6

Conclusions and Future Scope

6.1 Summary and Conclusions

In the present thesis, an attempt has been made to understand the mechanical properties (tension-stretch relation, turgor-stretch relation) of cell-wall of apple and potato tissues and structural properties (shrinkage, density, porosity, specific volume) of apple and potato. The primary goal of this work was to understand the tissue deformation (or damage) and changes in the structure occurred in apple and potato during the process of handling, packaging, transportation, storage and dehydration. The deformation (or damage) is the consequence of externally applied loads. The damage in apple and potato can be understand by analyzing mechanical properties of their soft tissues. On the other hand, structure related changes are the consequence of water removal and formation of pores during dehydration. The change in quality, texture and appearance can be understand by analyzing the variation in density, porosity, shrinkage and specific volume during water removal from these products.

The deformation of soft tissues is the complex process. To perceive the whole process, it is necessary to explore the factors behind the process. The whole methodology can be comprehend by developing mathematical models for deformation of cells or conglomerate of cells (or tissues). Formulation of constitutive equation plays a vital role in thorough understanding of tissue properties. Therefore, in Chapter 2, a new strain energy function was proposed and used to develop a constitutive model to investigate the mechanical properties

of apple and potato tissues. The developed model was capable to predict, why and how, the tension and stretch in the cell-wall get affected during mechanical loading of tissues. Therefore, this model can be applied to understand and control the tissue damage in more realistic loading regimes. Further, the work was extended to develop a relationship between turgor pressure and stretch ratio for apple and potato tissues, which is presented in Chapter - 3. The development of this relation was based on the strain energy function. It is evident that during transportation of food products, control of cell turgidity is necessary for reduction in bruise susceptibility and maintain apparent freshness. Chapter - 4 was mainly concern with the study of porosity variation in apple and potato during dehydration process. It was observed that current porosity is depended on initial porosity and pressure (or contraction stress in cells due to water removal). For study drying characteristics of apple and potato, a drying model was proposed in Chapter - 5. The proposed model was compared with other drying models cited in literature, and then it was used to obtain structural properties as a function of drying time. Throughout the thesis, models were validated with experimental data by using a very efficient Levenberg-Marquadt algorithm.

The freshness and quality of food products is dependent on the strength of the tissues. The strength is related to the failure of one or more cells or bonds in a tissues. Turgor pressure have great influence on the macroscopic fruit firmness and tissue strength. It is lost due to water loss through transpiration in apple or potato. Since, more damage in cells will occur during handling of highly turgid products, therefore, more work is required to control turgidity during transport and storage of food products.

Besides aforementioned drying methods (discussed in Chapter 5), moisture removal also comes into the picture during postharvest handling, storage and transportation of apple and potato (in general fruits and vegetables). The process of moisture loss from fresh fruits and vegetables is termed as transpiration. The transpiration process includes the evaporation of moisture from the surface of the fruits or vegetables to the surrounding air during storage [22]. Due to this process, moisture loss induces shrinkage, increase in porosity, wilting, and loss of firmness and crispness of apple and potato, and thus contrarily affects the texture, flavor, appearance and the mass of these products. During storage, the formation of pores in

fresh apple and potato is the consequence of water removal that is largely dependent on the air velocity, relative humidity and the heat of respiration. This loss of moisture can be reduced by minimizing the water vapor pressure difference between the air and the products and hence porosity increment can be minimized [22]. Additionally, at packaging time, various moisture-proof films and skin coatings can be used. As a result, mass loss and shrinkage can be reduced in these products that caused an improvement in firmness, appearance and overall storage life.

Following conclusions have been drawn from this study:

- A new strain energy function is used to develop the constitutive relation to explore the effects of stretch ratio on the cell-wall tension and effects of turgor pressure on stretch ratios for apple and potato tissues.

- The use of strain energy function is appropriate to study the mechanical properties (for example, tension-stretch relation, turgor-stretch relation) of apple and potato tissues. Further, an effort can be made to incorporate the mechanical properties of other fruits and vegetables by using this strain energy function.

- By the results of the present work, it is clear that the higher turgor pressure is responsible for cell-wall rupture, which is responsible for damage of cells and reduction in the freshness and quality of the products.

- It is observed that cell-wall tension increases as stretch ratios increases and stretch ratios increases as turgor pressure increases. Hence, it can be concluded that the cell-wall tension increases as turgor pressure increases.

- A successful understanding of parameters, which are responsible for tissue damage, one can leads to develop suitable methodology for damage control of tissues and thus maintain and enhance the quality of apple and potato.

- The porosity of apple and potato is largely depended on initial porosity and pressure. It increases due to moisture loss from these products.

- To obtain good dried food products, suitable drying methods and appropriate drying conditions are necessary, which can be investigated with the help of mathematical modeling.
- The study of structural properties as a function of drying time is invaluable, which can be used for allocation and optimization of resources in food drying industries.

6.2 Future Scope

The study of food related properties is the wide area of research. Although, we have explored some of the mechanical and structural properties of apple and potato, further work is needed to investigate other properties (e.g., optical, sensory, texture, physical, etc.) by means of mathematical modeling. Additionally, these properties can also be investigated for other fruits and vegetables.

Various techniques are available for preservation of fruits and vegetables. In this context, the radiation process technique is growing fast all over the world. Radiation is one of the latest methods in food preservation. Irradiation of food is one of the most effective ways of food preservation to inactivate microorganisms and destroy insect pests. In this technique, foods become safe for eating without changing in texture and freshness because radiation destroy bacteria from the foods. Further, foods do not gain any harmful toxic residues of radiation for two reasons. First, the gamma rays from *Cobalt-60*, used in food radiation, are not energetic enough to make it radioactive. Second, as the food never comes into contact with the source directly, it is not possible for the food to become contaminated with radioactive material. Disease causing organisms such as bacteria and parasites can be eliminated by the use of radiation.

Radiation in fruits and vegetables can be used for delaying ripening and/or sprouting, extend shelf-life, prevent spoilage or damage, kill infesting insects, destroy food borne pathogens and bacteria. Therefore, more research needs to be done to determine how radiation treatment interacts with commodity type, temperature and packaging for fruits and vegetables, specially apple and potato.

Bibliography

[1] Aghbashlo, M., Kianmehr, M. H., Khani, S., and Ghasemi, M. (2009). Mathematical modelling of thin-layer drying of carrot. *International Agrophysics*, 23(4):313–317.

[2] Akpinar, E. K. (2006). Determination of suitable thin layer drying curve model for some vegetables and fruits. *Journal of Food Engineering*, 73(1):75–84.

[3] Akyurt, M. (1969). *Constitutive Relations for Plant Materials*. Thesis, Purdue University.

[4] Al-Muhtaseb, A., McMinn, W. A. M., and Magee, T. R. A. (2004). Shrinkage, density and porosity variations during the convective drying of potato starch gel. In *Proceedings of the 14th International Drying Symposium*, volume C of *Drying 2004*, pages 1604–1611, Sao Paulo, Brazil.

[5] Alamar, M., Zarzo, M., Suay, R., Moltó, E., Vanstreels, E., Verlinden, B., Nicolaï, B., Loodts, J., Tijskens, E., and Ramon, H. (2005). Micromechanical behaviour of apple tissue in tensile and compression tests. In *Information and Technology for Sustainable Fruit and Vegetable Production FRUTIC 05*, pages 409–420.

[6] Alamar, M. C., Vanstreels, E., Oey, M. L., Moltó, E., and Nicolaï, B. M. (2008). Micromechanical behaviour of apple tissue in tensile and compression tests: Storage conditions and cultivar effect. *Journal of Food Engineering*, 86(3):324–333.

[7] Altisent, M. R. (1991). *Damage Mechanisms in the Handling of Fruits*, chapter 9, pages 231–257.

[8] Alvarez, M. D., Saunders, D. E. J., and Vincent, J. F. V. (2000). Effect of turgor pressure on the cutting energy of stored potato tissue. *European Food Research and Technology*, 210(5):331–339.

[9] Ang, K. C. and Mazumdar, J. N. (1997). Mathematical modelling of three-dimensional flow through an asymmetric arterial stenosis. *Mathematical and Computer Modelling*, 25(1):19–29.

[10] Araya, X. I. T. (2011). *Effects of High Pressure Processing on Carrot Tissue: A Microstructure Approach*. Thesis, Massey University, Palmerston North, New Zealand.

[11] Bai, Y., Rahman, M. S., Perera, C. O., Smith, B., and Melton, L. D. (2002). Structural changes in apple rings during convection air-drying with controlled temperature and humidity. *Journal of Agricultural and Food Chemistry*, 50(11):3179–3185.

[12] Bajema, R. W., Hyde, G. M., and Baritelle, A. L. (1998a). Effects of mannitol on turgor and on failure stress and strain in potato tuber tissue. *Postharvest Biology and Technology*, 14(2):199–205.

[13] Bajema, R. W., Hyde, G. M., and Baritelle, A. L. (1998b). Turgor and temperature effects on dynamic failure properties of potato tuber tissue. *Transactions of the ASAE*, 41(3):741–746.

[14] Bakal, S. B., Sharma, G. P., Sonawane, S. P., and Verma, R. C. (2012). Kinetics of potato drying using fluidized bed dryer. *Journal of Food Science and Technology*, 49(5):608–613.

[15] Ball, J. M. (1982). Discontinuous equilibrium solutions and cavitation in nonlinear elasticity. *Philosophical Transactions of the Royal Society A: Mathematical, Physical and Engineering Sciences*, 306(1496):557–611.

[16] Biderman, V. L. (1958). *Calculations of Rubber Parts*. Raschefina Prochnost 40, Moscow (in Russian).

[17] Boukouvalas, C. J., Bisharat, G. I., and Krokida, M. K. (2010). Structural properties of vegetables during air drying. *International Journal of Food Properties*, 13(6):1393–1404.

[18] Bruce, D. M. (2003). Mathematical modelling of the cellular mechanics of plants. *Philosophical Transactions of the Royal Society of London. Series B, Biological Sciences*, 358(1437):1437–1444.

[19] Brusewitz, G. H., Pitt, R. E., and Gao, Q. (1989). Effects of storage time and static preloading on the rheology of potato tissue. *Journal of Texture Studies*, 20(3):267–284.

[20] Cardello, A. V. (1998). *Perception of Food Quality. In: Food Storage Stability*. CRC Press LLC.

[21] Castleberry, H. C. (2013). *Development of Methods to Estimate or Reduce Pressure Flattening of Potatoes during Storage*. Thesis, Colorado State University, Department of Horticulture and Landscape Architecture, Fort Collins, Colorado.

[22] Chakraverty, A., Mujumdar, A., Raghavan, G., and Ramaswamy, H. S. (2003). *Handbook of Postharvest Technology: Cereals, Fruits, Vegetables, Tea, and Spices*. CRC Press, New York.

[23] Chang, C. S. (1988). Measuring density and porosity of grain kernels using a gas pycnometer. *Cereal Chemistry*, 65(1):13–15.

[24] Chang, W. J. and Pan, J. (2001). Cavitation instability in rubber with consideration of failure. *Journal of Materials Science*, 36(8):1901–1909.

[25] Chaturani, P. and Narasimman, S. (1990). Flow of power-law fluids in cone-plate viscometer. *Acta Mechanica*, 82:197–211.

[26] Chaturani, P. and Palanisamy, V. (1991). Pulsatile flow of blood with periodic body acceleration. *International Journal of Engineering Science*, 29(1):113–121.

[27] Chaturani, P. and Wassf Isaac, A. (1995). Blood flow with body aceleration forces. *International Journal of Engineering Science*, 33(12):1807–1820.

[28] Chayjan, R. A. (2012). Modeling some drying characteristics of high moisture potato slices in fixed, semi fluidized and fluidized bed conditions. *Journal of Agricultural Science and Technology*, 14(6):1229–1241.

[29] Chemkhi, S. and Zagrouba, F. (2011). Characterisation of potato slices during drying: Density, shrinkage, and thermodynamic of sorption. *International Journal of Food Engineering*, 7(3).

[30] Chen, P. and Pei, D. C. T. (1989). A mathematical model of drying processes. *International Journal of Heat and Mass Transfer*, 32(2):297–310.

[31] Chiputula, J. (2009). *Evaluating Mechanical Damage of Fresh Potato during Harvesting and Postharvest Handling*. Thesis, University of Florida, Florida.

[32] Chopra, C. S. and Singh, R. (2001). Studies on extraction of pulp from wood apple (limonia acidissima l.) fruit. *Beverage and Food World*, 28(2):25–27.

[33] Chou, S. K. and Chua, K. J. (2001). New hybrid drying technologies for heat sensitive foodstuffs. *Trends in Food Science & Technology*, 12(10):359–369.

[34] Cowin, S. C. and Doty, S. B. (2007). *Tissue Mechanics*. Springer, New York.

[35] Dal Fabbro, I. M., Murase, H., and Segerlind, L. J. (1980). Strain failure of apple, pear and potato tissue. *ASAE Paper No. 80-3048. ASAE, St. Joseph, MI*.

[36] Danielsson, M., Parks, D. M., and Boyce, M. C. (2004). Constitutive modeling of porous hyperelastic materials. *Mechanics of Materials*, 36(4):347–358.

[37] Darijani, H. and Naghdabadi, R. (2010). Hyperelastic materials behavior modeling using consistent strain energy density functions. *Acta Mechanica*, 213(3-4):235–254.

[38] Darvishi, H., Asl, A. R., Asghari, A., Najafi, G., and Gazori, H. A. (2013). Mathematical modeling, moisture diffusion, energy consumption and efficiency of thin layer drying of potato slices. *Journal of Food Processing & Technology*, 4:215(03).

[39] Datta, A. K. (2008). Status of physics-based models in the design of food products, processes, and equipment. *Comprehensive Reviews in Food Science and Food Safety*, 7(1):121–129.

[40] Datta, A. K. and Halder, A. (2008). Status of food process modeling and where do we go from here (synthesis of the outcome from brainstorming). *Comprehensive Reviews in Food Science and Food Safety*, 7(1):117–120.

[41] De Belie, N., Hallett, I. C., Harker, F. R., and De Baerdemaeker, J. (2000). Influence of ripening and turgor on the tensile properties of pears: A microscopic study of cellular and tissue changes. *Journal of the American Society for Horticultural Science*, 125(3):350–356.

[42] Diamante, L. M. and Munro, P. A. (1993). Mathematical-modeling of the thin-layer solar drying of sweet-potato slices. *Solar Energy*, 51(4):271–276.

[43] Doblar, M. and Aznar, G. (2010). Modelling living tissues: Mechanical and mechanobiological aspects. *Mathematics in Industry*, 15:3–8.

[44] Elnajjar, E., Haik, Y., Hamdan, M. O., and Khashan, S. (2013). Heat transfer characteristics of multi-walled carbon nanotubes suspension in a developing channel flow. *Heat and Mass Transfer*, 49(12):1681–1687.

[45] Erbay, Z. and Icier, F. (2010). A review of thin layer drying of foods: Theory, modeling, and experimental results. *Critical Reviews in Food Science and Nutrition*, 50(5):441–464.

[46] Esau, K. (1965). *Plant Anatomy*. John Wiley and Sons, Inc, New York.

[47] Fung, Y. C. (1967). Elasticity of soft tissues in simple elongation. *American Journal of Physiology*, 213(6):1532–1544.

[48] Fung, Y. C. (1984). Structure and stress-strain relationship of soft tissues. *American Zoologist*, 24(1):13–22.

[49] Gao, Q. and Pitt, R. E. (1991). Mechanics of parenchyma tissue based on cell orientation and microstructure. *Transactions of the ASAE*, 34(1):232–238.

[50] Gao, Q., Pitt, R. E., and Bartsch, J. A. (1989). Elastic-plastic constitutive relations of the cell walls of apple and potato parenchyma. *Journal of Rheology*, 33(2):233–256.

[51] Gao, Q., Pitt, R. E., and Ruina, A. (1990). A mechanics model of the compression of cells with finite initial contact area. *Biorheology*, 27(2):225–240.

[52] Gates, R. S., Pitt, R. E., Ruina, A., and Cooke, J. R. (1986). Cell wall elastic constitutive laws and stress-strain behavior of plant vegetative tissue. *Biorheology*, 23(5):453–466.

[53] Ghaemi, H., Behdinan, K., and Spence, A. (2006). On the development of compressible pseudo-strain energy density function for elastomers - part 1. theory and experiment. *Journal of Materials Processing Technology*, 178(1-3):307–316.

[54] Gibson, L. J., Ashby, M. F., Schajer, G. S., and Robertson, C. I. (1982). The mechanics of two-dimensional cellular materials. *Proceedings of the Royal Society of London Series A-Mathematical Physical and Engineering Sciences*, 382(1782):25–42.

[55] Gou, P. F. (1970). Strain energy function for biological tissues. *Journal of Biomechanics*, 3(6):547–550.

[56] Gupta, S. K. and Sowokinos, J. R. (2003). Physicochemical and kinetic properties of unique isozymes of UDP-Glc pyrophosphorylase that are associated with resistance to sweetening in cold-stored potato tubers. *Journal of Plant Physiology*, 160(6):589–600.

[57] Gupta, S. K., Sowokinos, J. R., and Hahn, I. S. (2008). Regulation of UDP-glucose pyrophosphorylase isozyme UGP5 associated with cold-sweetening resistance in potatoes. *Journal of Plant Physiology*, 165(7):679–690.

[58] Haik, Y., Chen, C.-J., and Chatterjee, J. (2002). Numerical simulation of biomagnetic fluid in a channel with thrombus. *Journal of Visualization*, 5(2):187–195.

[59] Haines, D. W. and Wilson, W. D. (1979). Strain-energy density function for rubber-like materials. *Journal of the Mechanics and Physics of Solids*, 27(4):345–360.

[60] Haman, J., Konstankiewicz, K., and Zdunek, A. (2000). Influence of water potential on the failure of potato tissue. *International Agrophysics*, 14(2):181–186.

[61] Henderson, S. M. (1974). Progress in developing the thin layer drying equation. *Transactions of the ASAE*, 17:1167–1172.

[62] Hepworth, D. G. and Bruce, D. M. (2000). Measuring the deformation of cells within a piece of compressed potato tuber tissue. *Annals of Botany*, 86(2):287–292.

[63] Hiller, S. and Jeronimidis, G. (1996). Fracture in potato tuber parenchyma. *Journal of Materials Science*, 31(11):2779–2796.

[64] Holt, J. E. and Schoorl, D. (1983). Fracture in potatoes and apples. *Journal of Materials Science*, 18(7):2017–2028.

[65] Holzapfel, G. A. (2000). *Nonlinear Solid Mechanics: A Continuum Approach for Engineering*. John Wiley & Sons Ltd, Chichester.

[66] Holzapfel, G. A., Gasser, T. C., and Ogden, R. W. (2000). A new constitutive framework for arterial wall mechanics and a comparative study of material models. *Journal of Elasticity*, 61(1-3):1–48.

[67] Hou, H. S. (1990). *Cavitation Instability in Solids*. Thesis, B.S., Solid Mechanics, Zhejiang University, Massachusetts Institute of Technology, Hangzhou, China.

[68] Humphrey, J. D. (2002). *Cardiovascular Solid Mechanics: Cell, Tissues, and Organs*. Springer, New York.

[69] Humphrey, J. D. and Yin, F. C. P. (1987). On constitutive relations and finite deformations of passive cardiac tissue: I. a pseudostrain-energy function. *Journal of Biomechanical Engineering*, 109(4):298–304.

[70] Isihara, A., Hashitsume, N., and Tatibana, M. (1951). Statistical theory of rubber-like elasticity. iv. (two-dimensional stretching). *The Journal of Chemical Physics*, 19(12):1508–1512.

[71] Jackman, R. L., Marangoni, A. G., and Stanley, D. W. (1992). The effects of turgor pressure on puncture and viscoelastic properties of tomato tissue. *Journal of Texture Studies*, 23(4):491–505.

[72] Karathanos, V. T., Kanellopoulos, N. K., and Belessiotis, V. G. (1996). Development of porous structure during air drying of agricultural plant products. *Journal of Food Engineering*, 29(2):167–183.

[73] Kaseem, A. S. (1998). Comparative studies on thin layer drying models for wheat. In *13th International Congress on Agricultural Engineering*, volume 6, pages 2–6.

[74] Kilani, M. I., Haik, Y. S., Jaw, S.-Y., and Chen, C.-J. (2005). Numerical simulation of flow in a screw-type blood pump. *Journal of Visualization*, 8(1):33–40.

[75] Kise'ák, J., Pardasani, K. R., Adlakha, N., Stehlík, M., and Agrawal, M. (2013). On some probabilistic aspects of diffusion models for tissue growth. *The Open Statistics and Probability Journal*, 5(1):15–22.

[76] Koç, B., Eren, I., and Kaymak Ertekin, F. (2008). Modelling bulk density, porosity and shrinkage of quince during drying: The effect of drying method. *Journal of Food Engineering*, 85(3):340–349.

[77] Konstankiewicz, K. and Zdunek, A. (2001). Influence of turgor and cell size on the cracking of potato tissue. *International Agrophysics*, 15(1):27–30.

[78] Krokida, M. and Maroulis, Z. (2001). *Quality Changes During Drying of Food Materials. In: Drying Technology in Agriculture and Food Science*. Science Publishers, USA.

[79] Krokida, M. K., Karathanos, V. T., and Maroulis, Z. B. (2000). Effect of osmotic dehydration on viscoelastic properties of apple and banana. *Drying Technology*, 18(4-5):951–966.

[80] Krokida, M. K., Kiranoudis, C. T., and Maroulis, Z. B. (1999). Viscoelastic behaviour of dehydrated products during rehydration. *Journal of Food Engineering*, 40(4):269–277.

[81] Krokida, M. K. and Maroulis, Z. B. (1997). Effect of drying method on shrinkage and porosity. *Drying Technology*, 15(10):2441–2458.

[82] Krokida, M. K. and Maroulis, Z. B. (1999). Effect of microwave drying on some quality properties of dehydrated products. *Drying Technology*, 17(3):449–466.

[83] Krokida, M. K., Zogzas, N. P., and Maroulis, Z. B. (1997). Modelling shrinkage and porosity during vacuum dehydration. *International Journal of Food Science and Technology*, 32(6):445–458.

[84] Kumar, P. S., Sagar, V. R., and Singh, U. (2006). Effect of tray load on drying kinetics of mango, guava and aonla. *Journal of Scientific & Industrial Research*, 65(8):659–664.

[85] Lewis, W. K. (1921). The rate of drying of solid materials. *Journal of Industrial & Engineering Chemistry*, 13(5):427–432.

[86] Liepsch, D. (2006). Biofluid mechanics - an interdisciplinary research area of the future. *Technology and Health Care*, 14:209–214.

[87] Lin, T. T. and Pitt, R. E. (1986). Rheology of apple and potato tissue as affected by cell turgor pressure. *Journal of Texture Studies*, 17(3):291–313.

[88] Lozano, J. E., Rotstein, E., and Urbicain, M. J. (1980). Total porosity and open-pore porosity in the drying of fruits. *Journal of Food Science*, 45(5):1403–1407.

[89] Lozano, J. E., Rotstein, E., and Urbicain, M. J. (1983). Shrinkage, porosity and bulk-density of foodstuffs at changing moisture contents. *Journal of Food Science*, 48(5):1497–1502 & 1553.

[90] Madiouli, J., Sghaier, J., Lecomte, D., and Sammouda, H. (2012). Determination of porosity change from shrinkage curves during drying of food material. *Food and Bioproducts Processing*, 90(C1):43–51.

[91] Marousis, S. N. and Saravacos, G. D. (1990). Density and porosity in drying starch materials. *Journal of Food Science*, 55(5):1367–1372.

[92] Mavroudis, N. E., Gekas, V., and Sjöholm, I. (1998). Osmotic dehydration of apples. Shrinkage phenomena and the significance of initial structure on mass transfer rates. *Journal of Food Engineering*, 38(1):101–123.

[93] May, B. K. and Perré, P. (2002). The importance of considering exchange surface area reduction to exhibit a constant drying flux period in foodstuffs. *Journal of Food Engineering*, 54(4):271–282.

[94] Mayor, L., Pissarra, J., and Sereno, A. M. (2008). Microstructural changes during osmotic dehydration of parenchymatic pumpkin tissue. *Journal of Food Engineering*, 85(3):326–339.

[95] Mayor, L. and Sereno, A. M. (2004). Modelling shrinkage during convective drying of food materials: a review. *Journal of Food Engineering*, 61(3):373–386.

[96] Mazumdar, J., Ghosh, A., Hewitt, J. S., and Bhattacharya, P. K. (2005). Elastic plastic analysis of shallow shells-a new approach. *The ANZIAM Journal*, 47(01):121–130.

[97] McCoy, E. L. (1989). The strain energy function in axial plant growth. *Journal of Mathematical Biology*, 27(5):575–594.

[98] McKenzie, M. J., Sowokinos, J. R., Shea, I. M., Gupta, S. K., Lindlauf, R. R., and Anderson, J. A. D. (2005). Investigations on the role of acid invertase and UDP-glucose pyrophosphorylase in potato clones with varying resistance to cold-induced sweetening. *American Journal of Potato Research*, 82:231–230.

[99] McMinn, W. A. M. and Magee, T. R. A. (1997). Physical characteristics of dehydrated potatoes - part I. *Journal of Food Engineering*, 33(1-2):37–48.

[100] Mernone, A. V. and Mazumdar, J. N. (2002). A mathematical study of peristaltic transport of a casson fluid. *Mathematical and Computer Modelling*, 35(7-8):895–912.

[101] Midilli, A., Kucuk, H., and Yapar, Z. (2002). A new model for single-layer drying. *Drying Technology*, 20(7):1503–1513.

[102] Mijovic, B. and Liepsch, D. (2003). Experimental flow studies in an elastic Y-model. *Technology and Health Care*, 11:115–141.

[103] Mohsenin, N. N. (1986). *Physical Properties of Plant and Animal Materials*. Gordon and Breach Science Publishers, New York.

[104] Mooney, M. (1940). A theory of large elastic deformation. *Journal of Applied Physics*, 11(9):582–592.

[105] Murase, H., Merva, G. E., and Segerlind, L. J. (1980). Variation of young's modulus of potato as a function of water potential. *Transactions of the American Society of Agricultural and Biological Engineers*, 23(3):794–796.

[106] Niklas, K. J. (1992). *Plant Biomechanics: An Engineering Approach to Plant Form and Function*. University of Chicago press.

[107] Nilsson, S. B., Hertz, C. H., and Falk, S. (1958). On the relation between turgor pressure and tissue rigidity. II. theoretical calculations on model systems. *Physiologia Plantarum*, 11(4):818–837.

[108] Oey, M. L., Vanstreels, E., De Baerdemaeker, J., Tijskens, E., Ramon, H., Hertog, M. L. A. T. M., and Nicolaï, B. (2007). Effect of turgor on micromechanical and structural properties of apple tissue: A quantitative analysis. *Postharvest Biology and Technology*, 44(3):240–247.

[109] Oey, M. L., Vanstreels, E., De Baerdemaeker, J., Tijskens, E., Ramon, H., and Nicolaï, B. (2006). Influence of turgor on micromechanical and structural properties of apple tissue. *IUFoST*, 855:1879–1889.

[110] Ogden, R. W. (2005). Mechanics of rubberlike solids. In *Proceedings of the 21st International Congress of Theoretical and Applied Mechanics*, pages 15–21.

[111] Oikonomopoulou, V. P. and Krokida, M. K. (2013). Novel aspects of formation of food structure during drying. *Drying Technology*, 31(9):990–1007.

[112] Oparka, K. J. and Wright, K. M. (1988). Influence of cell turgor on sucrose partitioning in potato tuber storage tissues. *Planta*, 175(4):520–526.

[113] Overhults, D. G., White, G. M., Hamilton, H. E., and Ross, I. J. (1973). Drying soybeans with heated air. *Transactions of the ASAE*, 16(1):112–113.

[114] Page, G. (1949). *Factors Influencing the Maximum Rate of Air Drying Shelled Corn in Thin-layers*. Thesis, Purdue University, West Lafayette, Indiana.

[115] Panchariya, P. C., Popovic, D., and Sharma, A. L. (2002). Thin-layer modelling of black tea drying process. *Journal of Food Engineering*, 52(4):349–357.

[116] Pang, D. W. (1993). *Prediction and Quantification of Apple Bruising*. Thesis, Massey University, New Zealand.

[117] Pardasani, K. R. and Adlakha, N. (1995). A study of thermal effect of epithelial tumor on temperature distribution in annular tissue layers of a human body. In *IEEE Engineering in Medicine & Biology*, pages 4.45–4.46.

[118] Pardasani, K. R. and Shakya, M. (2006). Three dimensional infinite element model to study thermal disturbances in human peripheral region due to tumor. *Journal of Biomechanics*, 39, Supplement 1(0):S634.

[119] Pitt, R. E. (1982). Models for the rheology and statistical strength of uniformly stressed vegetative tissue. *Transactions of the ASAE*, 25(6):1776–1784.

[120] Pitt, R. E. (1984). Stress-strain and failure characteristics of potato tissue under cyclic loading. *Journal of Texture Studies*, 15(2):131–155.

[121] Pitt, R. E. and Chen, H. L. (1983). Time-dependent aspects of the strength and rheology of vegetative tissue. *Transactions of the ASAE*, 26(4):1275–1280.

[122] Pitt, R. E. and Davis, D. C. (1984). Finite element analysis of fluid-filled cell response to external loading. *Transactions of the ASAE*, 27(6):1976–1983.

[123] Polignone, D. A. and Horgan, C. O. (1993). Cavitation for incompressible anisotropic nonlinearly elastic spheres. *Journal of Elasticity*, 33(1):27–65.

[124] Quevedo, R., Carlos, L. G., Aguilera, J. M., and Cadoche, L. (2002). Description of food surfaces and microstructural changes using fractal image texture analysis. *Journal of Food Engineering*, 53(4):361–371.

[125] Rahman, M. S. (2001). Toward prediction of porosity in foods during drying: A brief review. *Drying Technology*, 19(1):1–13.

[126] Rahman, M. S. (2003). A theoretical model to predict the formation of pores in foods during drying. *International Journal of Food Properties*, 6(1):61–72.

[127] Rahman, M. S. (2007). *Handbook of Food Preservation*. CRC press, Taylor & Francis Group, LLC, New York, second edition.

[128] Rahman, M. S. (2008). *Food Properties Handbook*. CRC Press, Taylor & Francis Group, LLC, New York, second edition.

[129] Rahman, M. S., Al-Zakwani, I., and Guizani, N. (2005). Pore formation in apple during air-drying as a function of temperature: porosity and pore-size distribution. *Journal of the Science of Food and Agriculture*, 85(6):979–989.

[130] Rao, M. A., Rizvi, S. S. H., and Datta, A. K. (2005). *Engineering Properties of Foods*. CRC Press, New York.

[131] Rassis, D. K., Saguy, I. S., and Nussinovitch, A. (1998). Physical properties of alginate-starch cellular sponges. *Journal of Agricultural and Food Chemistry*, 46(8):2981–2987.

[132] Ratti, C. (1994). Shrinkage during drying of foodstuffs. *Journal of Food Engineering*, 23(1):91–105.

[133] Rautela, S., Chopra, C. S., Pandey, A., and Raghav, M. (2009). Physico-chemical characteristics and chipping performance of organic potatoes (solanum tuberosum). In *National conference on Engineering for Food & Bio-Processing*, pages 312–316.

[134] Reeve, R. M. (1954). Histological survey of conditions influencing texture in potatoes. I. effects of heat treatments on structure. *Journal of Food Science*, 19(1-6):323–332.

[135] Rigbi, Z. and Hiram, Y. (1981). An approximate method for the study of large deformations of membranes. *International Journal of Mechanical Sciences*, 23(1):1–10.

[136] Rivlin, R. S. (1948). Large elastic deformations of isotropic materials. IV. further developments of the general theory. *Philosophical Transactions of the Royal Society of London. Series A, Mathematical and Physical Sciences*, 241(835):379–397.

[137] Roberts, K. (2007). *Handbook of Plant Science*. John Wiley & Sons Ltd., England.

[138] Ross, K. A. (2003). *Characterizing Porous Food Systems Using Fundamental*. Thesis, Purdue University, Purdue.

[139] Sablani, S. S. and Rahman, M. S. (2002). Pore formation in selected foods as a function of shelf temperature during freeze drying. *Drying Technology*, 20(7):1379–1391.

[140] Sacilik, K. and Elicin, A. K. (2006). The thin layer drying characteristics of organic apple slices. *Journal of Food Engineering*, 73(3):281–289.

[141] Sagar, V. R. and Suresh Kumar, P. (2010). Recent advances in drying and dehydration of fruits and vegetables: a review. *Journal of Food Science and Technology*, 47(1):15–26.

[142] Saha, S., Chimalwar, P. J., and Sherkar, B. D. (2007). Post harvest profile of potato. Report.

[143] Sahay, K. B. (1984). On the choice of strain energy function for mechanical characterisation of soft biological tissues. *Eng Med*, 13(1):11–14.

[144] Sahin, S. and Sumnu, S. G. (2006). *Physical Properties of Foods*. Springer Science+Business Media, LLC., New York.

[145] Saravacos, G. D. and Maroulis, Z. B. (2001). *Transport Properties of Foods*. CRC Press, New York.

[146] Scanlon, M. G., Pang, C. H., and Biliaderis, C. G. (1996). The effect of osmotic adjustment on the mechanical properties of potato parenchyma. *Food Research International*, 29(5-6):481–488.

[147] Shahari, N. A. (2012). *Mathematical Modelling of Drying Food Products. Application to Tropical Fruits*. Thesis, University of Nottingham.

[148] Sharaf-Eldeen, Y. I., Blaisdell, J. L., and Hamdy, M. Y. (1980). A model for ear corn drying. *Transaction of the ASAE*, 23(5):1261–1271.

[149] Sharma, P. R., Ali, S., and Katiyar, V. K. (2009a). Mathematical modeling of temperature distribution on skin surface and inside biological tissue with different heating. In *13th International Conference on Biomedical Engineering*, volume 23, pages 1957–1961. Springer Berlin Heidelberg.

[150] Sharma, P. R., Ali, S., and Katiyar, V. K. (2009b). Numerical study of temperature and thermal dose response of tumor tissue during hyperthermia treatment. In McGoron, A., Li, C., and Lin, W.-C., editors, *25th Southern Biomedical Engineering Conference*, volume 24, pages 377–378. Springer.

[151] Sharma, P. R. and Sharma, M. (2014). Oscillatory MHD free convective flow and mass transfer through porous medium bounded by a vertical porous channel with thermal source and slip boundary conditions. *Asian Journal of Multidisciplinary Studies*, 2(9):70–85.

[152] Sharma, R. R., Pal, R. K., Asrey, R., Sagar, V. R., Dhiman, M. R., and Rana, M. R. (2013). Pre-harvest fruit bagging influences fruit color and quality of apple cv. delicious. *Agricultural Sciences*, 04(09):443–448.

[153] Shekofteh, M., Cherati, F. E., Kamyab, S., and Hosseinpor, Y. (2012). Study of shrinkage of potato sheets during drying in thin-layer dryer. *Research Journal of Applied Sciences, Engineering and Technology*, 4(16):2677–2681.

[154] Silber, G., Alizadeh, M., and Salimi, M. (2010). Large deformation analysis for soft foams based on hyperelasticity. *Journal of Mechanics*, 26(03):327–334.

[155] Silber, G., Trostel, R., Alizadeh, M., and Benderoth, G. (1998). A continuum mechanical gradient theory with applications to fluid mechanics. *Le Journal de Physique IV*, 08(PR8):Pr8–365–Pr8–373.

[156] Singh, R. P. (1994). *Scientific Principles of Shelf Life Evaluation*, book section 1, pages 3–26. Springer US.

[157] Singh, R. P., Chopra, C. S., and Singh, I. S. (2000). Phsico-chemical composition of wood apple fruit (limonia acidissima l.). *Beverage and Food World*, 27(2):23–27.

[158] Sinha, N. (2011). *Handbook of Vegetables and Vegetable Processing*. John Wiley & Sons, USA.

[159] Sivaloganathan, J. (1986). Uniqueness of regular and singular equilibria for spherically symmetric problems of nonlinear elasticity. *Archive for Rational Mechanics and Analysis*, 96(2):97–136.

[160] Skalak, R., Tozeren, A., Zarda, R. P., and Chien, S. (1973). Strain energy function of red blood cell membranes. *Biophysical Journal*, 13(3):245–264.

[161] Slawinski, M. A. (2003). *Seismic Waves and Rays in Elastic Media*, volume 34. Oxford OX5 1 GB, UK, The Boulevard, Langford Lane Kidlington.

[162] Suzuki, K., Kubota, K., Hasegawa, T., and Hosaka, H. (1976). Shrinkage in dehydration of root vegetables. *Journal of Food Science*, 41(5):1189–1193.

[163] Taber, L. A. (2004). *Nonlinear Theory of Elasticity: Application in Biomechanics*. World Scientific Publishing Co. Pte. Ltd., Singapore.

[164] Tan, Y., Sun, D., Huang, W., and Cheng, S. H. (2008). Mechanical modeling of biological cells in microinjection. *IEEE Transactions on NanoBioscience*, 7(4):257–266.

[165] Tan, Y., Sun, D., Huang, W., and Cheng, S. H. (2010). Characterizing mechanical properties of biological cells by microinjection. *IEEE Transactions on NanoBioscience*, 9(3):171–180.

[166] Thakor, N. J., Sokhansanj, S., Sosulski, F. W., and Yannacopoulos, S. (1999). Mass and dimensional changes of single canola kernels during drying. *Journal of Food Engineering*, 40(3):153–160.

[167] Then, C., Vogl, T. J., and Silber, G. (2012). Method for characterizing viscoelasticity of human gluteal tissue. *Journal of Biomechanics*, 45(7):1252–1258.

[168] Tong, P. and Fung, Y. C. (1976). The stress-strain relationship for the skin. *Journal of Biomechanics*, 9(10):649–657.

[169] Treloar, L. R. G. (1975). *The Physics of Rubber Elasticity*. Oxford University Press Inc., New York.

[170] Valanis, K. C. and Landel, R. F. (1967). The strain-energy function of a hyperelastic material in terms of the extension ratios. *Journal of Applied Physics*, 38(7):2997–3002.

[171] Velić, D., Planinić, M., Tomas, S., and Bilić, M. (2004). Influence of airflow velocity on kinetics of convection apple drying. *Journal of Food Engineering*, 64(1):97–102.

[172] Verma, L. R., Bucklin, R. A., Endan, J. B., and Wratten, F. T. (1985). Effects of drying air parameters on rice drying models. *Transactions of the ASAE*, 28(1):296–301.

[173] Veronda, D. R. and Westmann, R. A. (1970). Mechanical characterization of skin-finite deformations. *Journal of Biomechanics*, 3(1):111–124.

[174] Walsh, M., McGloughlin, T., Liepsch, D. W., O'Brien, T., Morris, L., and Ansari, A. R. (2003). On using experimentally estimated wall shear stresses to validate numerically predicted results. *Proceedings of the Institution of Mechanical Engineers, Part H: Journal of Engineering in Medicine*, 217(2):77–90.

[175] Wang, J. and Chao, Y. (2002). Drying characteristics of irradiated apple slices. *Journal of Food Engineering*, 52(1):83–88.

[176] Wang, N. and Brennan, J. G. (1995). Changes in structure, density and porosity of potato during dehydration. *Journal of Food Engineering*, 24(1):61–76.

[177] Wayne, R. O. (2009). *Plant Cell Biology from Astronomy to Zoology*. Elsevier, UK.

[178] Weinberg, I. K. (2007). *Material Modeling of Microstructured Solids, Theory, Numeric and Applications*. Thesis, Technical University of Berlin, Berlin.

[179] White, G. M., Bridges, T. C., Loewer, O. J., and Ross, I. J. (1978). Seed coat damage in thin layer drying of soybeans as affected by drying conditions. *ASAE paper no. 3052*.

[180] Yaldýz, O. and Ertekýn, C. (2001). Thin layer solar drying of some vegetables. *Drying Technology: An International Journal*, 19(3-4):583–597.

[181] Yeoh, O. H. (1990). Characterization of elastic properties of carbon-black-filled rubber vulcanizates. *Rubber Chemistry and Technology*, 63(5):792–805.

[182] Zdunek, A., Gancarz, M., Cybulska, J., Ranachowski, Z., and Zgórska, K. (2008). Turgor and temperature effect on fracture properties of potato tuber (solanum tuberosum cv. irga). *International Agrophysics*, 22(1):89–97.

[183] Zhu, H. X. and Melrose, J. R. (2003). A mechanics model for the compression of plant and vegetative tissues. *Journal of Theoretical Biology*, 221(1):89–101.

[184] Zogzas, N. P., Maroulis, Z. B., and Marinos-Kouris, D. (1994). Densities, shrinkage and porosity of some vegetables during air-drying. *Drying Technology*, 12(7):1653–1666.

[185] Zulliger, M. A., Fridez, P., Hayashi, K., and Stergiopulos, N. (2004). A strain energy function for arteries accounting for wall composition and structure. *Journal of Biomechanics*, 37(7):989–1000.